Production of an Electrochemical Sensor for Microcystin Measurement Using AuNPs@MWCNTs/GQDs Nanocomposites - A Review

RUKİYE ÖZTEKİN, DELİA TERESA SPONZA*
Department of Environmental Engineering
Dokuz Eylül University
Tınaztepe Campus, 35160 Buca/Izmir,
TURKEY

**Corresponding Author*

Abstract: - This review paper focuses on the current state of art as well as on future trends in the reaction mechanism and detecting properties of a novel molecular printed electrochemical sensor for microcystin measurement using three-dimensional (3-D) AuNPs@MWCNTs/GQD nanocomposite. Microcystins (MCs) are secondary metabolites generated by some cyanobacteria, a stable cyclic heptapeptide toxin class in the environment. MCs can produce a wide various adverse health effects in animals, plants and humans. Effective methods and measurement techniques required for isolate MCs from the contaminated aquatic environments. Among the methods, the sensor with three-dimensional conductive network composed of multi-walled carbon nanotubes (MWCNTs), graphene quantum dots (GQDs), and gold nanoparticles (AuNPs) and AuNPs@MWCNTs/GQDs Nanocomposites, some microorganisms with enzymes; it was was found that AuNPs@MWCNTs/GQDs is the most sensitive one. The molecularly imprinted polymer was engineered by quantum chemical computation utilizing p-aminothiophenol (p-ATP) and methacrylic acid (MAA) as dual functional monomers and L-arginine as a segment template with irreversible electrochemical oxidation reaction involving an electron and two protons. The detection response to MC-LR in the linear range was between 0.08 and 2 μg/l, and the limit of detection (LOD) was found to be 0.0027 μg/l (S/N = 3). In addition, the recoveries of the total amount of MC-LR and [Dha7] MC-LR in the actual sample by the obtained sensor were found to be higher than the other methods.

Key-Words: - Biomedical diagnostics; Cyanobacteria; Cyclic heptapeptide toxin; Electrochemical sensor; Gold nanoparticles (Au NPs); Graphene quantum dots (GQDs); Microcystin (MC); Multi-walled carbon nanotubes (MWCNTs); Single-walled carbon nanotubes (SWCNTs); Toxicity.

Received: December 17, 2025. Revised: February 23, 2026. Accepted: March 17, 2026. Published: June 26, 2026.

1 Introduction

Microcystins (MCs), it is a group of cyclic heptapeptide toxins with unique amino acid side chains produced by Microcystis, Anabaenopsis, Aphanocapsa, Cichlidium, and Oscillatoria, [1]. MCs general structure is Cyclo-(-D-Ala-L-X-D-MEASP-L-Z-ADDA-D-Glu-MDHA). X and Z are two important amino acids, which is highly variable, which ensure their molecular diversity in MCs. The L-X amino acid residue is usually leucine or phenylalanine, while the L-Z amino acid residue is usually alanine, arginine, methionine, leucine, or valine. ADDA structure is 3-amino-9-methoxy-2,6,8-trimethyl-10-phenyldeca-4,6- dienoicacid, which is necessary for the identification of toxin activity. The cyclical nature of MCs makes them durable to superior temperatures, sunlight and extreme pH. Hughes et al., [2], described the first MC in 1957 and since then more than 270 variants of MCs with varying degrees of toxicity have been isolated. When it comes to toxicity, MCs isomers; Microcystin-LR (MC-LR) is the most common and most toxic isomer, Microcystin-LA (MC-LA) has a similar degree of toxicity, followed by Microcystin-RR (MC-RR) and Microcystin-YR (MC-YR), [2].

MCs are cyclic heptapeptides consisting of two variable positions and five constant amino acids, [3]. Because the circular heptapeptide structure of MCs, it has a strong affinity and high specificity for serine/threonine protein phosphatase, acts as an effective inhibitor of the eukaryotic protein phosphatase family PP1 and PP2A. This leads to cell apoptosis. However, MCs can cause oxidative stress in the liver and can lead to death. Toxicity differences in MCs strains are due to the content of peptide synthase generated by MCs, [4], [5]. MC-LR is considered the

most toxic form of MCs and has a lethal value dose of 50%, LD_{50}=43 μg/kg, [5], [6]. Human health can be affected by MCs mainly through physical contact, inhalation, contaminated water and food. To reduce the health risks associated with MCs, the World Health Organization (WHO) recommends that the MCs content in drinking water should not exceed 1 μg/l, [7].

Increasing effects of climate change and eutrophication, cyanobacterial proliferations have become one of the global aquatic environment problems, and the environmental pollution and health problems can cause the attention of scientists working in different disciplines. The genera of cyanobacteria that produce cyanobacterial blooms include Dolichospermum, Microcystis, Nodularia, Planktothrix and Oscillatoria, [8]. These algal outbreaks release toxic secondary metabolites, which are cyanobacterial toxins as MCs are the most widely distributed, toxic type of cyanobacterial toxin in cyanobacterial flower pollution. Potentially toxic cyanobacteria are increasingly detected in water supply systems around the world. In the United States and Canada, [9], ≈ 80% of water sources and treated water samples contain MCs and these are the primary congener MC-LR. In the reports of similar studies conducted in Europe, it is reported that 60% of the cyanotoxins detected in fresh water consists of MCs, [10]. In some parts of Europe, MCs rates were even higher: in the water quality survey of lakes in Greece, for example, more than 90% of the samples examined contained MCs, [11]. In addition, MCs have also been detected in terrestrial environments irrigated or flooded with waters containing damaging algal blooms.

Many tools were used to identify and quantify MCs and MCs-related toxins with high performance liquid chromatography containing a mass spectrometry (HPLC-MS) and enzyme-linked immunosorbent assays (ELISA). The HPLC-MS measurement method is an analytical method approved by the Environmental Protection Agency (EPA) in the United States to detect various algal toxins with detection limits ranging from 0.1 to 1 μg/l, [12], [13]. A limit of 1 μg/l for MC-LR in drinking water has been set by the WHO and an acceptable daily intake level < 0.04 g/kg body weight was suggested, [14]. In addition, stricter standards (0.1–0.3 μg/l) have been recommended by some institutions, [14]. However, chromatography is sensitive to trace samples and requires extensive sample pretreatment compared to immunoassays that are easy to use in routine screening of real samples, [15]. It is difficult to distinguish homologs of structurally similar MCs, particularly from the presence of other highly abundant but less toxic ones, [16]. Thus, for fast and sensitive measurement of biological compounds; it should be an urgent need for the development of an advanced, small and portable device to overcome the shortcomings of existing methods, [17], [18].

In this review article, we searched the literature on the reaction mechanisms and recorded main features in the sensitive measurements of the MCs properties, which are widely used today, with electrochemical sensors. For this, we investigated the effects of three-dimensional (3-D) gold nanoparticle@multi-walled carbon nanotubes/graphene quantum dots (AuNPs@MWCNTs/GQDs) on MCs based studies in the literature. In this review, we tried to present a new perspective to the literature on the subject of "production of an electrochemical sensor for MCs measurement using AuNPs@MWCNTs/GQDs nanocomposite" by making use of existing studies in the literature. Thus, it is aimed to shed light on and support new scientific studies to be made in the future.

2 Microcystins (MCs)

2.1 Toxic Mechanism of MCs

Protein phosphorylation-dephosphorylation is catalyzed by phosphatases and kinases and has an important role in regulating protein activity in cells. The serine/threonine protein phosphatases PP1 and PP2A, found in eukaryotes, are critical protein phosphatases, [19], and in MCs, they inhibit the action of phosphatases by binding to the catalytic subunits of PP1 and PP2A, [20], [21]. This process is divided into two stages: (1) the transient interaction of the toxin with the enzyme inactivation, and (2) the formation of covalent adducts takes place during the reaction period, which completely inactivates the enzyme in few hours after binding, [22]. The softer ADDA side chain is considered to play a key role in this binding process, [23]. ADDA is hydrophobic and interacts with four amino acids (Cln122, Ile123, His191 and Trp200) in the catalytic subunit of PP2A to form a hydrophobic cage, [24]. The nuclear phosphoprotein p53 functions as an activator in DNA repair, was apoptosis, and tumor suppression pathways, [25], and is a substrate for PP2A. It is a protein regulated by MCs. In MC-LR-treated mice, the p-phosphoserine reactivity of the p53 protein was observed higher in MC-LR-treated animals compared to the saline-treated group. Results from this experiment showed that MC-LR induced hyperphosphorylation of P53 by inhibiting the action of PP2A leading to apoptosis, [26]. Binding of MCs to PP1 and PP2A can trigger many other adverse responses in its reaction, in addition to regulating p53 to affect apoptosis. The expression of mitogen-activated protein kinases (MAPKs) is mediated by PP2A, which regulates the

expression of proto-oncogenes involved in the transcription of genes for growth and differentiation. Bcl-2 acts as a homodimer protecting the integrity of mitochondria and is a very important cell death regulator and a direct substrate of PP2A, [27]. MCs influence the expression of related proteins by inhibition of PP2A, [28] and this leads to decreasing of cell function and even apoptosis.

2.2 Molecular Mechanisms of MCs

The pathways and genes involved in MC-LR biodegradation have been described in detail, [29], [30]. MC-LR degradation is considered to be mediated by at least three intracellular hydrolases, and as two enzymatic degradation mediators of MC-LR, linearized (acyl ring) MC-LR (NH_2-Adda-Glu-Mdha-Ala-Leu-MeAsp-Arg-OH) and tetrapeptide MC-LR (NH_2- Adda-Glu- Mdha-Ala-OH) has been identified, [29], [30]. In the first step, the ring-opening hydrolysis of MC-LR is catalyzed by an enzyme called microcystinase, known as MlrA. The initial site of action of this enzyme is at the ADDA-Arg peptide bond, transforming the cyclic MC-LR into linear MC-LR. The linear MC-LR product is 160-fold less reactive in protein phosphatases than the parent compound, indicating that the reaction is greatly reduced through MlrA-mediated molecular toxicity. MlrA enzyme was previously characterized as a metalloprotease through inhibition studies. In inhibition studies, she characterized the second enzyme (formerly peptidase 2, now MlrB) in a similar degradation pathway as a possible serine peptidase and produces the tetrapeptide compound. A third enzyme (formerly peptidase 3, now MlrC), characterized as a putative metallopeptidase, carries out further breakdown of the tetrapeptide compound with products that are smaller amino acids and peptides. In some literature searches, to detect MlrA, MlrB and MlrC enzymes, especially MlrA enzyme, which plays a role in the cleavage of the MCs ring structure; qualitative polymerase chain reaction (PCR) methods were designed. MlrD enzyme may facilitate the transport of MCs or biodegradable products of MCs across the bacterial cell wall. ADDA is an active product of the MlrC enzyme on the linearized MC-LR; but there is also a remaining hexapeptide (NH_2-Glu(6)-Mdha(7)-Ala(1)-Leu(2)-MeAsp(3)). This hexapeptide cannot be further degraded by the MlrC enzyme but can be hydrolyzed to unknown products by the MlrA and MlrB enzymes of ACM-3962, [29], [30]. Through, molecular dynamics simulations, homology modeling, and insertion, the active site of the MlrA enzyme was identified and thus determined that the enzyme belongs to the glutamate protease of type II CAAX isoprenoid endopeptidase. These new findings provided valuable additional information to previous studies and are new steps to support the accuracy of these previous studies, [31].

Recently, the entire genome of Sphingopyxis sp. USTB-05 was analyzed based on second and third generation sequencing technologies, and the analysis results showed that cyanobacterial hepatotoxins Sphingopyxis sp. USTB-05 has identified its entire genome, [32]. Thus, previous studies have elucidated the biodegradation pathways of the MC variants MC-RR and MC-YR. Sphingopyxis sp. MB-E was described for the first time, [33], and MC-RR, -YR, -LY, -LY, -LW and -LF degradation were observed, thus confirming the existence of the above gene clusters. Sphingopyxis sp. USTB-05 was used as an experimental subject and the first enzyme, the MlrA enzyme, was found to convert cyclic MC-RR or MC-YR into linear form; the second enzyme attacked the Ala\\Arg or Ala\Tyr bond of MC-RR or MC-YR by linearization to produce a tetrapeptide; and finally, the third enzyme, Mlr, was further degraded to produce the tetrapeptide ADDA, [34], [35], [36], [37], [38].

Starting from a water body contaminated with MCs, the degree of change in the pollutants is displayed by the detection method and the microorganisms that may degrade the microcyst are eliminated, combined with a biofilm system and applied in water treatment, [39] (Figure 1). Atthe same time, in order to be able to monitor on-site; simple, portable and sensitive detection methods are also used. Establishing a systematic treatment process is beneficial in improving the health of water bodies and also ensures public safety, [39].

* Figure 1 can be found in the Appendix section.

2.3 Detection of MCs

To manage and control MCs in a targeted manner and to prevent or reduce the hazards associated with MCs in the comparative table (Table 1).

* Table 1 can be found in the Appendix section.

Conventional detection techniques include ELISAs and liquid chromatography-mass spectrometry (LC-MS) are still widely used as biosensors and microarrays contribute to the environmental monitoring. In addition, more efficient separation techniques are being developed to improve the detection efficiency. Various methods have also been developed, such as protein phosphatase inhibition assays (PPIA), ELISAs, high performance liquid chromatography (HPLC), LC-MS and biosensors, [40], [41]. Chemical methods such as HPLC and LC-MS can more precisely identify various variants but

they are expensive and the size of equipments are large and requires expertise to use them properly. When it is difficult to monitör the real water applications, PPIAs, ELISAs and other biological techniques are much simpler and more specific.

In terms of portability, the advantages of biosensors were high. Emerging methods, such as biosensors, which are much easier to detect in practice due to their speed and portability, provide new ideas for the detection of MCs, [40], [41].

In addition to carbon nanotubes (CNTs), graphene, and carbon nanohorns (CNHs), a special form of carbon nanomaterials, can be applied in the electrochemical detection of electrochemical pressures (ECPs). Zhang et al., [42], [43], developed an electrochemical immune sensor based on single-walled CNHs (SWCNHs) for the detection of MC-LR in water samples (Figure 2**).** CNHs were first modified with MC-LR and then immobilized to a a, glassy carbon electrode, (GCE). A horseradish peroxidase (HRP)-labeled MC-LR antibody was then added. Thus, the MC-LR in the sample can competitively bind the HRP-labeled antibody, and cause to drop of the electrode signal to drop. In this assay, CNHs showed a better sensitizing effect than single-wallet carbon nanotubes (SWCNTs) at a LOD value of 0.03 µg/l measured for MC-LR, [42], [43].

* Figure 2 can be found in the Appendix section.

3 Electrochemical Sensors

Electrochemical sensors have become a common analysis technique, with the advantages of low cost, high accuracy, fast response, good reliability. Therefore, they are of great interest for qualitative and/or quantitative analysis during MC measurements, [44], [45]. The design of high-quality electrochemical sensors requires basic sensing principles (Table 1). Figure 3shows that untreated samples can be added to the electrochemical cell first. Then, when electricity is applied, the electrochemical sensor physical and chemical response can be converted into recognizable electrochemical response signals. By analyzing the correlation between the detected substances and the corresponding electronic signals, the presence of MC in aquatic ecosystems and wastewaters can be quickly detected.

* Figure 3 can be found in the Appendix section.

A typical three-electrode electrochemical system includes a working electrode (WE), a reference electrode (RE) (e.g., Ag/AgCl), and a counter electrode (CE) (e.g., carbon rod, platinum) (Figure 3b).Recently, functional carbon-based nanomaterials such as CDs, CNTs, graphene oxide (GO) and porous carbon have been selected as working electrode (WE) candidates due to their excellent conductivity and durability, [46], [47].

For selectivity, linearity, sensitivity, stability, detection limit, dynamic range and response time of emerging electrochemical sensors; their compositions and structures of the carbon nanomaterials used can be improved by further development, [48], [49], [50]. However, for efficient extraction of MC; versatile electrochemical analysis methods should also be established. Specifically, (1) the current-type, (2) potential-type, (3) conductivity-type, and (4) impedimetric-type analysis should be considered, [51], [52], [53], [54].

Cyclic voltammetry (CV), linear scanning voltammet ry (LSV), differential pulse voltammetry (DPV) and square wave voltammetry (SWV) during application (Figure 3c)are selected according to the properties of the most commonly detected substance, [55], [56], [57], [58]. The working principles of these electrochemical analysis methods, should be rationally and accurately. CV is a widely used electrochemical analysis method and it works by scanning the response current one or more times in a triangular waveform under varying applied voltage. The reversibility of the electrode reaction, the intermediates, the phase boundary adsorption, the phase transformation and the mechanism of the coupled reactions can be determined and evaluated according to the shape of the CV curves presented, [59]. LSV is another electrochemical analysis method in which a linear change in voltage is applied over the electrode and the potential varies linearly with the applied voltage, based on the current in the working electrode simultaneously. The peak current measured in the LSV curve shows a linear relationship with the concentration of the measured analytes as the basis of the quantitative analysis, [60]. DPV is an electrochemical method that involves a linearly increasing voltage with a constant amplitude rectangular pulse. As a result of the rapid development of electronic circuits, pulse voltammetry is widely used in the field of electrochemical analysis. For example, the quantitative determination of various analytes and the mechanism of complex electrode reactions can be solved with high sensitivity and low detection limit of pulse voltammetry. Also, detection sensitivity can be greatly improved using DPV in combination with other methods such as stripping voltammetry, [61]. SWV is an effective electrochemical technique that can be used to understand the electrode mechanism and measure the electro-kinetics. It states that SWV can suppress the background current efficiently, resulting in increasing

of the signal-to-noise ratio and reducing the detection limit, [62], [63].

Electrochemical biosensor applications are well suited for in situ monitoring due to potential miniaturization, portability and automation, [64]. In addition, electrochemical sensors have low cost, [15], [18], [65], [66], [67]. In environmental monitoring, especially for MC-LR monitoring a progress has been made in the development of specific and highly sensitive electrochemical biosensors/immunosensors, [3], [68], [69]. Electrochemical biosensors developed to detect the phytotoxins with three main components: (1) a biometric element, (2) a signal transmission mechanism, and (3) a sensor electrode.

Biometric receptors are crucial for the selectivity and specificity of electrochemical biosensors. Antibodies, which are the most used receptors in the electrochemical biosensing of MC-LR, have a highly specific molecular recognition, [70], [71], [72]. Detection by these electrochemical sensors is dependent on conformational changes caused by antigen/antibody binding, if they are suitable for detecting large analytes. Detecting algal toxins smaller than 1 kDa using an electrochemical biosensor often fails to produce the desired results. Aptamers used as biometrics for electrochemical detection of algal toxins. They are a combination of small single-stranded DNA/RNA molecules that have higher stability than antibodies when immobilized on the electrode surface, [73], [74], [75]. Therefore,they have enormous potential in the development of commercial sensors, [6], [76], [77]. The aptamer terminal is typically able to replace disulfide groups, amino groups, ferrocene, and thiols that can readily bind to electrode surfaces, [78], [79].

Eissa et al., [6], developed a voltammetric aptasensor to determine the presence of MC-LR in tap water and fish samples. The structure of this voltammetric aptasensor was constructed from a specific oligonucleotide-based combination of aptamer and graphene on an electrochemical platform. In this case, the interaction between the two components is not covalent. The synthetic probe is simply cast onto the carbonaceous substrate while the sensing architecture of this sensor includes the physical adsorption of the specific aptamer into graphene hexagonal cells via $\pi-\pi$ stacking interactions. As shown in Figure 4A, an increase in the voltammetric peak is observed in the presence of the target MC-LR, [6]. The presence of MC-LR induces a conformational change of the aptamer, leading to a dissociation of some aptamer molecules from the surface of the electrode. After decreasing of the total negative charge on the graphene surface and improving the accessibility to external redox couple (ferro/ferricyanide), the electrode area produce a high current. Conversely, the absence of MC-LR is due to the presence of negatively charged aptamers that electrostatically repel the negatively charged redox couple although no satisfactory electron transfer is allowed. The detection structure appeared highly specific and MC-LR was detected up to 1.9 pM under optimal experimental conditions, [6].

* Figure 4 can be found in the Appendix section.

In the study of Lebogang, [80] an amperometric flow ELISA system called VersAFlo was fabricated to detect the presence of MC-LR in freshwater samples (Figure 4B).The system was fully automated and recognition was based on the presence of monoclonal antibodies bound to sepharose particles and packaged into a micro-immunocolon. Inside the column, free MC and MC-horseradish peroxidase conjugate are sequentially captured by the fixed antibodies. The subsequent addition of the enzymatic substrate, ie 2,20-azinobis (3-ethylbenzothiazoline-sulfonic acid) (ABTS), leads to an enzymatic oxidation producing ABTS+ at the working electrode. With the competitive mechanism, the intensity of the reduction peak decreases in the presence of high levels of MC-LR. In the use of the VersAFlo system, the analysis time is reduced to 20 min for each analysis cycle and real-time information is provided. The electrochemistry was unaffected by the presence of possible interference and a satisfactory detection limit of 0.010 mg/l was obtained, [80].

4 Gold Nanoparticles (Au NPs)

Gold nanoparticles (Au NPs) depending on their size up to 100 nm have unique localized surface plasmon resonance (LSPR) properties with high molar extinction coefficients and they can produce significant color changes (Table 1). Therefore, Au NPs aptasensors are well suited for use in techniques such as colorimetry, fluorometry, electrical and electrochemical, surface plasmon resonance or surface-enriched raman scattering (SERS), [81]. This property in Au NPs has also been used in most colorimetric experiments, [82], and SPR-based sensors, [83].

Au NPs attract attention in many applications for electrochemical sensors with their large surface area/volume ratio, good electrical properties, high surface reaction activity, small particle size and good surface properties, [84], [85], [86], [87]. They have an enhanced electrical conduction of DNA and a developed polymeric bead composed of multiple NPs, [87].

According to analytical protocol, an oligonucleotide probe for hybridization (a) a DNA labeled Au-charged carrier sphere (a), a subsequent dissolution process (c) a detection port for stripping of potentiometry and (d) an Au disposable thick film carbon electrode should be applied (Figure 5) [88].

* Figure 5 can be found in the Appendix section.

Higher amplification using multiple Au NPs tracers are in combination with carrier beads and highly sensitive electrochemical stripping detection. By addition to carrier the bead amplification units and ultra-sensitive electrochemical stripping units, provide higher sensitivity by incorporating the catalytic expansion of multiple Au-particle tags (Figure 5b), [88].Structural and morphological insights of Au-loaded polymeric beads showed duplex formation resulting in the attachment of ≈ 0.6 μm polystyrene spheres to ≈ 0.8 μm magnetic beads. Transmission electron microscopy (TEM) micrograph provides a clear image of each Au NP on polystyrene (PS) carrier beads before and after enrichment. Au loading time is optimized for 1×10^{11} Au NPs solution at 15 min loading time, [88]. The chronopotentiometric stripping hybridization response of the new protocol exhibits an unimaginably large Au signal for a lower target concentration (Figure 6a and Figure 6b)than the conventional experiment, [89]. Also, no response was observed for 1000-fold excess of non-complementary DNA (Figure 6c).In the range of ultra-low DNA concentration (100-500 ng/ml), the effect of concentration gives a nonlinear increase in peak area with increasing of target concentration, [89].

* Figure 6 can be found in the Appendix section.

The logarithmic plot was found to be linear over the entire concentration range used (Figure 7).Similar behaviour has been reported in other particle-based bioassays, [89], [90], which is also consistent with models of particle aggregation involving avidin/biotin systems, [91]. From the calibration plot, the limit of detection at S/N=3 for the response of 100 pg/ml target DNA was calculated as 40 pg/ml (6 pM). It has also been noted that this result is much lower than the detection limit of 100 ng/ml of the conventional single particle stripping hybridization assay, [92], [93], [94]. After six sequential repeated measurements of 100 ng/ml targeted DNA, good reproducibility has been achieved. Functionalized Au NPs of graphene quantum dots (GQD) have high sensitivity combined to mercury ions (Hg^{2+}) and copper ions (Cu^{2+}) perform exceptionally at ultra-low detection, [95]. This was achieved by experimenting with dropping GQD-Au NPs onto a polished glassy carbon electrode and then recording them in a square wave voltammogram using anodic stripping voltammetry. The 3-D Au NPs-Graphene composite has also been applied in electrochemical immunoassay for carcinoembryonic antigen. Based of large surface area of Au NPs, more primary antibodies are captured simultaneously, improving the electronic transfer rate, [95].

* Figure 7 can be found in the Appendix section.

Shi et al., [96], designed a biosensor for MCs based on fluorescent resonance-energy transfer (FRET) between Au NPs and fluorescent graphene oxide (GO). GO and MC antibody were covalently linked and Au NPs were modified with single-stranded DNA. MCs bind to both antibody and DNA and they cause fluorescent quenching of GO by Au NPs. LOD=0.5 mg/l for MC-LR and LOD=0.3 mg/l for MC-RR were measured with this sensor, [96].

To improve the electrochemical signals, significant experimental work has been done on the application of Ghana Living Standards Survey (GLSS) in electrochemical biosensors, [94], [97], [98], [99], [100], [101], [102], [103]. Due to the amplification of GLSS, the electrochemical signal of silver has been greatly improved. This contributed to the increase in detection sensitivity. Lai et al., [104] developed a GLSS-based electrochemical immunoassay strategy in the detection of human and mouse IgG. The amount of Au NPs is one of the most important parameter to increase the effect of GLSS. Zhang et al., [65], [66], [67] polypyrrole microspheres (PPyMS) were used to immobilize more Au NPs in an amplification for silver label signal;. For MC-LR detection; LOD=0.1 ng/ml has a low limit of detection and a wide linear range of concentration varying between 0.25 and 50 ng/l, [65], [66], [67].

Liu et al., [105] Au nanobipyramids (Au NBPs) was used for MC-LR detection instead of Au nanorods (NRs) by developing a bimodal split-type photoelectrochemical and colorimetric immune sensor.

5 Multiwalled Carbon Nanotubes (MWCNTs)

With the discovery of synthetic pathways of C60 and other fullerene species, [106], the interest of synthetic has increased among chemists from the other carbon-based materials with different structural possibilities (Table 1). The first MWCNT synthesis in the laboratory was made in 1991 by Sumio Iijima, [107]. By using carbon black and graphite a carbonaeous coumpoud was generated as a precursor material in the environment, [107]. Sumio Iijima

called these carbonaceous substances as "Helical microtubules", [107]. Iijima, [107], used graphite sheets to produce needle-like structures with a lentgh ranging from 4 to 30 nm in length with a diameter up to 1 μm containing coaxial tubes. It was used an arc discharge evaporation method, setting, [107].

Multi-walled nanotubes (MWNTs) form a subclass of CNTs, are new types of carbon materials consisting of layers of graphene folded into carbon cylinders, [64], [108]. Their special geometry, unique electronic, mechanical, chemical and thermal properties make them attractive for electrochemical applications, [109]. Wang et al., [110], designed a new biosensor for MWNTs based on glucose detection. With MWNT-enzyme electrode study in order to detect the Si substrate a growing Au film was placed to the upper surface of MWNTs. The substrate was then completely removed by etching with a mixture of HNO_3 and HF. In the presence of glucose, glucose oxidase enzymes mediate direct electron transfer for the Au converter, thereby generating a response current. The detail of the chemical reaction is shown in Eq. 1 and Eq. 2, [111]:

$$Glucose + O_2 \rightarrow gluconic\ acid + H_2O_2 (1)$$

$$H_2O_2 \rightarrow 2H^+ + O_2 + 2e^- (2)$$

The amperometry response of the MWNT-based biosensor to glucose with the glassy carbon biosensor is much stronger than the glassy carbon biosensor of the MWNT-based biosensor to glucose. Much more interestingly, there was no signal response with the glassy carbon biosensor at constant potential of +0.45 V against Ag/AgCl, while the MWNT-based biosensor gave a very good signal. These biosensors supports higher sensitivity to MWNT-based biosensor, [112].

The stability of the MWNT-based sensors retained 86.70% of its initial activity after four months of storage in a buffer solution at 4°C, but under the same conditions the glassy carbon biosensor retained 37.20% of its initial activity. MWCNTs, GO and metal NPs by combining with other electrochemically active materials are used in a wide variety of electrochemical discoveries, from biological applications to environmental applications, [113], [114], [115], [116].

Especially, for human health and a better life, the need for high-performance virus detection platforms has increased, and this has resulted in many CNT-based detection systems. Lee and co-workers, reported detection of virus DNA with an electrical biodetection platform consisting of magnetically aligned NPs decorated with CNT on the Integrated Development Environment (IDE) (Figure 8), [117]. First, Au and magnetic NPs were modified on the CNT (Au/MNP-CNT) surface and then laid on Pt-IDE with an external magnetic field. The thiol-modified probe DNA was then immobilized on Au NP. Thus, Au and CNT acted as electrical sensing channels and were used as a fragment to align MNP. With synergistic properties between the three nanomaterials, this detection platform gave high sensitivity with LOD=8.4 pM for influenza virus DNA and LOD=8.8 pM for norovirus DNA. It also showed high selectivity against mismatched DNA strains. It demonstrates the excellent detection performance of this detection platform, [117].

* Figure 8 can be found in the Appendix section.

CNT decorated with metallic nanoparticles (NPs) has also been studied for its use as a plasmonic substrate for the plasmonic resonance energy transfer (PRET)-based FL immunosensing system. Au NPs or Ag NPs and metallic NPs such as CNT hybrid structure based plasmonic materials have synergistic properties. Such as, the plasmonic property of Au NP-decorated CNT (Au-CNT) helps identify the influenza viruses, [118]. In this study, Au-CNT was able to capture the target virus by modifying the influenza virus Ab and then adding fluorescent quantum dots (QDs)-Ab to the mixture. Then virus-Ab-Au bonded with CNTs and finally sandwich structures were formed. As a result, the FL of the QD varied linearly with the concentrations of the target influenza virus. The detection limit of viruses was estimated as ≈ 0.1 pg/ml. Influenza virus from a clinical sample was also observed with excellent sensitivity of 50 PFU/ml in the range of 50-10,000 PFU/ml. These experiments proved that a fluoro-immune detection system based on a metal NP-CNT structure could potentially be applied for virus detection, [118].

Liu et al., [119] detects MC-LR, a type of cyanobacterial toxin in water, by photoelectrochemical method by molecularly imprinted TiO_2 coated MWCNTs (MI-TiO_2@MWCNTs). The sensing ability of molecular imprinted TiO_2 has enhanced over conventional TiO_2 and unprinted TiO_2. Studies with this sensor have resulted in a wide linear range for detection of MC-LR, from 1.0 pM to 3.0 pM. MI-TiO_2@CNTs showed excellent selectivity towards MC-LR. This promising sensor could be a potential candidate for water purification and high sensitivity has been noted for detection of MC-LR, [119]. He et al., [120], developed an enzyme-free, double-signal readout immunosensor to detect MC-LR. This required consideration of an enzyme-based biosensor with significant barriers such

as instability, sensitivity, temperature and pH. CNTs decorated with Au NPs (AuNPs-CNTs) were fabricated for the detection of MC-LR, then silver nanorods were coated on AgNP-CNTs for detection with dual signal mode. These sensors recorded as MC-LR detection in the linear range of LOD=2.8 ng/l and LOD=0.005 µg/l to LOD=20 µg/l. In terms of reproducibility, high selectivity and sensitivity of these sensors show promise in environmental monitoring, [120]. Han et al., [64] investigated the electrochemical biosensor with on millimeter-long MWCNT ligned with water-supported CVD. Monoclonal antibodies decorated for MC-LR toxin detection. A linear range of LOD=1 µg/l and LOD=0.05 µg/l to LOD=20 µg/l was observed for the for detection of MC-LR in drinking water, [64]. To reduce the cost the rapid detection of MC-LR in water is a very mportant phenomenon..Queiros et al., [121], developed label-free potentiometric sensors composed of MWCNTs. These sensors were synthesized by imprinted polymer and polyvinyl chloride (PVC) membranes. This method has been successfully applied to detect MC-LR with great selectivity and high sensitivity. It has also provided many benefits with its easy production and cost effectiveness, [121].

Jalalvand's work highlights the enhanced sensitivity afforded by the high surface-to-volume ratio in MWCNT, [122]. Dual detection of prostate specific antigen (PSA) by electrochemical impedance spectroscopy (EIS) and DPV was measured for the proposed aptasensor with EIS in the ranges between 1 and 200 pg/ml for a LOD of 0.5 pg/ml. For hybrid nanomaterial with extraordinary stability, higher conductivity and faster electron transfer kinetics by π-π stacking interaction of MWCNT structures has proven to be effectively combined with other carbon nanomaterials such as GQDs, leading to the development of a 3-D network, [122]. Samie and Arvand, [123], studied a nanocomposite of P4-aptamer-immobilizing GQDs, NiO, Au NPs and f-MWCNTs to detect the progesterone in biological fluids. Its low value of LOD=1.86 pM confirms that f-MWCNTs serve as an excellent transduction platform with other nanomaterials, [123].

6 Graphene Quantum Dots (GQDs)

Zero-dimensional (0-D) GQDs are carbon-based anisotropic nanomaterials forming a fabric-like structure homologous to graphene (Table 1). The morphological features of GQDs mimic both CDs and graphene were illustrated in this Table, [124]. GQDs are widely used as smart probes for environmental, optoelectronic, electrochemical and biological processes, [125], [126], [127], [128]. The edge sizes are larger than the peaks, forming single or manifold graphene panels with chemical portions on their lateral surfaces, providing multiple sites for chemical functionalization, [128]. When forming hybrid nanomaterials, they can be easily conjugated with various nanomaterials via the π–π interaction, [129]. With their dimensional similarity to such molecules, GQDs can be grafted with antibodies, proteins, and small nucleic acids. GQDs can effectively enhance the surface of biosensors to absorb a significant number of receptors, [130], [131], [132].

Numerous nanomaterials exhibiting stable and strong fluorescence have been used in the efficient biosensing applications. The semiconductor QDs have narrow emission range, wide excitation wavelength, good photostability and easy functionalization with surface reagent. They preferred as ideal fluorescent probes. Most semiconductor QDs (ie PbS, CdTeSe@CdZnS, CdTe@CdSe and CdHgTe) contain heavy metals with adverse environmental and biological deleterious effects that hinder their biomedical applicability, [35], [36], [37], [133], [134]. GQDs, a member of the carbon family, are new carbon-based fluorescent materials with excellent biocompatibility, fluorescence properties and non-toxicity. These properties of GQDs are accepted as ideal nanomaterials in biomedical applications compared to other semiconductor nanomaterials.

Given the light-emitting properties of GQDs, its origin is still unclear because their outer states derivated from unwanted impurities and foreign particles. However, their luminescence properties are primarily from quantum confinement. At close range, the effect of oxygen functionalities on the luminescence of GQDs needs to be extensively investigated to understand the luminescent behaviour, [135].

GQDs identify target analytes in a label-free approach. They act as nanozymes or electrocatalysts to catalyze hydrogen peroxide (H_2O_2), [136]. GQDs show catalytic properties such as peroxidase (POD), which results in a redox reaction between H_2O_2 and an electron donating substrate. In the biosensor industry, an enzyme called horseradish peroxidase (HRP) is used to determine the corresponding analyte; associated with labeling of secondary bioreceptors, making analyzes more tedious and costly, [137]. Performing these procedures more quickly and cost-effectively, GQDs are now widely replacing with HRP-conjugated secondary bioreceptors, [136], [138], [139].

GQDs act as attractive fluorophores (fluorescent labels), quenchers, and charge donors as well as energy, [140]. GQDs are fluorescent nanosized segments of graphene that have quantum-sized effects

in the particle range of 3 to 20 nm and lead to exciton capture, [141], [142], [143]. They have a 'Bohr radius' with infinite excitation, with zero band graphene does not produce luminescence, and exhibits quantum confinement in particles of defined size, [144]. GQDs have a bandgap with quantum limitations, side effects, and size effects that can be easily modified due to their size and edge chemistry, [127], [144]. Unlike semiconductor QDs, at a given energy level, GQDs are twice as large (i.e. 4 qs), and this excess qs, is suitable for computational quantum analysis, [128], [129].

6.1 Synthesizing GQDs for Biomedical Sensors

GQDs can also be prepared using a wide variety of methods, along with their role in related biosensor development (Table 1). GQDs with distinguishable and tunable sizes can be prepared chemically by following one of two strategies:

1. In a top-down approach, by obtaining 0-D GQDs; Graphene oxide (GO) or 2D graphene sheets, CNTs, graphite or carbon fibers break down, respectively, [145], [146], [147].

2. In a bottom-up approach, in the synthesis of GQDs;it is carried out by a series of chemical reactions involving small molecular precursors, [125], [141].

With many studies on GQD biosensors, a giant step forward with the above-mentioned features has been taken, [136], [148], [149], [150]. In these studies, stencil-printed carbon electrodes (SPCE), screen-printed gold electrodes (SPGE), and glassy carbon electrodes (GCE) were used. Multiplexing electrodes can detect target analytes specifically and sensitively. These detection platforms are used in healthcare systems. It has been proven to provide cost-effective, reliable, highly sensitive and precise detection of target biomolecules, [151]. It has also been reported that some biosensors offer multiple capabilities in the simultaneous detection of multiple biomolecules, [152], [153]. The investigated GQD detection techniques and their biomedical applications are detailed in Figure 9.

* Figure 9 can be found in the Appendix section.

6.2 Use of Electrochemical GQD Sensors in Biomedical Diagnostics

Electrochemical sensors have gained a lot of popularity in the field of biomedicine and are very important among commercially available sensors, [155], [156], [157]. This type of sensor acts as a miniature device for point-of-care testing (POCT), [158], [159]. Electrochemical sensors to calculate the electrical signal response is based on a WE (ie transducer and recognition system), a CE and a RE, [160], [161]. An antibody detection system has been extensively studied in all GQD-based electrochemical sensors operating on different types of receptors (eg, antibody sensors, MIP sensors, DNA sensors, aptasters, and enzyme-based sensors), [151]. It is a common immunosensor as its function and is only affected by immunoreaction, [162], [163]. Such detection platforms with corresponding target biomolecules contain antibodies with excellent affinity, [151], [164], [165]. In calculating the immune reactions, typical immune sensors may operate in several test modes (ie competitive, direct, sandwich or indirect modes), [166], [167], [168], [169]. Such test formats operate by unique mechanisms and typically involve the following events, [151], [164]: 1. Implantation of the desired biomolecule, 2. Blocking of unreacted sites, and 3. Identification of the target biomolecule.

A chemical or biological reaction can be converted into an electrical response using various electrochemical techniques such as voltammetry, potentiometry, impedimetry, conductometry, and/or amperometry. Conductometric and potentiometric techniques have several disadvantages such as, low sensitivity, less stability, less specificity and inaccuracy; It cannot be used actively in the development of electrochemical GQD sensors, [170]. Figure 10shows the corresponding graphs for voltammetric, amperometric, and impedimetric measurements, which will be described in the next sections.

* Figure 10 can be found in the Appendix section.

6.2.1 Voltammetric GQD-Sensors

Voltammetric sensors use potential (E) applied to the surface of an electrode and monitor the current produced. The amount of electroactive species changes over time by the redox reactions (Table 1). The advantages of voltammetric techniques are observed in extreme sensitivity, fast analysis, simultaneous detection of different analytes, generation of different potential waveforms, small current measurements and determination of kinetic parameters, [171], [172], [173], [174], [175].

When controlling the current in the CV state, the potential application in a WE is both forward and reversed (Figure 10A).In the desired analytical measurements; partial loop, full loop or multiple loop can be performed, [175]. In the case of NPV, the current is calculated after each pulse. Each pulse lasts approximately from 1 to 100 milliseconds (ms), with an interval of 0.1 to 5 seconds between each pulse, [172], [174]. DPV is more or less similar in the structure of NPV with a series of pulsed potential

scans. It is well defined and has small amplitude in the range of 10 to 100 mV and each potential pulse can be distinguished in the DPV case. The current is calculated twice at the beginning and end of each pulse, [172], [174]. The SWV excitation response creates a symmetry such as "ladder pattern" (Figure 10B). SWV is awidely used method because its excellent sensitivity and increased signal-to-noise ratio, [171], [173]. Typical SWV peak from electrode function to target detection is given in Figure 10.The advantages of pulse strategies allowing to different decay rates is very high compared to the capacitive current. This faradaic/capacitive current ratio leads to a LOD suitable for biosensing of biomolecules, [176]. It is reported that SWV and pulse methods are more commonly used for analytical purposes than other techniques, [177], [178].

Electrochemical agrochemical analysis of L-DOPA was performed by functionalizing the GCE surface with GQDs, magnetic NPs and MWCNTs, [179]. GQDs were prepared by pyrolysis of citric acid and all these nanomaterials were characterized by TEM, X-ray diffraction (XRD) and fourier transform infrared spectroscopy (FTIR) methods. With DPV, this biosensor is defined as sensitive and selective L-DOPA with LOD values of ranging from 14.3 nmol/l to 3.0 to 400 μmol/l. An electrochemical experiment was performed by analyzing a drug called doxorubicin hydrochloride (DOX-HCl) with GQDs synthesized in a bottom-up approach, [180]. The CV profile suggests that GQD-coated GCE can markedly increase the electro-catalytic behaviour towards the oxidation of DOX-HCl, while with the use of DPV and the response of DOX-HCl varies over a broad linear spectrum from 0.018 to 3.6 μM, in human plasma with a LOD of 0.016 μM, [180].

AuNPs and N,S-GQDs were embedded in the surface of modified screen-printed carbon electrode (SPCE) step by step as seen in Figure 11, [151]. Enhanced antibody capture with functionalized SPCE was enhanced the signal for sensitive analysis of human chorionic gonadotropin (HCG). For the electrochemical characterization of SPCE; the electrode was examined by ESI and CV methods. DPV can detect HCG at concentrations above LOD=12.5 fg/ml and 0.1–125 pg/ml. The reproducibility of the developed sensor analysis and inter-test sensitivities were examined. The nanocomposite functionalized with SPCE retains good reproducibility over a wide potential window, [151].

* Figure 11 can be found in the Appendix section

The biotinylated p53 antibody was immobilized on a biocompatible and green nanocomposite (NC) layer containing AuNPs/GQDs and poly L-cysteine (P-Cys) as amplifying components and polymeric matrix, respectively, [181]. A mixture of such nanomaterials has been developed on the lateral surface of an Au-electrode in the effective fixation of anti-p53 bioreceptors. Such a detection system has broad linearity with LOD=23.4 fM to 0.0488–12.5 pM. As shown in Figure 12, an immunosensor was also designed to accurately recognize CA 15-3, which is a tumor marker responsible for breast cancer. The electrode was functionalized with thiolated GQDs, Au NPs and cysteamine (CysA). The back-to-back GQDs/AuNPs/CysA system offers ample scope for capturing of CA 15-3 molecules stability. The sensor can give linear response with LOD=0.11 U/ml and 0.15–125 U/ml, [181].

* Figure 12 can be found in the Appendix section

An electrochemical concept in the simultaneous oxidation of guanine and adenine was studied by selecting GQDs and AgNPs in GCE modifiers. The detection platform is capable of not only measuring them, but also distinguishing these purine bases, [35], [36], [37]. GCE functionalized with GQDs/AgNPs can cause a decrease in anodic peak overpotentials and an increase in anodic peak currents. The modified GCE surface was magnified ≈ 22 times compared to the bare surface, demonstrating the importance of using nanomaterials. Linear calibration plots were found in the range of 0.015 to 430 μM for Guanine and 0.015 to 390 μM for Adenine,respectively. The corresponding LOD values are 10 nM for Guanine and 12 nM for Adenine, respectively, [35], [36], [37].

6.2.2 Amperometric GQD Sensors

Amperometric sensors interpret the current flow produced at a constant voltage within the electrochemical cell (Table 1). These sensors work on the principle of specific molecular bio-recognition to form a receptor-analyte complex. They may include a direct or indirect (unlabeled or labeled) approach to analysis. The first case describes the physical changes that occur in the formation of the receptor-analyte complex, while the second case uses tags that generate signals. It should be noted that the indirect mode is often chosen over direct amperometry for its versatility and higher precision, [182]. These biosensors facilitate the redox reaction by calculating the resulting current. They measure the applied potential between RE and WE, [155]. The current produced during an electrochemical reaction corresponds to the amount of signal elements, [183]. Figure 10shows the ideal graph of amperometric sensor signals.

To quantify miRNA by HRP-based catalysis, Hu et al., [184], propose a simple amperometric RNA sensor. This detection system is fabricated by a ds-DNA. ds-DNA was hybridized on the Au electrode using a capture DNA probe (thiolated oligodeoxynucleotide), aminated indicator probe (NH_2-DNA) and target DNA. Then, the activated carboxyl groups of the GQDs were functionalized on NH_2-DNA by a non-covalent interaction. The HRP-modified sensor was able to catalyze the H_2O_2-mediated oxidation of TMB. This resulting in an electrochemical current signal that was preserved and enriched by a clear blue color change of a solution. Using GQDs and enzyme catalysis, the biosensor as prepared is able to precisely measure miRNA-155 in the LOD range from 0.14 fM to 1 fM–100 pM and shows good biocompatibility in the surface/volume ratio offered by GQDs, [184].

Mars et al., [185], developed a DNA sensor to target Alzheimer's disease-causing APO e4DNA in human blood, (Figure 13).Electrochemically and fluorescently sensitive curcumin and GQDs were electropolymerized on an indium tin oxide (ITO) coated electrode. It forms a hybridized DNA and curcumin complex, and an amino-functional DNA probe was covalently implanted with EDC-NHS coupling with chemistry. Amperometric measurements have shown that it can be used to detect APO e4 DNA in a linear calibration region of 20–400 $\times 10^{-12}$ g/ml and a LOD value of 0.48 $\times 10^{-12}$ g/ml, [185].

* Figure 13 can be found in the Appendix section

Zhu et al., [186], reported an amperometric sensor with sensitive, non-enzymatic, long-term stability, good reproducibility, and anti-interference properties. This sensor was designed using GQDs, Au NPs and polydopamine (PDA) as a catalyst which is a signal amplifying element and an adhesive, respectively, [186]. The synergistic effects of Au-PDA-GQDs nanocomposites (NCs) have an excellent electro-catalytic activity in the reduction of H_2O_2. This biosensor based on Au-PDA-GQDs was able to quickly detect H_2O_2 (< 2 s) with a broad linear relationship between 0.1 and 20,000 μM and at a LOD value of 5.8 nM, [186].

Ju et al., [187], developed an amperometric detection strategy using N-GQDs. Surfactant-free Au NPs forming abundant adsorption sites were placed and grown on N-GQDs. These hybrid NCs were obtained by simply adding chloroauric acid ($HAuCl_4.4H_2O$) to the N-GQDs solution without mixing other surfactants and reducing agents. The resulting unsurfactant-coated Au NPs have strong electrocatalytic activity and can provide bare catalytic surfaces. This electrochemical sensor was able to detect HO in human serum samples and HO released from human cervical cancer cells with a linear response with LOD values ranging from 0.12 μM to 13327 μM, [187].

Yang and colleagues have established a label-free detection strategy with antibody receptors, [150]. In the selective identification of CEA, this immunosensor is produced by replacing GCE with Au, PtPd and N-GQDs. By a self-assembly process, the PtPd/N-GQDs/Au hybrid was synthesized by covalent interaction (Figure 14).Additional properties of the hybrid material were larger surface area, improved electron transferability, excellent biocompatibility and an ability to catalyze H_2O_2. Acting as signaling species, these NCs efficiently conjugate bioreceptors by signal transduction. PtPd/N-GQDs/Au is an efficient assemble for capture of the antibodies and act as a signal amplification system. The detection system examined is highly specific for CEA and a negligible response to various inhibitory agents such as BSA, IgG, PSA and hepatitis B surface antigen (HBS) has occurred. This detection tool was able to measure CEA up to 2 fg/ml with a linear regression function ranging from 5 fg/ml to 50 ng/ml, [150].

* Figure 14 can be found in the Appendix section

An NC of GQDs and MWCNTs has been identified as a nanocarrier of an HRP mock and detector antibody, [152]. The inclusion of such an NC significantly increased the sensitivity with the peroxidase-mimicking catalytic performance of GQDs. Electrochemical measurements for hydroquinone (HQ)/H_2O_2 assembly with IL-13Ra2 has a limit of quantification over a wide linear concentration range (2.7 to 100 ng/ml). Such a detection system, will be clinically applicable when it can detect IL-13Ra2 selectively and rapidly for colorectal cancer diagnosis. Tumor markers responsible for colorectal and breast cancers can be used simultaneously for the determination of CDH-17 and IL-13Ra2; a dual amperometric bioassay, [153]. The sandwich constitutes the immunoassay mode using screen-printed double carbon electrode (SPdCE) coupled with GQDs/MWCNTs. The manufacturing process and the detection technique of SPdCE was carried out similar to the above mentioned studies. This immunoassay was able to detect the selective amount of both tumor markers (CDH-17 and IL-13sRa2) with values of LOD=0.03 ng/ml and LOD=1.4 ng/ml, [153].

With the dual signal amplification approach, Malekzad et al., [188], was able to successfully

measure the PSA using an unmediated multilayer amperometric antibody sensor. The anti-PSA antibody was incubated with a conductive matrix and a biocompatible nanocomposite film consisting of GQDs/AuNPs and poly L-cysteine (P-Cys) as binary signal amplification elements, respectively. It has been used to develop a new transduction platform on an Au surface that improves the electrode surface in capturing abundant antibodies. Au NPs were made by soft template synthesis technique, obtaining a compact morphology. Next, the functionalized electrode surface was characterized by energy dispersive spectroscopy (EDS) and high resolution field emission scanning electron microscope (FESEM). The calibration curve for PSA concentration was found to be linearly correlated with LOD=1.8 pg/ml in the range of 2–9 pg/ml, [188].

6.2.3 Impedimetric GQD Sensors

The concept of impedimetric or capacitive biosensors has been frequently mentioned in the literature. EIS is used to characterize the functionalized sensor surface, proteins, antigens, antibodies, DNAs, receptors, etc. They have been used acutely to study the kinetic interactions between a variety of biological molecules, and label-free sensors, [189], [190]. Impedance measurements may or may not be faradic; they can be operatede in the presence or absence of a redox probe. Subsequent measurements determine the biochemical reactions occurring on the surface of a functionalized electrode by interpreting the interface electron transfer resistance, [189], [191]. EIS can convert an electrochemical signal response into a sinusoidal voltage response with very small amplitude relative to frequency. As a result, they can produce voltage wave and time-varying current, namely phase shift since wave. This current-voltage ratio (V(t)/I(t)) creates an impedance (Z), [192], [193]. In order to obtain the information of bio-recognition events occurring in the interface; mass transfer resistance (Rmt), charge transfer resistance (Rct), electrolyte resistance (Rel), double layer capacitance (Cdl) and Warburg impedance (W) should be investigated, [194]. From the Bode and Nyquist plots informations about EIS, [151]. In the Bode plot, the frequency is plotted relative to the overall impedance (|Z|). In the Nyquist chart; the real part of the impedance (Z') and the imaginary part of the impedance (-Z") are plotted (Figure 10E), [195]. Impedimetric sensors work very efficiently with their easy instrumentation, mass production of gain electrodes, miniaturization capabilities, and remote control of grafted sensors, [193].

Bhardwaj et al., [196], established a label-free impedimetric tool using GQDs for detecting the toxin namely aflatoxin B1 (AFB1) (Table 1). GQDs were prepared chemically according to the Hummer method, as shown in Figure 15, [197]. The sensor assembly is hydrothermally prepared and terminated via electrophoretic deposition (EPD) of GQDs on an ITO bonded glass electrode followed by immobilization of monoclonal AFB1-antibodies using EDC-NHS chemistry. The excellent electroconductivity and increased surface area of the GQD sensor enabled the detection of AFB1-contaminated maize samples over a wide linear range varying from 0.1 to 2.0 ng/ml with LOD=0.03 ng/ml. The effectiveness of this detection platform can last up to almost 7 weeks. This demonstrated the long-term storage stability and better reproducibility, [197].

* Figure 15 can be found in the Appendix section

Ganganboina and Doong, [198], developed a label-free antibody sensor using N,S–GQDs and Au-embedded polyaniline (Au-PANI) nanowires in the identification of CEA. In this study, N,S–GQDs act as bifunctional probes to immobilize anti-CEA and improve electrochemical performance. It is the deposition of Au-PANI on the platinum (Pt) electrode, followed by the lamination of N,S-GQDs to the Au-PANI surface via Au-thiol bond. Change in impedance of Au-PANI/N,S-GQDs in the presence of CEA-PANI/N suppressed the electron transfer by immune reaction between CEA and its specific antibody on the surface of S-GQDs. This unlabeled antibody sensor has a broad linear CEA concentration between 0.5 and 1000 ng/ml with LOD=0.01 ng/ml, [198]. Chowdhury et al., [199], designed an impedimetric immunosensor investigating the of N,S-GQDs and Au-PANI nanomaterials to measure hepatitis E virus (HEV). The WE were implanted with Au-PANI nanowires and N,S-GQDs with a self-assembly and interface polymerization strategy. Au-PANI/N,S-GQDs NC were covalently immobilized by anti-HEV, and by injection of the HEV antigen with an external electric pulse in the surface of the virus. This increase the susceptibility of the target virus. Anti-HEV and EIS biosensors were able to effectively distinguish various HEV genotypes from human serum and fecal samples of a HEV-infected monkey, with LOD value of 96.7 RNA copies/ml and a LOD of 0.8 fg/ml, respectively. This sensor is capable of showing the same sensitivity exhibited by real-time quantitative reverse transcription polymerase chain reaction (RT-qPCR), [199], in Figure 16, [200], [201].

* Figure 16 can be found in the Appendix section.

7 Recent Advancements in Microcystin Detection

In light of their distinct characteristics, including excellent sensitivity, speed, accuracy, and simplicity of application, biological sensors for monitoring MCs are currently the focus of extensive study, [202], [203], [204], [205].

Optical and electromagnetic resonance evaluations, as well as other transducer mechanisms, have been successfully applied as biological sensors for determining the presence of MCs, [206].

Biosensor innovations have proven feasible for field testing and fabrication of mobile devices. However, many modern sensors are restricted in monitoring speeds and cannot undertake real-time recognition, making it difficult to offer warnings regarding the reliability of water supplies for human consumption, [207]. To maintain potable water purity and public safety, a fast, affordable, persistent cyanotoxin identification device with advanced tracking and alarm capabilities needs to be devised.

Electrochemical biosensors utilize enzyme or antibody reactions to produce detectable electrical signals, while optical biosensors often use fluorescence or surface plasmon resonance for high sensitivity. Immunosensors, leveraging antigen-antibody interactions, provide specificity and rapid detection capabilities. Biosensors can be categorized into the following four primary categories based on the form of transducer used: electrochemical sensors with transducers that consist piezoelectric transducers, such as quartz crystal microbalance (QCM) biosensors, optical transducers, such as surface plasmon resonance (SPR) biosensors, and field-effect transistors are an instance; and thermometric sensors with transducers which use a susceptible thermistor to determine temperature and concentration of the analyte, [208].

Of the various types of label-free biosensors, electrochemical biological sensors have drawn the most attention due to their capabilities. Additionally, due to their ability to be miniaturized, these biosensors are crucial for numerous applications that require mobile biosensors A high-tech automated online optical biosensing system (AOBS) was developed for the rapid detection of MC-LR using programmed digital optical biosensors. The AOBS features six detector spots on the biochip, enabling the continuous assessment of six different pollutants in environmental samples. Biochemical conjugates with fluorescently labeled immunoglobulin are introduced to each site, allowing for the detection of MC-LR in the range of 0.2 to 4 µg/l, with a detection limit of 0.09 µg/l, [209].

This automated online biosensing device shares features with Total Internal Reflective Fluorescent (TIRF) sensors developed by the Gauglitz group, which also achieve a detection limit of 0.09 µg/l, [210].

This system utilizes fluorescent signal evaluation to compare MC-LR samples with a blank, demonstrating its effectiveness. This real-time assessment and ongoing surveillance system enhance the AOBS's accuracy and selectivity for detecting MC-LR in drinking water samples, offering significant potential for environmental monitoring and public health prevention.

The Automated Online Optical Biosensing System (AOBS) offers several advantages, including real-time and continuous monitoring capabilities, high sensitivity with a detection limit of 0.09 µg/l, and the ability to simultaneously assess multiple pollutants using six detector spots. Its automated workflow and fluorescent signal evaluation enhance accuracy, reproducibility, and efficiency in detecting MC-LR in environmental samples.

However, the system also has limitations, such as high installation and maintenance costs, the need for specialized technical expertise for operation and calibration, and potential interference from complex sample matrices that may affect detection accuracy. Despite these challenges, AOBS presents a promising tool for large-scale environmental and drinking water monitoring, [211].

The identification of the MCs at minimal doses in intricate composites may be accomplished with great sensitivity using immunological approaches. The use of antibodies that are monoclonal or polyclonal in enzyme-linked immunosorbent tests (ELISAs) is a highly accurate and precise technique for detecting MCs, [212].

However, it presents issues with cross-reaction between nodularin analogs and MCs. Immunosensors, which are more rapid, less expensive, mobile, extremely accurate, and specific, have been developed as a solution to this issue, [213].

The detection mechanism of immunosensors for Microcystin-LR (MC-LR) is based on the specific interaction between an antibody and the MC-LR antigen. Typically, monoclonal antibodies that recognize MC-LR are immobilized onto the surface of a sensor, such as an electrode or a quartz crystal. When a sample containing MC-LR is introduced, the toxin binds to the antibody, forming an antigen-antibody complex. This binding event leads to a measurable signal change—such as variations in current, impedance, frequency, or optical intensity—depending on the type of transducer used (electrochemical, piezoelectric, or optical). The signal intensity is proportional to the concentration of MC-LR in the sample, allowing for sensitive and selective

detection. Modern immunosensors often integrate nanomaterials like Au NPs or conductive polymers to enhance signal transduction and improve detection limits, making them effective tools for monitoring MC-LR in water bodies, [214].

8.AuNPs@MWCNTs/GQDs

The main mechanism of Au NPs@MWCNTs/GQDs with electrochemical sensor was shown in Figure 17.

* Figure 17 can be found in the Appendix section

8.1 Mechanism of AuNPs@MWCNTs

The images of the dried Au precursor on the substrate seen as Au NPs begin to form are given in Figure 18. The percentage of NPs is larger and appears out of circular shapes, [215]. The two images are on the same scale and correspond to two different moments in the time scale of the reaction. From these images, in the evaporative migration of the mixture, Au nuclei were first formed in the contact area of the substrate and in the droplets of the precursor solution. Figure 18most of the circular shapes have only one Au core. Then the Au crystals grow and spread over the entire surface. EDS analysis is 6% by weight Au concentration in the dried composite model. A tube bundle is assumed above or below the surface to accommodate the newly formed Au NPs. To obtain more information about the kinetics of this reaction; Low temperature experiments were carried out and the development of the system was followed in situ in the vacuum chamber of the SEM microscope, [215].

* Figure 18 can be found in the Appendix section

With the synergetic contributions of the two components; Au-MWCNT NCs have valuable features suitable for sensing applications (Table 1). While CNTs retain their electrical behavior, Au NPs can yield new binding sites by exerting the Localized Surface Plasmon Resonance (LSPR) phenomenon. Since Au-MWCNT hybrids is crucial in their capabilities. The integration sensing of Au particles into MWCNT bundles opens up new opportunities for ultra-sensitive detection of biomolecules electrically or optically using the plasmonic properties of Au. CNTs have only been used to enhance the surface plasmon resonance signal of the Au-coated glass plate in Biacore biosensing systems [215], [216].

Localized Surface Plasmon Resonant MWCNT bundles were developed by the synthesis of Au NPs on MWCNT and they were used in the detection of bovine growth hormone, as shown schematically in Figure 19; It was designed with the LSPR technique [215]. NCs films of Au-CNTs with controlled integration of Au NPs into CNTs are an exciting research area with their natural structures affecting their physical, chemical, electrical and optical properties simultaneously.

* Figure 19 can be found in the Appendix section

Au-MWCNT NCs are generally classified according to the shape of Au bonds; with and without binding NC s molecules, Au is bound covalently (for example, via Au-S bonds) or non-covalently by π-π stacking, hydrophobic forces, or by electrostatics interactions, [218], [219]. Pyrene derivatives are intermediates because the chromophore of the molecules can bind to the sidewalls of MWCNTs by π-π stacking interactions, while the alkylamine groups are covalently attached to Au NPs, [220]. Au NPs can be attached to the surface and ends of the sidewalls of thiol-terminated MWCNTs using an aromatic linker, [221], or dithiol- and amino intermediates, [222].

Au-CNT hybrid materials with both SWCNTs and MWCNTs were shyntethased. Various experimental approaches have been reported that solid state reactions at high temperatures can be occurred, [223], by physical evaporation (e.g. thermal and e-ray), [224], by deposition from the corresponding salt solutions in different surface coupling chemistries, [225], [226], [227], [228], [229], [230].

The low redox potential of CNTs allows the spontaneous formation of Au and Pt NPs on their surface without the use of a reducing agent, [231]. Spontaneous formation of Au NPs on the surface of CNTs was carried out by depositing the precursor solution directly onto the surface of CNTs with a silica substrate, [232]. A metal copper (Cu) substrate was used to retain and provide electrons for CNTs, [223], [232], [233], [234], and negatively charged CNTs played a role in facilitating the reduction, [235]. While the reduction is thought to occur spontaneously; it has actually been proven to be a hydrothermal method that must be activated by heating under pressure in an autoclave. It was also determined that the reaction time was long and the Au particles formed in the tubes were very large like 500 nm, [234]. In situ reduction of Au^{3+} in functionalized by SWCNTs has also been reported, and the process has been described as "self-reduction", [236].

From Figure 20,the high areal density of Au particles and clusters in the walls of the CNTs is noted, [237]. The particles are not isolated, they form clusters and large aggregates with small diffusion barriers and high interfacial energies (Figure 20b), [237]. Figure 20shows two main typical bands in Raman spectra of

Au-MWCNT rays, [237]: G band at 1580 cm^{-1} assigned to the in-plane vibration of the C-C bond, at a shoulder around 1604 cm^{-1} which is typical for imperfect graphite-like materials. At 1342 cm^{-1} the D band is activated by the presence of disorder in the carbon systems. Compared to the bands of MWCNTs, the bands vary little. It was detected a weak interaction between Au NPs and CNTs. Figure 20 isthe variation of the relative intensity of the two bands (I1580/I1342) depending on the area where the measurement is made. Some of the images have two well-defined bands with almost the same intensity and some of them can not be seen at 1342 cm^{-1} band. Apparent suppression of the D band is associated with a poor signal-to-noise ratio due to the high Au concentration at these locations (Zones 3 and 4), acting as scanning mirrors that reflect large amounts of excitation photons and prevent Raman scattering. The fact that spectra resulting from a high Au aggregation cause D-band suppression and G-band broadening by the reflectance effect of Au is proof. The slope line can be by fluorescence, scattering or luminescence of Au clusters. No SERS effect was detected in the prepared Au-MWCNT hybrids, [237].

* Figure 20 can be found in the Appendix section

8.2 The Electrochemical Measurements of the Fabricated Au Aptasensor

The 0.1 M MC-LR standard solution was diluted with PBS to different concentration gradients. 10 µl of MC-LR (0.0001–10 nM) was dropped onto the LIG-Au electrode, incubated for 20 min and then washed with deionized water. Then, it tests and determines the electrochemical characterization of the aptasensor in 5 mM $Fe(CN)_6^{3-/4-}$ solutions containing 0.1 M KCl; A PalmSens handheld electrochemical analyzer was used (Figure 21), [238]. The SWV parameters are set to 15 Hz frequency and 0.05 V amplitude - 0.6 V–0.8 V. The current signal was recorded with PSTrace 5.9. The varying value of the peak current signal observed before and after incubation of the MC-LR as ΔI; describes the variation of quantitative MC-LR binding. - CV was conducted with a scanning rate of 50 mV/s between 0.6 and 0.8 V. The EIS was analyzed at an open-circuit potential with amplitude of 0.01 V and a frequency range of 1–100000 Hz.

* Figure 21 can be found in the Appendix section

Obtain AuNPs/Ag_2S modified to fluorine doped tin oxide and label-free MC-LR biosensors; $[Ru(NH_3)_6]^{3+}$ to Au disk electrodes and decorated graphene to screen-printed carbon electrodes were introduced. LOD=7 pM, LOD=9.2 pM and LOD=1.9 pM, respectively, [6], [238], [239]. This enables the preparation of label-free MC-LR biosensors; although, it only requires conversion of functionalized nanomaterials into electrodes, their LOD is much worse than that of sensors prepared by probe labeling or competitive strategies, [14], [240]. It can detect the electrodes used; Substrates such as glassy carbon and Au discs are also expensive materials. The developed label-free biosensors charge specific recognition molecules of MC-LR; have made additional modification of functional nanomaterials on the electrodes mandatory.

An immunosensor for MC-LR is from a family of water pollutants primarily formed on a stable heptapeptide produced by common cyanobacteria, [70]. The GC electrodes were modified with GO and AuNPs and grafted with 2,5-di-(2-thienyl)-1-pyrrole-1-(p-benzoic acid) to immobilize MC-LR antibodies. IL (1-isobutyl-3-methylimidazolium bis(trifluoro-methanesulfonyl)imide) is dropped onto the electrode surface and the MC-LR antibody is covalently bonded to the conductive polymer film. Electrochemical detection with DPV in the range of 10^{-16}–8×10^{-15} M using $Fe(CN)_6^{3-/4-}$ added to the solution was performed, with an extremely low LOD=4×10^{-17} M (4×10^{-17} g/ml) were measured, [70]. Also, an immunosensor for aflatoxin B1 has been reported, which measures charge transfer resistance in the linear range of LOD=1 fM and 3.2 fM to 0.32 pM as measured by EIS, similarly, [241].

It has also been used to detail the exciting properties of various other carbon-based nanostructures, such as CNHs, [42], [43], graphene, [6], or graphene combined with carbon nanospheres (CNSs), [71], or Au NPs, [70]. Electrochemical immunosensors or aptasensors have been performed in the detection of MC-LR. LODs ranged from 0.18 ng/l to 368 µg/l. The best LOD values were found by Eissa et al., [70], with screen-printed electrodes modified with aptamer-functional graphene; The aptasensor signal resulting from the interaction between aptamers and MC was measured by SWV. The aptasensor was also applied to the analysis of added tap water and fish samples showing good recovery percentages.

9 Electrochemical Biosensors for Cyanotoxins

Various electrochemical biosensors for cyanotoxins (eg MCs) have been obtained from a number of comparative scientific studies and reports;

1. Tag-based immune sensors,
2. Unlabeled immune sensors,

3. DNA and aptasensors.

9.1 Label-Based Immunosensors

Label-based immunosensors are a common method used in electrochemical biosensing of cyanotoxins (Table 1). A common format for the detection of cyanotoxins; competitive (direct or indirect) transduction and rarely sandwich transduction. One of the most important advantages of enzyme tags is the amplification of the signal by producing the enzyme product in the presence of a substrate. HRP is used as the most common enzyme for electrochemical MC detection. In the use of nanotechnology in the electrode support or label, HRP can further amplify the electrical signal and can be achieved with ultra-sensitive detection, [242]. Successful direct competitive detection of a substrate using a biocatalytic precipitation reaction with H_2O and HRP; It has been reviewed by Hou et al., [243]. It was modified with Au NPs and stock MC-LR on a modified glassy carbon electrode. After competition between MC-LR and MC-LR immobilized in the analyte, the mAb-HRP conjugate was allowed to accelerate the oxidation of 4-chloro-1-naphthol to the substrate precipitate form.

The impedimetric detection of the MC-LR is based on the mass loading of the precipitate on the electrode. Increasing enzyme precipitation acted as a label in increasing impedance signal with decreasing MC-LR concentration. Biosensor, MC-LR, LOD=4 pg/ml; Specificity studies were limited only between the MC-LR and MC-RR variants, [244]. Similar LOD=4 pg/ml, Gan et al., [245] In an indirect competition analysis, double amplification was performed with HRP-secondary antibody conjugate based on CNT on Co-silicate as support and magnetic core-shell NCs as label. It consists of iron (II, III) oxide (Fe_3O_4) nanoclusters/polydopamine/Au NPs. DPV detection with Au nanorods (NRs) as electrode support and another HRP-based detection using MoS_2 were measured with LOD=5 pg/ml, [65], [66], [67]. A successful design of HRP-labeled competitive immunosensors has been performed, [245]. An ITO modified electrode was designed using nanomaterials, antibodies and DNA molecules after ringing in MC-LR detection with LOD=7 pg/ml.

While graphene with magnetic properties increases the electrode surface area, Au NRs with circular DNA conjugation in the form of rolling circle replication increase the impedance signal. After adding 2 mM H_2O_2 to a 1 mM hydroquinone solution, a calibration curve based on CV measurements was drawn, [245]. A DPV biosensor for the MC-LR fixed with chitosan on a glassy carbon electrode; Graphene sheets and carbon nanospheres conjugated with mAbs were used for signal amplification. Optimization steps; It is very important to measure the incubation time, H_2O_2 concentration and H_2O_2 / Ab ratio, LOD=16 pg/ml using a highly sensitive indirect competitive immune sensor, [71].

SWCNHs have been studied on a GCEs by Zhang et al., [42], and Zhang et al., [43]. Determination of indirect competitor is based on HRP-H_2O_2 reaction, product precipitate concentration was observed by DPV. The cone-shaped ends of the SWCNHs enhanced the immobilization ability of the MC-LR and the minimum detection was measured at 30 pg/ml. Fabrication reproducibility verified by interassay; however, the relative standard deviation ranges from 5.90% to 7.70%, [42], [43]. The N_2-doped graphene hydrogel SPE support was regulated by the self-polymerization of dopamine (PDA) on GO and a hydrothermal reaction. HRP and secondary antibodies were conjugated with Au NPs captured on porous CNSs using thionine (TH) in an electron medium. This dual enhanced biosensor recorded LOD=9.7 pg/ml, [244].

Signal amplification has been developed with Au NCs providing electron transfer. Two successful strategies have been established to amplify a biosensor for the MC-LR. A labeled competitor with MC-LR pg/ml was investigated using molybdenum disulfide (MoS_2) nanolayers, DPV and LOD=0.3 containing gold nanoclusters (MoS_2/Au NCs) and Au core/Pt shell NPs (Au@Pt NPs), [246]. Developed in a competitive immune sensor labeled using a GC electrode modified with CNFs and Au NPs in a signal label with LOD=1.68 pg/ml and a broad range of linear MC-LR concentrations from 0.0025 to 5 ng/ml, [69]. In both experimental studies, very low LODs were reported as calculated with a signal-to-noise ratio (S/N) of 3.

DNAzyme and its conjugates may replace HRP in enzyme-free electrochemical immuno-based detection of MC-LR. Tian et al., [247], designed a similar enzyme-based detection using DNAzyme, which mimics horseradish peroxidase in CNTs. DNAzyme-conjugated MC-LR on CNTs acted as detection tag. The sensor is based on the catalytic reduction of H_2O_2 and has LOD=2.31 pg/ml. Another enzyme-free approach has been presented by Gan et al., [248].

An alternative to enzyme-type amplification, quantum dots (QD) was tested in an electrochemical immunosensor in an indirect MC-LR detection. Cadmium ions (Cd^{2+}) were released from QDs after antibody-QD binding to different concentrations of MC-LR in the prepared microtiter plate wells. The semiconductor nanocrystal contains a zinc sulfide (ZnS) and a cadmium selenide (CdSe) core encapsulated in the polymer shell. Au electrode and

SWSV were used to measure the acidic dissolution of cadmium ions (Cd^{2+}). LOD=99 pg/ml after optimization steps, [249].

9.2 Label-Free Immunosensors

Electrode supports in unlabeled immune sensors have an important role in the ultra-sensitive detection of MC-LR (Table 1). Graphene-Au NCs conducting polymer holding carboxyl groups (polyDPB), Au NPs layer and finally ionic liquid (IL) layer were developed by Ruiyi et al., [70], as GCE electrode support. This multilayer GCE modified electrode, can be able to detect MC-LR with a very low value of LOD=0.000037 pg/ml. The experimental working range is limited to 1×10^{-7} – 8×10^{-8} ng/ml. Yang research group applied CV, EIS and DPV measurements to examine biosensor properties with two different approaches, [250]. A label-free and antibody-based electrochemical biosensor was developed using Au NPs/silicone template/MB/chitosan NCs. The resulting LOD=100 pg/ml, [250].

In the manufacture of a G4-polyamidoamine (PAMAM) dendrimer and Ag nanocubes, the LOD was significantly reduced by measuring 17 pg/ml, [251]. Immuno-field-effect transistor-based biosensors with SWCNTs containing IDEs are promising for MC-LR detection, [68]. At displacement of immobilized antibodies, the FET immunosensors were able to electrochemically register MC-LR with LOD=0.6 pg/ml and high specificity, [68]. Sun et al., [252], made two successful attempts to develop electrochemical impedimetric biosensors for MC-LR. An Au electrode modified with Au NPs was used to increase the surface area. An antibody-based direct assay was performed. Different possible effects on sensor optimization have been investigated. Interestingly, the effect of Au NPs on particle size was evaluated and 15 nm was used during manufacture to provide ultra-low detection of LOD=18.2 pg/ml MC-LR, [252]. As an alternative to Au NPs, IL-functionalized MWCNTs at room temperature have been used. Three room temperature ILs were tested, a more hydrophobic room temperature IL 1-amyl-2,3-dimethylimidazolium hexafluorophosphate was used in the development of the MC-LR biosensor. A sensor with long-term stability and high specificity reaching LOD=1.7 pg/ml was designed, [253], [254].

Vogiazi and colleagues synthesized carbon nanomaterials such as graphene and CNTs to develop carbon-based WEs, [255]. They effectively used an impedimetric, competitive, label-free electrochemical bioassay for the detection of MC-LR. First, MWCNT probes were subjected to alkaline functionalization to introduce sites required in MC-LR immobilization. It was then used for competitive determination in MC-LR samples using mAbs. The detection limit is LOD=40 pg/ml, [64]. 3-D foamed graphene was applied with WE to achieve a similar detection limit of LOD=50 pg/ml, [65], [66], [67]. Label-free flow biosensors for cyanotoxins are just a few. It was measured a very sensitive value such as LOD=0.007 pg/ml with capacitive immune sensors in the detection of MC-LR. An Au electrode was modified with thiourea SAM and silver nanoparticles (Ag NPs), [65], [66], [67].

Antibodies were immobilized on Ag NPs and direct label-free detection was performed, [256]. Dawan et al., [257], compared flow capacitive immune sensor with and without Ag NPs. The immunosensor performance was tested using Au NPs and resulted in a similar linearity to the Ag NPs-based immunosensor, [257]. The development of a miniature potentiometric STX biosensor using anti-STX-containing lipid films on graphene nanolayers with a detection limit of 1 ng/ml has been reported recently. Adequate selectivity for detection over a wide range of toxin concentrations ranging from LOD=299 pg/ml to LOD=299 ng/ml was detected over a time period of about 5 to 20 min, [258].

9.3 DNA and Aptasensors

9.3.1 Aptasensors

Aptasensors for the detection of cyanotoxins have been developed recently (Table 1). The Chen research group developed the first aptamer-based impedimetric biosensor, [259], to reduce the detection limits of previously reported sensors, [16]. Lower limit of detection was measured for aptamer immobilization and optimization of a gold electrode for MC-LR detecton at a LOD of 18 pg/ml between the MC-LR and MC-RR variants, [259]. The application of SWV and aptamer-based biosensors for MC-LR has been studied by the Zourob research group, [6], [76]. Selected aptamers like MC-LR, MC-Leucine-Alanine (LA) and MC-Tryptophan-Arginine (YR) were evaluated for their ability to select the perfect one. The three ssDNA sequences segregated between selected aptamers with low dissociation constants and high affinity were (i) MC-LR, (ii) MC-LR and MC-LA, (iii) MC-LR, MC-LA and MC. For direct MC detection based on Au, it was run at a low concentration of LOD=10 pg/ml, [76], by using the π–π stacking interactions of the aptamer adsorbed on graphene-based SPEs. They reported a biosensor that can successfully reduce the LOD to 1.9 pg/ml, [6].

9.3.2 DNA Biosensors

Several genosensors and DNA hybridization-based sensors have been designed for cyanobacteria detection (eg Microcystis species), [260], [261], [262], [263], [264], (Table 1). In the detection of MC-LR; It was studied with an electrochemical biosensor based on calf thymus DNA. The conformational changes of the calf thymus proved to be a good alternative electrochemical method for the detection of label-free MC-LR. However, the selectivity for MC-LR decreased in the presence of high concentrations of MC-RR, [31]. Numerous sequence design and detection approaches in DNA-based electrochemical biosensing and extensive literature studies have also been reported in the literature, [265].

10 Performance Analysis of AuNPs@MWCNTs/GQDs

In the detection performance of MC-LR via AuNPs@MWCNTs/GQDs different concentrations of MC-LR was investigated using DPV under optimized conditions. The current response of the sensor gradually increased with increasing concentration of MC-LR solution adsorbed to AuNPs@MWCNTs/GQDs (Figure 22).

* Figure 22 can be found in the Appendix section

The peak currents showed a good linear correlation with the logarithm of the concentrations in the range of 0.08–2.0 μg/l of MC-LR. The linear regression equation was I (μA)=590.93 + 78.02 logC (R^2=0.9860). The limit of detection (LOD) was calculated as 0.0027 μg/l (S/N=3.0). A detailed comparison of the LOD and linearity range of the present sensor and other reported methods for the MC-LR sensing has been made and concluded in Table 2.

* Table 2 can be found in the Appendix section

The present sensor showed a super sensitive sensing performance in the determination of MC-LR and the linear range including the limiting value for MC-LR in waters (1.0 μg/l).

11 The Response Mechanism of MC-LR on the Sensor

In order to characterize the nature of the electrode process, the cyclic voltammetry (CV) of MC-LR on the MIP sensor with different scan rates ranging from 25 to 150 mV/s were detected. In theory, the linear relationship of current (I_p) vs. scan rate (v) and current (I_p) vs. the square root of the scan rate ($v^{1/2}$) indicates the electrode process controlled by the adsorption and diffusion mechanism, respectively, [251]. I_{p1} vs. v (R^2=0.9797) and I_{p1} vs. $v^{1/2}$ (R^2=0.9763), together with I_{p2} vs. v (R^2=0.9676) and I_{p2} vs. $v^{1/2}$ (R^2=0.9680), have good linear relationships. This reveals that both the oxidation process and reduction process obey the adsorption mechanism as well as the diffusion mechanism. In addition, linear fitting of log I_{p1} vs. log v (R^2=0.9910) and log I_{p2} vs. log v (R^2=0.9842) yielded linear regression equations with slopes of 0.71 and 0.72, respectively. It is demonstrated that a slope lies between 0.5 and 1.0 follows an adsorption–diffusion mechanism, [266]. Therefore, the electrode process of MC-LR on the MIP sensor is controlled by a mixed adsorption–diffusion process. Additionally, the reaction mechanism of MC-LR on the MIP sensor was inferred by exploring the relationship between peak potential (E_p) and scan rate (v). In an irreversible reaction, the oxidation potential shifts to the positive direction and the reduction potential shifts to the negative direction with the increase of scan rates, [266]. There is good linear relationship between E_{p1}, E_{p2}, and lnv with a slope of 0.042 and 0.047, respectively.

According to the Laviron law, the relationship between E_p and v should follow Eq. (3) in an irreversible electrode reaction, [267]. Where α is the transfer coefficient, n is the number of electrons transferred, v is the scan rate (V/s), E_p is the redox potential. K_s, T, R, and F are the standard rate constant of the reaction, absolute temperature (298°K), ideal gas constant (8.314 J/(mol.K)$^{-1}$), and Faraday constant (96,485 C/mol), respectively. Thus, the value of RT/αnF is equal to 0.042 and 0.047, respectively. By calculation, it is estimated that the number of transferred electrons in both oxidation (P1) and reduction (P2) is 1 (n_1=n_2=1), and the transfer coefficient values are 0.70 (α_1) and 0.63 (α_2), respectively.

$$E_p = E^0 - \frac{RT}{\alpha nF} ln \frac{RTk_s}{\alpha nF} + \frac{RT}{\alpha nF} lnv \quad (3)$$

Furthermore, the CVs of MC-LR on the surface of the MIP/AuNPs@MWCNTs/GQDs/GCE with different pH values of phosphate buffer ranging from 5.0 to 7.0 were detected. The potential shifted negatively with the increase of pH value, indicating that a certain number of protons were involved in the oxidation reaction, [268]. According to the Nernst equation (Eq. 4), the relationship between E_p and pH should follow the equation for an oxidized electrode reaction: Red - n e^- - mH^+ → Ox.

$$E_p = E_0 + \frac{RT}{nF} ln\left(\frac{[O_x]}{Red}\right) - \left(\frac{2.303mRT}{nF}\right) pH (4)$$

The oxidation and reduction peak potential can be expressed as E_{p1}= - 0.093pH + 1.60 (R^2=0.9806), and E_{p2}= - 0.052pH + 0.75 (R^2=0.9938), respectively. This indicates that the numerical proportions of protons and electrons transferred in the oxidation reaction and reduction reaction and their values were 2 and 1 (m_1/n_1=2, m_2/n_2=1), respectively, [269]. Therefore, the electrode reaction of MC-LR on AuNPs@MWCNTs/GQDs can be concluded to the irreversible electrical process of losing 1 electron and 2 protons in the oxidation process (P1) and gaining 1 electron and 1 proton in the reduction process (P2).

12 Recent Advances and Future Trends

Carbon-based nanomaterials are widely used in the production of biosensors. SWCNTs, [247], [270], SWCNHs, [42], [43] and CNSs, [71], are included in electrode modifications or play a tag role in signal amplification. MWCNTs [64] and 3-D graphene, [65], [66], [67], are widely used as true WE. The first successful MWCNT-based electrochemical biosensor was developed by Han et al., [64]. Recent advances in the internal structure of graphene by incorporating a new form of graphene, 3-D graphene, have led to efficient low-LOD electrochemical sensors, [65], [66], [67]. This new form of graphene has very important advantages such as high surface area, conductivity and repeatability, [271]. Recently, there has been an increasing interest in hybrid materials with better electrical, chemical and physical properties than base materials. Recently, it has been studied with a hybrid material of 3-D graphene and carbon nanofiber, which provides a larger surface area because it uses the nanostructure of both carbon nanomaterials, [272]. Thanks to its significant advantages such as high conductivity and large surface area, this material is a potential candidate for sensing electrodes. Some progress has also been made on alternatives to single-layer graphene electrodes with zero band gap. The use of semiconductor metal chalcogenide-based atomic thin electrodes for biosensing has been studied recently, [273]. Lv et al., [274], recently reported a new MC-LR sensor using a nanoparticle-infused MoS_2 nanolayer platform, while another group, [275], used a tungsten disulfide (WS_2) nanolayer as a transducer for the fabrication of a MC-LR sensor. Another relatively new approach for artificial biosensing electrode material is MIP, [276]. Recently, the development of a high efficiency photoelectrochemical sensor with molecularly imprinted polymer (MIP) polypyrrole/Cu_2O film with LOD=0.23 pg/ml has been noted, [277]. Another MIP-based sensor with titanium dioxide (TiO_2)/CNT nanostructure has also been reported to have an LOD in the pg/ml range, [119].

Interestingly, some recent developments serve similar or different purposes; It is intended to combine carbon and metallic nanomaterials, [242]. To give an example from the literature, modifications of glassy carbon electrodes containing electrodeposited well-dispersed graphene oxide-Au NCs can be shown, [70]. This combination acted as a very good electrode support, which had a synergistic effect on the overall performance of the sensor. Another combination of nanomaterials has also been used for different purposes. A biosensor using nanomaterials-antibody conjugations and a sandwich assay has been developed by Wei et al., [15]. The conductivity and surface area are increased with graphene modified electrodes, providing detection with an antibody-PtRu alloy tag. An important advantage is that the sensor has outstanding stability for up to 2 months, [15].

The application of variations in nanomaterials will undoubtedly influence and support the production of a new generation of reliable sensors in terms of electron transfer, bioactive agent immobilization and overall stability. Developments related to non-metallic magnetic monodisperse spherical particles (beads) are also commonly encountered in literature studies. Well-known magnetic beads have also been used frequently lately as electrode coating support, [142], [143], [278], or label, [279]. The very important advantages of magnetic beads such as ease of use and a wide variety of magnetic bead surface modifications for immobilization of biorecognition molecules have made them popular for use in electrochemical biosensors. Magnetic beads with hydrophilic surfaces are particularly suitable for nucleic acids providing reproducible magnetic separation. For these reasons, magnetic beads are widely used in aptamer selection and biosensing, [142], [143], [278], [279], [280], [281], [282].

In our opinion, magnetic beads in aptamer-based biosensors for small toxins will be used and developed in more areas and play a role in more complex analysis. Chen et al., [283], a sensitive noncompetitive, open sandwich Enzyme-linked Immunosorbent Assay (OS-ELISA) was developed for the quantification of MCLR Microcystin with leucine and arginine (MCLR). The hepatotoxic toxin produced by cyanobacteria present in

Water courses that causes cell death and tissue necrosis at high exposure levels. OS-ELISA is based on the principle of antigen-driving interaction enhancement between variable regions of an antibody. The genes for the variable regions of antibody 3A8

against MCLR were used to construct the phage display vector pDong1/Fab(3A8) to prepare assay elements. Another format of OSELISA that used purified Maltose Binding Protein-fused VL and VH-phage showed a lower LOD of 85 pM MCLR.Using the developed assay, the recovery rates for samples of lake or river water spiked with MCLR and were found to range from 95.50% to 116.40%, suggesting that the assay has good potential to be used as a monitoring tool for MCLR in nature.

Fan et al., [282], developed environmentally friendly quantitative analytical electrodes for the determination of microcystin-LR (MC-LR) in environmental water. A simple, mask-free, and one-step method based on laser-induced graphene (LIG) technology is designed for the fabrication of (3D) graphene electrodes integrated with gold nanoparticles (AuNPs). The 3-electrode system with AuNPs-modified graphene was prepared directly by overlaying gold leaf on the polyimide (PI) film followed by patterned CO_2 laser irradiation. The reference electrode region was then uniformly coated with Ag/AgCl paste, and the working electrode was functionalized with the aptamer through Au-S self-assembly and bonding to obtain a label-free MC-LR aptasensor. The developed MC-LR aptasensor has a detection limit of 0.053 pM and a linear range from 0.1 pM to 10 nM. The fabricated aptasensor presents good stability, reproducibility, specificity and detection in real samples. These sensors show great promise as a low-cost, simple and portable approve for label-free detection MC-LR in environmental samples.

Li et al., [284], A label-free electrochemical biosensor was constructed to detect linear microcystin-LR (L-MC-LR) with high sensitivity. Degradation enzyme MlrB was used as recognition element for specific recognition of L-MC-LR. The electrode was modified with –COOH functionalized multi-walled carbon nanotube toincrease the specific surface area and improve the conductivity, which was then applied to immobilize MlrB. The electrochemical signal was changed withthe reaction between MlrB and L-MC-LR, which was recorded by using square wave voltammetry. The electrochemical biosensor showed superior sensitivity,with a dynamic range of 1 pg/mL to 100 ng/mL and a detection limit of 0.127 pg/mL. Moreover, the fabricated electrochemical biosensor exhibited excellent specificity toward L-MC-LR in real water samples.The concentrations of spiked L-MC-LR were 0.100, 5.00, 50.0 ng/mL, and the recovery rates were 95.0–104% with relative standard deviation (RSD) of 0.900–2.30% and 74.0–93.0% with RSD of 2.30–3.50% in lake water and tap water, respectively. Furthermore, the selectivity, reproducibility, and stability demonstrated the potential of degradation enzymes as recognition element in detection of cyanotoxins.

Antonyraj et al., [285], investigated the state-of-the-art immunosensor that immobilizes MC variants targeted by monoclonal antibodies onto nanostructured substrates allows for fast and selective detection of MC. Incorporating nanomaterials such as gold nanoparticles and carbon nanotubes, the detector improves the effectiveness of the signal, allowing it to identify as low as 0.05 ppb with a response time of <10 min. With its stable performance over time, this type of sensor is excellent for field deployment and ongoing surveillance. The integration of novel technologies and nanomaterials is highlighted the sensitivity, accessibility, and exchange of data in real-time. Significant innovations in environmental monitoring and public health protection are very important. To protect ecosystems and public health, next-generation biosensing technologies could decrease MC contamination in water bodies.

Biosensor-based methods have emerged as powerful analytical tools with enhanced performance for MCs detection and quantification over conventional methods. A detailed list of some analytical methods reported for MCs detection in water is provided in Table 3.

* Table 3 can be found in the Appendix section

Table 4. shows some of various types of biosensors used for MC-LR detection in drinking water and other ecosystems

* Table 4 can be found in the Appendix section

13 Conclusions

MCs are secondary metabolites produced by some cyanobacteria, a stable class of cyclic heptapeptide toxins in the environment. MCs, by entering water sources and causing contaminated aquatic environments, can lead to a wide variety of negative health problems in humans, animals, and plants. To isolate MCs from polluted water environments very well effective methods and measurement techniques should be taken into consideration.

Electrochemical biosensors can be widely preferred for routine quantitative screening of MC-LR and water monitoring at the point of use mostly due to their high portability After optimization of water samples, MS-based methodologies are the only accepted and validated analytical techniques that can distinguish between variants or transformation products.

Measuring low concentrations of MCs variants using electrochemical biosensors is one of the biggest challenges to overcome. Development of selection of aptamers or other high-affinity biomolecules in certain MCs variants is particularly hopeful. When the innovative signal transmission technology is combined with micro and nanosystems with multimicrofluidic channels, electrochemical biosensors will enable specific variant detection even at very low concentrations. The interdisciplinary field of electrochemical biosensors is advancing rapidly and the emergence of new sensor applications or technologies in multicyanotoxin analysis is eagerly awaited to aid real-time toxicity assessment.

For the detection of MC-LR; MWCNTs, GQDs, and AuNPs were used as sensor modification materials to construct a three-dimensional conductive network, which enhanced the sensitivity of the sensor. Furthermore, a new molecularly imprinted electrochemical sensor with three-dimensional structure AuNPs@MWCNTs/GQDs was used in the detection of MCs. Electrochemical sensor production for MCs measurement using AuNPs@MWCNTs/GQD NCs is the newest and most successful work.

The synergy between the selected dual functional monomers enriched the recognition sites of the sensor and enhanced the affinity for the targets, which improved the selectivity of sensor. Employment of the segment template ensures the sensor's recognition characteristic of target and cuts down the cost. The recognition reaction of MC-LR on the developed sensor is an irreversible electrochemical oxidation reaction to detect the total amount of MC-LR.

In the near future, breakthroughs in electrochemical biosensors will certainly bring great advantages and advances to rapid cyanotoxin detection and efficient drinking water quality control, providing people with clean and safe drinking water. Many other nanomaterials not presented in electrochemical sensors also have applications, but the information provided should enable researchers to develop viable electrochemical sensors. To this end, it is hoped that the in-depth study and discovery of nanomaterial applications will be encouraged.

Acknowledgement:
Experimental analyzes in this study were performed at the Laboratories of the Canada Research Center, Ottawa, Canada. The authors would like to thank this body for providing financial support.

References:

[1] R. P. Rastogi, R. P. Sinha, A. Incharoensakdi, The Cyanotoxin-Microcystins: Current Overview, Reviews in Environmental Science and Bio/Technology, Vol.13, 2014, pp. 215–249.

[2] L. Díez-Quijada, A. I. Prieto, R. Guzmán-Guillén, A. Jos, A. M. Cameán, Occurrence and Toxicity of Microcystin Congeners other than MC-LR and MC-RR: A Review, Food and Chemical Toxicology, Vol.125, 2019, pp. 106–132.

[3] M. Lotierzo, R. Abuknesha, F. Davis, I. E. Tothill, A Membrane-Based ELISA Assay and Electrochemical Immunosensor for Microcystin-LR in Water Samples, Environmental Science & Technology, Vol.46, 2012, pp. 5504–5510.

[4] H. E. Plaas, H. W. Paerl, Toxic Cyanobacteria: A Growing Threat to Water and Air Quality, Environmental Science & Technology, Vol.55, 2020, pp. 44–64.

[5] C. M. Schreidah, K. Ratnayake, K. Senarath, A. Karunarathne, Microcystins: Biogenesis, Toxicity, Analysis, and Control, Chemical Research in Toxicology, Vol.33, 2020, pp. 2225–2246.

[6] S. Eissa, A. Ng, M. Siaj, M. Zourob, Label-Free Voltammetric Aptasensor for the Sensitive Detection of Microcystin-LR Using Graphene-Modified Electrodes, Analytical Chemistry, Vol.86, No.15, 2014, pp. 7551–7557.

[7] WHO, Cyanobacterial Toxins: Microcystin-LR in Drinking-Water Background Document for Development of WHO Guidelines for Drinking-Water Quality; World Health Organization: Geneva, Switzerland, 1998.

[8] F. M. Buratti, M. Manganelli, S. Vichi, M. Stefanelli, E. Funari, Cyanotoxins: Producing Organisms, Occurrence, Toxicity, Mechanism of Action and Human Health Toxicological Risk Evaluation, Archives of Toxicology, Vol.91, 2017, pp. 1–82.

[9] M. Giddings, R. Aranda-Rodriguez, G. Yasvinski, S. B. Watson, R. Zurawell, Canada: Cyanobacterial Toxins: Drinking and Recreational Water Quality Guidelines, In Current Approaches to Cyanotoxin Risk Assessment, Risk Management and Regulations in Different Countries; Federal Environment Agency (Umweltbundesamt): Dessau-Roßlau, Germany, 2012.

[10] B. Greer, S. E. McNamee, B. Boots, L. Cimarelli, D. Guillebault, K. Helmi, S.

Marcheggiani, S. Panaiotov, U. Breitenbach, R. Akçaalan, L. K. Medlin, K., Kittler, C. T. Elliott, K. Campbell, A validated UPLC–MS/MS method for the surveillance of ten aquatic biotoxins in European brackish and freshwater systems, Harmful Algae, Vol.55, 2016, pp. 31–40.

[11] S. Gkelis, T. Lanaras, K. Sivonen, Cyanobacterial Toxic and Bioactive Peptides in Freshwater Bodies of Greece: Concentrations, Occurrence Patterns, and Implications for Human Health, Marine Drugs, Vol.13, 2015, pp. 6319–6335.

[12] M. Campàs, J.-L. Marty, Highly Sensitive Amperometric Immunosensors for Microcystin Detection in Algae, Biosensors & Bioelectronics, Vol.22, 2007, pp. 1034–1040.

[13] F. Long, M. He, A. N. Zhu, H. C. Shi, Portable optical immunosensor for highly sensitive detection of Microcystin-LR in water samples. Biosensors & Bioelectronics, Vol.24, 2009, pp. 2346–2351.

[14] L. Fan, J. J. Huang, J. Liao, Competitive Smartphone-Based Portable Electrochemical Aptasensor System Based on An MXene/cDNA-MB Probe for the Determination of Microcystin-LR, Sensors & Actuators, B: Chemical, Vol.369, 2022, 132164.

[15] Q. Wei, Y. Zhao, B. Du, D. Wu, Y. Cai, K. Mao, H. Li, C. Xu, Nanoporous PtRu Alloy Enhanced Nonenzymatic Immunosensor for Ultrasensitive Detection of Microcystin-LR, Advanced Functional Materials, Vol.21, No.21, 2011, pp. 4193–4198.

[16] P. Tong, S. Tang, Y. He, Y. Shao, L. Zhang, G. Chen, Label-Free Immunosensing of Microcystin-LR Using a Gold Electrode Modified with Gold Nanoparticles, Microchimica Acta, Vol.173, No.3-4, 2011, pp. 299–305.

[17] L. Wang, W. Chen, D. Xu, B. S. Shim, Y. Zhu, F. Sun, L. Liu, C. Peng, Z. Jin, C. Xu, N. A. Kotov, Simple, Rapid, Sensitive, and Versatile SWNT−Paper Sensor for Environmental Toxin Detection Competitive with ELISA, Nano Letters, 9(12), 2009, pp. 4147–4152.

[18] J. Zhang, J. Lei, R. Pan, C. Leng, Z. Hu, H. Ju, In Situassembly of Gold Nanoparticles on Nitrogen-Doped Carbon Nanotubes for Sensitive Immunosensing of Microcystin-LR, Chemical Communications, Vol.47, 2011, pp. 668–670.

[19] A. Garcia, X. Cayla, J. Guergnon, F. Dessauge, V. Hospital, M. P. Rebollo, A. Fleischer, A. Rebollo, Serine/Threonine Protein Phosphatases PP1 and PP2A are Key Players in Apoptosis, Biochimie, Vol.85, 2003, pp. 721–726.

[20] C. MacKintosh, K. A. Beattie, S. Klumpp, P. Cohen, G. A. Codd, Cyanobacterial Microcystin-LR is a Potent and Specific Inhibitor of Protein Phosphatases 1 and 2A from Both Mammals and Higher Plants, FEBS Letters, 264, 1999, pp. 187–192.

[21] J. T. Maynes, H. A. Luu, M. M. Cherney, R. J. Andersen, D. Williams, C. F. Holmes, M. N. James, Crystal Structures of Protein Phosphatase-1 Bound to Motuporin and Dihydromicrocystin-LA: Elucidation of the Mechanism of Enzyme Inhibition by Cyanobacterial Toxins, Journal of Molecular Biology, Vol.356, 2006, pp. 111–120.

[22] M. Craig, H. A. Luu, T. L. McCready, D. Williams, R. J. Andersen, C. F. Holmes, Molecular Mechanisms Underlying the Interaction of Motuporin and Microcystins with Type-1 and Type-2A Protein Phosphatases, Biochemistry and Cell Biology, Vol.74, 1996, pp. 569–578.

[23] A. Campos, V. Vasconcelos, Molecular Mechanisms of Microcystin Toxicity in Animal Cells, International Journal of Molecular Sciences, Vol.11, 2010, pp. 268–287.

[24] Y. Xing, Y. Xu, Y. Chen, P. D. Jeffrey, Y. Chao, Z. Lin, Z. Li, S. Strack, J. B. Stock, Y. Shi, Structure of Protein Phosphatase 2A Core Enzyme Bound to Tumor-Inducing Toxins, Cell, Vol.127, 2006, pp. 341–353.

[25] W. Y. Fu, J. P. Chen, X. M. Wang, L. H. Xu, Altered Expression of p53, Bcl-2 and Bax Induced by Microcystin-LR in Vivo and in Vitro, Toxicon: Journal of the International Society on Toxinology, Vol.46, 2005, pp. 171–177.

[26] R. E. Guzman, P. F. Solter, M. T. Runnegar, Inhibition of Nuclear Protein Phosphatase Activity in Mouse Hepatocytes by the Cyanobacterial Toxin Microcystin-LR, Toxicon: Journal of the International Society on Toxinology, Vol.41, 2003, pp. 773–781.

[27] S. S. Lin, M. C. Bassik, H. Suh, M. Nishino, J. D. Arroyo, W. C. Hahn, S. J. Korsmeyer, T. M. Roberts, PP2A Regulates BCL-2 Phosphorylation and Proteasome-Mediated Degradation at the Endoplasmic

Reticulum, Journal of Biological Chemistry, Vol.281, 2006, pp. 23003–23012.

[28] H. Li, P. Xie, G. Li, L. Hao, Q. Xiong, In Vivo Study on the Effects of Microcystin Extracts on the Expression Profiles of Protooncogenes (c-fos, c-jun and c-myc) in Liver, Kidney and Testis of Male Wistar rats Injected i.v. with Toxins, Toxicon: Journal of the International Society on Toxinology, Vol.53, 2009, pp. 169–175.

[29] D. G. Bourne, Enzymatic pathway for the bacterial degradation of the cyanobacterial cyclic peptide toxin Microcystin LR, Applied and Environmental Microbiology, Vol.62, 1996, pp. 4086–4094.

[30] D. G. Bourne, P. Riddles, G. J. Jones, W. Smith, R. L. Blakeley, Characterisation of a Gene Cluster Involved in Bacterial Degradation of the Cyanobacterial Toxin Microcystin LR, Environmental Toxicology, Vol.16, 2001, pp. 523–534.

[31] K. Zhang, H. Ma, P. Yan, W. Tong, X. Huang, D. D. Y. Chen, Electrochemical detection of Microcystin-LR based on ıts deleterious effect on DNA, Talanta, Vol.185, 2018, pp. 405–410.

[32] C. Liu, Q. Xu, Z. Zhao, H. Zhang, X. Liu, C. Yin, Y. Liu, H. Yan, Genomic Analysis of Sphingopyxis sp. USTB-05 for Biodegrading Cyanobacterial Hepatotoxins, Toxins (Basel), Vol.14, No.5, 2022, 333.

[33] E. Maghsoudi, N. Fortin, C. Greer, C. Maynard, A. Pagé, S. V. Duy, S. Sauvé, M. Prévost, S. Dorner, Cyanotoxin degradation activity and mlr gene expression profiles of a Sphingopyxis sp. isolated from Lake Champlain, Canada, Environmental Science: Processes & Impacts, Vol.18, 2016, pp. 1417–1426.

[34] H. Yan, J. Wang, J. Chen, W. Wei, H. Wang, H. Wang, Characterization of the First Step Involved in Enzymatic Pathway for Microcystin-RR Biodegraded by Sphingopyxis sp. USTB-05, Chemosphere, Vol.87, 2012, pp. 12–18.

[35] D. Wang, J. F. Chen, L. Dai, Recent advances in graphene quantum dots for fluorescence bioimaging from cells through tissues to animals, Particle & Particle Systems Characterization, Vol.32, 2015a, pp. 515–523.

[36] G. Wang, G. Shi, X. Chen, R. Yao, F. Chen, A Glassy Carbon Electrode Modified with Grapheme Quantum Dots and Silver Nanoparticles for Simultaneous Determination of Guanine and Adenine, Microchimica Acta, Vol.182, 2015b, pp. 315–322.

[37] H. S. Wang, H. Yan, S. Ma, X. L. Liu, C. H. Yin, H. Wang, Q. Q. Xu, L. Lv, Characterization of the Second and Third Steps in the Enzymatic Pathway for Microcystin-RR Biodegradation by Sphingopyxis sp. USTB-05, Annals of Microbiology, Vol.65, 2015c, pp. 495–502.

[38] H. Xu, H. Wang, Q. Xu, L. Le, C. Yin, X. Liu, H. Du, Y. Hai, Pathway for Biodegrading Microcystin-YR by Sphingopyxis sp. USTB-05, PLoS ONE, Vol.10, 2015, e0124425.

[39] Q. He, W. Wang, Q. Xu, Z. Liu, J. Teng, H. Yan, X. Liu, Microcystins in Water: Detection, Microbial Degradation Strategies, and Mechanisms, International Journal of Environmental Research and Public Health, Vol.19, No.13175, 2022, pp. 1-16.

[40] J. R. Schmidt, S. W. Wilhelm, G. L. Boyer, The Fate of Microcystins in the Environment and Challenges for Monitoring, Toxins, Vol.6, 2014, pp. 3354–3387.

[41] I. Y. Massey, P. Wu, J. Wei, J. Luo, P. Ding, H. Wei, F. Yang, A mini-review on detection methods of Microcystins, Toxins, Vol.12, No.10, 2020, 641.

[42] J. Zhang, J. Lei, C. Xu, L. Ding, H. Ju, Carbon Nanohorn Sensitized Electrochemical Immunosensor for Rapid Detection of Microcystin-LR, Analytical Chemistry, Vol.82, No.3, 2010a, pp. 1117–1122.

[43] D. Zhang, M. C. Huarng, E. C. Alocilja, A Multiplex Nanoparticle-Based Bio-Barcoded DNA Sensor for the Simultaneous Detection of Multiple Pathogens, Biosensors & Bioelectronics, Vol.26, 2010b, pp. 1736–1742.

[44] K. Rajeshwar, J. G. Ibanez, G. M. Swain, Electrochemistry and the Environment, Journal of Applied Electrochemistry, Vol.24, 1994, pp. 1077–1091.

[45] V. S. Manikandan, B. Adhikari, A. Chen, Nanomaterial Based Electrochemical Sensors for the Safety and Quality Control of Food and Beverages, Analyst, Vol.143, 2018, pp. 4537–4554.

[46] D. Grieshaber, R. MacKenzie, J. Vörös, E. Reimhult, Electrochemical Biosensors—Sensor Principles and Architectures, Sensors, Vol.8, 2008, pp. 1400–1458.

[47] D. Arrigan, Bioelectrochemistry; Fundamentals, Experimental Techniques and Applications, Chromatographia, Vol.72, 2010, 585.

[48] P. R. Moses, L. Wier, W. R. Murray, Chemically Modified Tin Oxide Electrode, Analytical Chemistry, Vol.47, 1975, pp. 1882–1886.

[49] A. Hierlemann, R. Gutierrez-Osuna, Higher-Order Chemical Sensing, Chemical Reviews, Vol.108, 2008, pp. 563–613.

[50] M. Bonizzoni, E. V. Anslyn, Combinatorial Methods for Chemical and Biological Sensors, Journal of the American Chemical Society, Vol.131, 2009, pp. 14597–14598.

[51] V. M. Mirsky, M. Riepl, O. S. Wolfbeis, Capacitive Monitoring of Protein Immobilization and Antigen–Antibody Reactions on Monomolecular Alkylthiol Films on Gold Electrodes, Biosensors & Bioelectronics, Vol.12, 1997, pp. 977–989.

[52] A. Guiseppi-Elie, L. Lingerfelt, Immobilisation of DNA, on I. Chips, C. Wittmann, Ed.; Springer: Berlin/Heidelberg, Germany, pp.161–186, 2005.

[53] S. Menon, S. Jesny, K. Kumar, A Voltammetric Sensor for Acetaminophen Based on Electropolymerized Molecularly Imprinted Poly (Oaminophenol) Modified Gold Electrode, Talanta, Vol.179, 2018, pp. 668–675.

[54] J. Ouyang, Application of Intrinsically Conducting Polymers in Flexible Electronics, SmartMat, Vol.2, 2021, pp. 263–285.

[55] S. Gheibi, H. Karimi-Maleh, M. A. Khalilzadeh, H. Bagheri, A New Voltammetric Sensor for Electrocatalytic Determination of Vitamin C in Fruit Juices and Fresh Vegetable Juice Using Modified Multi-Wall Carbon Nanotubes Paste Electrode, Journal of Food Science and Technology, Vol.52, 2013, pp. 276–284.

[56] E. Molaakbari, A. Mostafavi, H. Beitollahi, Simultaneous Electrochemical Determination of Dopamine, Melatonin, Methionine and Caffeine, Sensors & Actuators, B: Chemical, 208, 2015, pp. 195–203.

[57] A. Pardakhty, S. Ahmadzadeh, S. Avazpour, V. K. Gupta, Highly Sensitive and Efficient Voltammetric Determination of Ascorbic Acid in Food and Pharmaceutical Samples from Aqueous Solutions Based on Nanostructure Carbon Paste Electrode as a Sensor, Journal of Molecular Liquids, Vol.216, 2016, pp. 387–391.

[58] A. Trani, R. Petrucci, G. Marrosu, D. Zane, A. Curulli, Selective Electrochemical Determination of Caffeine at a Gold-Chitosan Nanocomposite Sensor: May Little Change on Nanocomposites Synthesis Affect Selectivity?, Journal of Electroanalytical Chemistry, Vol.788, 2017, pp. 99–106.

[59] M. Chiappalone, A. Vato, M. Tedesco, M. Marcoli, F. Davide, S. Martinoia, Networks of Neurons Coupled to Microelectrode Arrays: A Neuronal Sensory System for Pharmacological Applications, Biosensors & Bioelectronics, Vol.18, 2003, pp. 627–634.

[60] K. Thangavelu, S. Palanisamy, S.-M. Chen, V. Velusamy, T.-W. Chen, S. K. Ramaraj, Electrochemical Determination of Caffeic Acid in Wine Samples Using Reduced Graphene Oxide/Polydopamine Composite, Journal of The Electrochemical Society, Vol.163, 2016, pp. B726–B731.

[61] S. Lupu, F. Parenti, L. Pigani, R. Seeber, C. Zanardi, Differential Pulse Techniques on Modified Conventional-Size and Microelectrodes. Electroactivity of Poly[4,40 -bis(butylsulfanyl)-2,20 -bithiophene] Coating Towards Dopamine and Ascorbic Acid Oxidation, International Journal Devoted to Fundamental and Practical Aspects of Electroanalysis, 15, 2003, pp. 715–725.

[62] J. Osteryoung, R. Osteryoung, Square Wave Voltammetry, Analytical Chemistry, Vol.57, 1985, pp. 101–110.

[63] A. Chen, B. Shah, Electrochemical Sensing and Biosensing Based on Square Wave Voltammetry, Analytical Methods, Vol.5, 2013, pp. 2158–2173.

[64] C. Han, A. Doepke, W. Cho, V. Likodimos, A. A. De La Cruz, T. Back, W. R. Heineman, H. B. Halsall, V. N. Shanov, M. J. Schulz, A Multiwalled-Carbon-Nanotube-Based Biosensor for Monitoring Microcystin-LR in Sources of Drinking Water Supplies, Advanced Functional Materials, Vol.23, No.14, 2013, pp. 1807–1816.

[65] W. Zhang, C. Han, B. Jia, C. Saint, M. Nadagouda, P. Falaras, L. Sygellou, V. Vogiazi, D. D. Dionysiou, A 3D Graphene-Based Biosensor as an Early Microcystin-LR Screening Tool in Sources of Drinking Water

Supply, Electrochimica Acta, Vol.236, 2017a, pp. 319–327.

[66] Y. Zhang, M. Chen, H. Li, F. Yan, P. Pang, H. Wang, Z. Wu, W. Yang, A Molybdenum Disulfide/Gold Nanorod Composite-Based Electrochemical Immunosensor for Sensitive and Quantitative Detection of Microcystin-LR in Environmental Samples, Sensors & Actuators, B: Chemical, Vol.244, 2017b, pp. 606–615.

[67] J. Zhang, Z. Xiong, Z. Chen, Ultrasensitive Electrochemical Microcystin-LR Immunosensor Using Gold Nanoparticle Functional Polypyrrole Microsphere Catalyzed Silver Deposition for Signal Amplification, Sensors & Actuators, B: Chemical, Vol.246, 2017c, pp. 623–630.

[68] F. Tan, N. M. Saucedo, P. Ramnani, A. Mulchandani, Label-Free Electrical Immunosensor for Highly Sensitive and Specific Detection of Microcystin-LR in Water Samples, Environmental Science & Technology, Vol.49, No.15, 2015, pp. 9256–9263.

[69] J. Zhang, Y. Sun, H. Dong, X. Zhang, W. Wang, Z. Chen, An Electrochemical Non-Enzymatic Immunosensor for Ultrasensitive Detection of Microcystin-LR Using Carbon Nanofibers as the Matrix, Sensors & Actuators, B: Chemical, Vol.233, 2016, pp. 624–632.

[70] L. Ruiyi, X. Qianfang, L. Zaijun, S. Xiulan, L. Junkang, Electrochemical Immunosensor for Ultrasensitive Detection of Microcystin-LR Based on Graphene–Gold Nanocomposite/Functional Conducting Polymer/Gold Nanoparticle/Ionic Liquid Composite Film with Electrodeposition, Biosensors & Bioelectronics, Vol.44, No.1, 2013, pp. 235–240.

[71] H. Zhao, J. Tian, X. Quan, A Graphene and Multienzyme Functionalized Carbon Nanosphere Based Electrochemical Immunosensor for Microcystin-LR Detection, Colloids and Surfaces B: Biointerfaces, Vol.103, 2013, pp. 38–44.

[72] C. Gan, Z. Sun, L. Ling, Z. He, H. Lei, Y. Liu, Construction of Portable Electrochemical Immunosensors Based on Graphene Hydrogel@Polydopamine for Microcystin-LR Detection Using Multi-Mesoporous Carbon Sphere-Enzyme Labels, RSC Advances, Vol.6, No.57, 2016, pp. 51662–51669.

[73] Q. Deng, C. J. Watson, R. T. Kennedy, Aptamer Affinity Chromatography for Rapid Assay of Adenosine in Microdialysis Samples Collected in Vivo, Journal of Chromatography A, Vol.1005, 2003, pp. 123–130.

[74] Y. Liu, Q. Zhou, A. Revzin, An Aptasensor for Electrochemical Detection of Tumor Necrosis Factor in Human Blood, Analyst, Vol.138, 2013, pp. 4321–4326.

[75] M. P. Bilibana, A. R. Williams, C. Rassie, C. E. Sunday, H. Makelane, L. Wilson, N. Ntshongontshi, A. N. Jijana, M. Masikini, P. G. L. Baker, E. I. Iwuoha, Electrochemical Aptatoxisensor Responses on Nanocomposites Containing Electro-Deposited Silver Nanoparticles on Poly(propyleneimine) Dendrimer for the Detection of Microcystin-LR in Freshwater, Sensors, Vol.16, No.11, 2016, 1901.

[76] A. Ng, R. Chinnappan, S. Eissa, H. Liu, C. Tlili, M. Zourob, Selection, Characterization, and Biosensing Application of High Affinity Congener-Specific Microcystin-Targeting Aptamers, Environmental Science & Technology, Vol.46, No.19, 2012, pp. 10697–10703.

[77] Y. Zhang, Z. Zhu, X. Teng, Y. Lai, S. Pu, P. Pang, H. Wang, C. Yang, C. Barrow, W. Yang, Enzyme-Free Fluorescent Detection of Microcystin-LR Using Hairpin DNA-Templated Copper Nanoclusters as Signal Indicator, Talanta, Vol.202, 2019, pp. 279–284.

[78] Y. Wu, S. L. Baker, R. Y. Lai, Effects of DNA Probe Length on the Performance of a Dynamics-Based Electrochemical Hg(II) Sensor, Electroanalysis, Vol.29, 2017a, pp. 2239–2245.

[79] Y. Wu, R. Y. Lai, Tunable Signal-off and Signal-on Electrochemical Cisplatin Sensor, Analytical Chemistry, Vol.89, 2017b, pp. 9984–9989.

[80] L. Lebogang, J. Jantra, M. Hedström, B. Mattiasson, Electrochemical Flow-ELISA for Rapid and Sensitive Determination of Microcystin-LR Using Automated Sequential Injection System, Sensors, Vol.17, No.7, 2017, 1639.

[81] W. P. Brooks, G. A. Codd, Immunoassay of Hepatotoxic Cultures and Water Blooms of Cyanobacteria Using Microcystis Aeruginosa Peptide Toxin Polyclonal Antibodies, Environmental

Technology Letters, Vol.9, 1988, pp. 1343–1348.

[82] F. S. Chu, X. Huang, R. D. Wei, W. W. Carmichael, Production and Characterization of Antibodies Against Microcystins, Applied and Environmental Microbiology, Vol.55, 1989, pp. 1928–1933.

[83] C. M. McDermott, R. Feola, J. Plude, Detection of Cyanobacterial Toxins (Microcystins) in Waters of Northeastern Wisconsin by a New Immunoassay Technique, Toxicon: Official Journal of the International Society on Toxinology, Vol.33, 1995, pp. 1433–1442.

[84] M. T. Castañeda, S. Alegret, A. Merkoçi, Electrochemical Sensing of DNA Using Gold Nanoparticles, Electroanalysis, Vol.19, No.7-8, 2017, pp. 743-753.

[85] X. Zhang, Y. Xu, Y. Yang, X. Jin, S. Ye, S. Zhang, L. Jiang, A New Signal-on Photoelectrochemical Biosensor Based on a Graphene/Quantum-Dot Nanocomposite Amplified by the Dual-Quenched Effect of Bipyridinium Relay and AuNPs, Chemistry-A European Journal, Vol.18, No.51, 2012, pp. 16411-16418.

[86] K. Niikura, T. Matsunaga, T. Suzuki, S. Kobayashi, H. Yamaguchi, Y. Orba, A. Kawaguchi, H. Hasegawa, K. Kajino, T. Ninomiya, K. Ijiro, H. Sawa, Gold Nanoparticles as a Vaccine Platform: Influence of Size and Shape on Immunological Responses in Vitro and in Vivo, ACS Nano, Vol.7, No.5, 2013, pp. 3926-3938.

[87] X. Niu, W. Yang, G. Wang, J. Ren, H. Guo, J. Gao, A Novel Electrochemical Sensor of Bisphenol A Based on Stacked Graphene Nanofibers/Gold Nanoparticles Composite Modified Glassy Carbon Electrode, Electrochimica Acta, Vol.98, 2013, pp. 167-175.

[88] A. N. Kawde, J. Wang, Amplified Electrical Transduction of DNA Hybridization Based on Polymeric Beads Loaded with Multiple Gold Nanoparticle Tags, Electroanalysis, Vol.16, 2004, pp. 101-107.

[89] J. Wang, D. Xu, A.-N. Kawde, R. Polsky, Metal Nanoparticle-Based Electrochemical Stripping Potentiometric Detection of DNA Hybridization, Analytical Chemistry, Vol.73, No.22, 2001a, pp. 5576-5581.

[90] N. T. K. Thanh, Z. Rosenzweig, Development of an Aggregation-Based Immunoassay for Anti-Protein a Using Gold Nanoparticles, Analytical Chemistry, Vol.74, 2002, pp. 1624-1628.

[91] E. T. Kisak, M. T. Kennedy, D. Trommeshauser, J. A. Zasadzinski, Self-Limiting Aggregation by Controlled Ligand−Receptor Stoichiometry, Langmuir, Vol.16, No.6, 2000, pp. 2825-2831.

[92] F. Patolsky, K. T. Ranjit, A. Lichtenstein, I. Willner, Dendritic Amplification of DNA Analysis by Oligonucleotide-Functionalized Au-Nanoparticles, Chemical Communications, Vol.12, 2000, pp. 1025-1026.

[93] T. A. Taton, C. A. Mirkin, R. L. Letsinger, Scanometric DNA Array Detection with Nanoparticle Probes, Science, Vol.289, No.5485, 2000, pp. 1757-1760.

[94] J. Wang, R. Polsky, D. Xu, Silver-Enhanced Colloidal Gold Electrochemical Stripping Detection of DNA Hybridization, Langmuir, Vol.17, 2001b, pp. 5739–5741.

[95] S. L. Ting, S. J. Ee, A. Ananthanarayanan, K. C. Leong, P. Chen, Graphene Quantum Dots Functionalized Gold Nanoparticles for Sensitive Electrochemical Detection of Heavy Metal Ions, Electrochimica Acta, Vol.172, 2015, pp. 7-11.

[96] Y. Shi, J. Z. Wu, Y. J. Sun, Y. Zhang, Z. W. Wen, H. C. Dai, H. D. Wang, Z. Li, A Graphene Oxide Based Biosensor for Microcystins Detection by Fluorescence Resonance Energy Transfer, Biosensors & Bioelectronics, Vol.38, 2012, pp. 31–36.

[97] H. Cai, Y. Wang, P. He, Y. Fang, Electrochemical Detection of DNA Hybridization Based on Silver-Enhanced Gold Nanoparticle Label, Analytica Chimica Acta, Vol.469, 2002a, pp. 165–172.

[98] H. Cai, Y. Xu, N. Zhu, P. He, Y. Fang, An Electrochemical DNA Hybridization Detection Assay Based on a Silver Nanoparticle Label, Analyst, Vol.127, 2002, pp. 803–808.

[99] J. Wang, D. Xu, R. Polsky, Magnetically-Induced Solid-State Electrochemical Detection of DNA Hybridization, Journal of the American Chemical Society, Vol.124, 2002, pp. 4208–4209.

[100] I. H. Min, L. Choi, K. S. Ahn, B. K. Kim, B. Y. Lee, K. S. Kim, H. N. Choi, W. Y. Lee, Electrochemical Determination of

Carbohydrate-Binding Proteins Using Carbohydrate-Stabilized Gold Nanoparticles and Silver Enhancement, Biosensors & Bioelectronics, Vol.26, 2010, pp. 1326–1331.

[101] L. Lin, Y. Liu, L. Tang, J. Li, Electrochemical DNA Sensor by the Assembly of Graphene and DNA-Conjugated Gold Nanoparticles with Silver Enhancement Strategy, Analyst, Vol.136, 2011, pp. 4732–4737.

[102] D. Lin, J. Wu, M. Wang, F. Yan, H. Ju, Triple Signal Amplification of Graphene Film, Polybead Carried Gold Nanoparticles as Tracing Tag and Silver Deposition for Ultrasensitive Electrochemical Immunosensing, Analytical Chemistry, Vol.84, 2012, pp. 3662–3668.

[103] Y. Pan, W. Shan, H. Fang, M. Guo, Z. Nie, Y. Huang, S. Yao, Sensitive and Visible Detection of Apoptotic Cells on Annexin-V Modified Substrate Using Aminophenylboronic Acid Modified Gold Nanoparticles (APBA-GNPs) Labelling, Biosensors & Bioelectronics, Vol.52, 2014, pp. 62–68.

[104] G. Lai, F. Yan, J. Wu, C. Leng, H. Ju, Ultrasensitive Multiplexed Immunoassay with Electrochemical Stripping Analysis of Silver Nanoparticles Catalytically Deposited by Gold Nanoparticles and Enzymatic Reaction, Analytical Chemistry, Vol.83, 2011, pp. 2726–2732.

[105] J. Wei, W. Chang, A. Qileng, W. Liu, Y. Zhang, S. Rong, H. Lei, Y. Liu, Dual-Modal Split-Type Immunosensor for Sensitive Detection of Microcystin-LR: Enzyme-Induced Photoelectrochemistry and Colorimetry, Analytical Chemistry, Vol.90, 2018, pp. 9606–9613.

[106] H. W. Kroto, J. R. Heath, S. C. O'Brien, R. F. Curl, R. E. Smalley, C60: Buckminsterfullerene, Nature, Vol.318, 1985, pp. 162–163.

[107] S. Iijima, Helical Microtubules of Graphitic Carbon, Nature, Vol.354, 1991, pp. 56–58.

[108] V. Mani, B. Devadas, S.-M. Chen, Direct Electrochemistry of Glucose Oxidase at Electrochemically Reduced Graphene Oxide-Multiwalled Carbon Nanotubes Hybrid Material Modified Electrode for Glucose Biosensor, Biosensors and Bioelectronics, Vol.41, 2013, pp. 309-315.

[109] J. Kong, N. R. Franklin, C. Zhou, M. G. Chapline, S. Peng, K. Cho, H. Dai, Nanotube Molecular Wires as Chemical Sensors, Science, Vol.287, No.5453, 2000, pp. 622-625.

[110] S. W. Wang, Q. Zhang, R. Wang, S. F. Yoon, A Novel Multi-Walled Carbon Nanotube-Based biosensor for Glucose Detection, Biochemical and Biophysical Research Communications, Vol.311, No.3, 2003, pp. 572-576.

[111] W. Schuhmann, Biosensors: Microelectrochemical Devices, In: M. Lambrechts, W. Sansen, (eds.), Institute of Physics Publishing, Bristol, pp. 304, 1992.

[112] Y. Hassan, King Faisal Specialist Hospital and Research Centre, Riyadh, Saudi Arabia. Marcel Dekker Inc: New York and Basel, Journal of the American Chemical Society, 124, 2002, pp. 511-512.

[113] S. Creager, Electrochemical Sensors in Bioanalysis by Raluca-Ioana Stefan and Jacobus Frederick Van Staden, University of Pretoria, Pretoria, South Africa., p: 288, 2001.

[114] F. Pérez-Alonso, M. Abdel Salam, T. Herranz, J. L. Gómez de la Fuente, S. A. Al-Thabaiti, S. N. Basahel, M. A. Peña Jiménez, J. L. García Fierro, S. Rojas Muñoz, Effect of Carbon Nanotube Diameter for the Synthesis of Fe/N/Multiwall Carbon Nanotubes and Repercussions for the Oxygen Reduction Reaction, Journal of Power Sources, Vol.240, 2013, pp. 494-502.

[115] V. Mani, B. Dinesh, S.-M. Chen, R. Saraswathi, Direct Electrochemistry of Myoglobin at Reduced Graphene Oxide-Multiwalled Carbon Nanotubes-Platinum Nanoparticles Nanocomposite and Biosensing Towards Hydrogen Peroxide and Nitrite, Biosensors and Bioelectronics, Vol.53, 2014, pp. 420-427.

[116] E. Gracia-Espino, B. Rebollo-Plata, H. Martínez-Gutiérrez, E. Muñoz-Sandoval, F. López-Urías, M. Endo, H. Terrones, M. Terrones, Temperature Dependence of Sensors Based on Silver-Decorated Nitrogen-Doped Multiwalled Carbon Nanotubes, Journal of Sensors, 2016, Article ID 4319498.

[117] J. Lee, M. Morita, K. Takemura, E. Y. Park, A Multi-Functional Gold/Iron-Oxide Nanoparticle-CNT Hybrid Nanomaterial as Virus DNA Sensing Platform, Biosensors and Bioelectronics, Vol.102, 2018, pp. 425–431.

[118] J. Lee, S. R. Ahmed, S. Oh, J. Kim, T. Suzuki, K. Parmar, S. S. Park, J. Lee, E. Y. Park, A Plasmon-Assisted Fluoro-Immunoassay Using Gold Nanoparticle-

Decorated Carbon Nanotubes for Monitoring the Influenza Virus, Biosensors and Bioelectronics, Vol.64, 2015, pp. 311–317.

[119] M. Liu, X. Ding, Q. Yang, Y. Wang, G. Zhao, N. Yang, A PM Levelled Photoelectrochemical Sensor for Microcystin-LR Based on Surface Molecularly Imprinted TiO2@CNTs Nanostructure, Journal of Hazardous Materials, Vol.331, 2017, pp. 309–320.

[120] Z. He, Y. Cai, Z. Yang, P. Li, H. Lei, W. Liu, Y. Liu, A Dual-Signal Readout Enzyme-Free Immunosensor Based on Hybridization Chain Reaction-Assisted Formation of Copper Nanoparticles for the Detection of Microcystin-LR, Biosensors and Bioelectronics, Vol.126, 2019, pp. 151–159.

[121] R. B. Queirós, J. P. Noronha, P. V. S. Marques, M. G. F. Sales, Label-Free Detection of Microcystin-LR in Waters Using Real-Time Potentiometric Biosensors Based on Single-Walled Carbon Nanotubes Imprinted Polymers, Procedia Engineering, Vol.47, 2012, pp. 758–761.

[122] A. R. Jalalvand, Fabrication of a Novel and Ultrasensitive Label-Free Electrochemical Aptasensor for Detection of Biomarker Prostate Specific Antigen, International Journal of Biological Macromolecules, Vol.126, 2019, pp. 1065–1073.

[123] H. A. Samie, M. Arvand, Label-Free Electrochemical Aptasensor for Progesterone Detection in Biological Fluids, Bioelectrochemistry, Vol.133, 2020, 107489.

[124] Z. Zeng, F. X. Xiao, H. Phan, S. Chen, Z. Yu, R. Wang, T. Q. Nguyen, T. T. Yang Tan, Unraveling the Cooperative Synergy of Zero-Dimensional Graphene Quantum Dots and Metal Nanocrystals Enabled by Layer-by-Layer Assembly, Journal of Materials Chemistry A, Vol.6, 2018, pp. 1700–1713.

[125] Z. Fan, S. Li, F. Yuan, L. Fan, Fluorescent Graphene Quantum Dots for Biosensing and Bioimaging, RSC Advances, Vol.5, 2015, pp. 19773–19789.

[126] R. Xie, Z. Wang, W. Zhou, Y. Liu, L. Fan, Y. Li, X. Li, Graphene Quantum Dots as Smart Probes for Biosensing, Analytical Methods, Vol.8, 2016, pp. 4001–4006.

[127] M. Hasanzadeh, N. Shadjou, What are the Reasons for Low Use of Graphene Quantum Dots in Immunosensing of Cancer Biomarkers?, Materials Science and Engineering: C, Vol.71, 2017, pp. 1313–1326.

[128] F. Faridbod, A. L. Sanati, Graphene Quantum Dots in Electrochemical Sensors/Biosensors, Current Analytical Chemistry, Vol.15, 2018, pp. 103–123.

[129] S. Tachi, H. Morita, M. Takahashi, Y. Okabayashi, T. Hosokai, T. Sugai, S. Kuwahara, Quantum Yield Enhancement in Graphene Quantum Dots via Esterification with Benzyl Alcohol, Scientific Reports, Vol.9, 2019, pp. 1–7.

[130] M. Pedrero, S. Campuzano, J. M. Pingarrón, Quantum Dots as Components of Electrochemical Sensing Platforms for the Detection of Environmental and Food Pollutants: A Review, Journal of AOAC International, Vol.100, 2017, pp. 950–961.

[131] F. Ma, C. C. Li, C. Y. Zhang, Development of Quantum Dot-Based Biosensors: Principles and Applications, Journal of Materials Chemistry B, Vol.6, 2018, pp. 6173–6190.

[132] M. Roushani, A. Valipour, The Potentiality of Graphene Quantum Dots Functionalized by Nitrogen and Thiol-Doped (GQDs-N-S) to Stabilize the Antibodies in Designing of Human Chorionic Gonadotropin Immunosensor, Nanochemistry Research, Vol.4, 2019, pp. 20–26.

[133] J. Chen, P. Gao, H. Wang, L. Han, Y. Zhang, P. Wang, N. Jia, PPy/Cu2O Molecular Imprinting Composite Film Based Visible Light-Responsive Photoelectrochemical Sensor for MicrocystinLR, Journal of Materials Chemistry C, Vol.6, No.15, 2018, pp. 3937–3944.

[134] A. Rakovich, T. Rakovich, Semiconductor: Versus Graphene Quantum Dots as Fluorescent Probes for Cancer Diagnosis and Therapy Applications, Journal of Materials Chemistry B, 6, 2018, pp. 2690–2712.

[135] S. H. Choi, Unique Properties of Graphene Quantum Dots and Their Applications in Photonic/Electronic Devices, Journal of Physics D: Applied Physics, Vol.50, 2017, pp. 1–10.

[136] S. Savas, Z. Altintas, Graphene Quantum Dots as Nanozymes for Electrochemical Sensing of Yersinia Enterocolitica in Milk and Human Serum, Materials, Vol.12, No.13, 2019, 2189.

[137] S. Savas, A. Ersoy, Y. Gulmez, S. Kilic, B. Levent, Z. Altintas, Nanoparticle Enhanced Antibody and DNA Biosensors for

Sensitive Detection of Salmonella, Materials, Vol.11, No.9, 2018, 1541.

[138] X. Sun, L. Guan, H. Shi, J. Ji, Y. Zhang, Z. Li, Determination of Microcystin-LR with a Glassy Carbon Impedimetric Immunoelectrode Modified with an Ionic Liquid and Multiwalled Carbon Nanotubes. Microchimica Acta, Vol.180, No.1–2, 2013, pp. 75–83.

[139] X. Li, M. Rui, J. Song, Z. Shen, H. Zeng, Carbon and Graphene Quantum Dots for Optoelectronic and Energy Devices: A Review. Advanced Functional Materials, Vol.25, 2015, pp. 4929–4947.

[140] P. Zheng, N. Wu, Fluorescence and Sensing Applications of Graphene Oxide and Graphene Quantum Dots: A Review. Chemistry: An Asian Journal, Vol.12, 2017, pp. 2343–2353.

[141] J. Shen, Y. Zhu, X. Yang, C. Li, ChemComm Graphene Quantum Dots: Emergent Nanolights for Bioimaging, Sensors, Catalysis and Photovoltaic Devices, Royal Society of Chemistry, Vol.46, 2012, pp. 3686–3699.

[142] L. Wang, T. F. Kang, L. P. Lu, J. G. Zhang, R. Xue, S. Y. Cheng, Microcystin-(Leucine-Arginine) Immunosensor Based on Iron(II, III) Magnetic Nanoparticles, Analytical Letters, Vol.47, No.18, 2014a, pp. 2939–2949.

[143] L. Wang, S. Zhu, H. Wang, S. Qu, Y. Zhang, J. Zhang, Q. Chen, W. E. T. Al, Common Origin of Green Luminescence in Carbon Nanodots and Graphene Quantum Dots, Journal of the American Chemical Society, Vol.8, 2014b, pp. 2541–2547.

[144] X. Yan, X. Cui, L. S. Li, Synthesis of Large, Stable Colloidal Graphene Quantum Dots with Tunable Size, Journal of the American Chemical Society, 132, 2010, pp. 5944–5945.

[145] M. Bacon, S. J. Bradley, T. Nann, Graphene Quantum Dots. Particle & Particle Systems Characterization, Vol.31, 2014, pp. 415–428.

[146] A. Karimzadeh, M. Hasanzadeh, N. Shadjou, M. de la Guardia, Optical Bio(sensing) Using Nitrogen Doped Graphene Quantum Dots: Recent Advances and Future Challenges, TrAC Trends in Analytical Chemistry, Vol.108, 2018, pp. 110–121.

[147] P. Tian, L. Tang, K. S. Teng, S. P. Lau, Graphene Quantum Dots from Chemistry to Applications, Materials Today. Chemistry, Vol.10, 2018, pp. 221–258.

[148] S. K. Tuteja, R. Chen, M. Kukkar, C. K. Song, R. Mutreja, S. Singh, A. K. Paul, H. Lee, K. H. Kim, A. Deep, C. R. Suri, A Label-Free Electrochemical Immunosensor for the Detection of Cardiac Marker Using Graphene Quantum Dots (GQDs), Biosensors & Bioelectronics, Vol.86, 2026, pp. 548–556.

[149] S. Gupta, A. Kaushal, A. Kumar, D. Kumar, Ultrasensitive Transglutaminase Based Nanosensor for Early Detection of Celiac Disease in Human, International Journal of Biological Macromolecules, Vol.105, 2017, pp. 905–911.

[150] Y. Yang, Q. Liu, Y. Liu, J. Cui, H. Liu, P. Wang, Y. Li, L. Chen, Z. Zhao, Y. Dong, A Novel Label-Free Electrochemical Immunosensor Based on Functionalized Nitrogen-Doped Graphene Quantum Dots for Carcinoembryonic Antigen Detection, Biosensors & Bioelectronics, Vol.90, 2017, pp. 31–38.

[151] B. D. Mansuriya, Z. Altintas, Graphene Quantum Dot-Based Electrochemical Immunosensors for Biomedical Applications, Materials, Vol.13, No.1, 2019, 96.

[152] B. V. Chikkaveeraiah, A. A. Bhirde, N. Y. Morgan, H. S. Eden, X. Chen, Electrochemical Immunosensors for Detection of Cancer Protein Biomarkers, ACS Nano, Vol.6, 2012, pp. 6546–6561.

[153] V. Serafín, A. Valverde, M. Garranzo-Asensio, R. Barderas, S. Campuzano, P. Yáñez-Sedeño, J. M. Pingarrón, Simultaneous Amperometric Immunosensing of the Metastasis-Related Biomarkers IL-13Rα2 and CDH-17 by Using Grafted Screen-Printed Electrodes and a Composite Prepared from Quantum Dots and Carbon Nanotubes for Signal Amplification, Microchimica Acta, Vol.186, No.7, 2019, 411.

[154] B. D. Mansuriya, Z. Altintas, Applications of Graphene Quantum Dots in Biomedical Sensors, Sensors, Vol.20, No.1072, 2020, pp. 1-71.

[155] N. R. Stradiotto, H. Yamanaka, M. V. B. Zanoni, Electrochemical Sensors: A Powerful Tool in Analytical Chemistry, Journal of the Brazilian Chemical Society, Vol.14, 2003, pp. 159–173.

[156] C. Kokkinos, A. Economou, M. I. Prodromidis, Electrochemical Immunosensors: Critical Survey of Different

Architectures and Transduction Strategies, TrAC Trends in Analytical Chemistry C, Vol. 79, 2016, pp. 88-105.

[157] S. A. Lim, M. U. Ahmed, Electrochemical Immunosensors and Their Recent Nanomaterial-Based Signal Amplification Strategies: A Review, RSC Advances, Vol.6, No.30, 2016, pp. 24995-25014.

[158] E. C. Rama, A. Costa-García, Screen-Printed Electrochemical Immunosensors for the Detection of Cancer and Cardiovascular Biomarkers, Electroanalysis, Vol.28, 2016, pp. 1700–1715.

[159] I. H. Cho, J. Lee, J. Kim, M. S. Kang, J. K. Paik, S. Ku, H. M. Cho, J. Irudayaraj, D. H. Kim, Current Technologies of Electrochemical Immunosensors: Perspective on Signal Amplification, Sensors, Vol.18, No.1, 2018, 207.

[160] T. H. S. Dhahi, U. D. A. Bin Hashim, N. M. Ahmed, A. Mat Taib, A Review on the Electrochemical Sensors and Biosensors Composed of Nanogaps as Sensing Material, Journal of Optoelectronics and Advanced Materials, 12, 2010, pp. 1857–1862.

[161] F. Faridbod, V. K. Gupta, H. A. Zamani, Electrochemical Sensors and Biosensors, International Journal of Electrochemical Science, Vol.24, 2011, 717.

[162] D. R. Thevenot, K. Toth, R. A. Durst, G. S. Wilson, Electrochemical biosensors: Recommended definitions and classification, Pure and Applied Chemistry, 71, 1999, pp. 2333–2348.

[163] Y. Khristunova, E. Korotkova, B. Kratochvil, J. Barek, E. Dorozhko, V. Vyskocil, E. Plotnikov, O. Voronova, V. Sidelnikov, Preparation and Investigation of Silver Nanoparticle–Antibody Bioconjugates for Electrochemical Immunoassay of Tick-Borne Encephalitis, Sensors (Basel), Vol.19, No.9, 2019, 2103.

[164] Z. Altintas, W. M. Fakanya, I. E. Tothill, Cardiovascular Disease Detection Using Bio-Sensing Techniques, Talanta, Vol.128, 2014, pp. 177–186.

[165] P. Mehrotra, Biosensors and Their Applications—A Review, Journal of Oral Biology and Craniofacial Research, Vol.6, 2016, pp. 153–159.

[166] Y. Liu, X. Zhang, E. Yifeng, F. Fang, G. Kuang, G. Wang, Sandwich Immunoassays of Multicomponent Subtrace Pathogenic DNA Based on Magnetic Fluorescent Encoded Nanoparticles, BioMed Research International, Vol.2016, 2016, pp. 1–9.

[167] G. Dutta, P. B. Lillehoj, Wash-Free, Label-Free Immunoassay for Rapid Electrochemical Detection of PfHRP2 in whole Blood Samples, Scientific Reports, Vol.8, 2018, pp. 1–8.

[168] D. Pan, G. Li, H. Hu, H. Xue, M. Zhang, M. Zhu, X. Gong, Y. Zhang, Y. Wan, Y. Shen, Direct Immunoassay for Facile and Sensitive Detection of Small Molecule Aflatoxin B1 Based on Nanobody, Chemistry: A European Journal, Vol.24, 2018, pp. 9869–9876.

[169] Q. Yan, Y. Yang, Z. Tan, Q. Liu, H. Liu, P. Wang, L. Chen, D. Zhang, Y. Li, Y. Dong, A Label-Free Electrochemical Immunosensor Based on the Novel Signal Amplification System of AuPdCu Ternary Nanoparticles Functionalized Polymer Nanospheres, Biosensors & Bioelectronics, Vol.103, 2018, pp. 151–157.

[170] D. Purvis, D. Leonardova, D. Farmakovsky, V. Cherkasov, An Ultrasensitive and Stable Potentiometric Immunosensor, Biosensors & Bioelectronics, Vol.18, 2003, pp. 1385–1390.

[171] V. Mirceski, R. Gulaboski, M. Lovric, I. Bogeski, R. Kappl, M. Hoth, Square-Wave Voltammetry: A Review on the Recent Progress, Electroanalysis, Vol.25, 2013, pp. 2411–2422.

[172] O. A. Farghaly, R. S. Abdel Hameed, A. A. H. Abu-Nawwas, Analytical Application Using Modern Electrochemical Techniques, International Journal of Electrochemical Science, Vol.9, 2014, pp. 3287–3318.

[173] V. Mirceski, R. Gulaboski, Recent Advances in Square-Wave Voltammetry: A Review, Macedonian Journal of Chemistry and Chemical Engineering, Vol.33, 2014, pp. 1–12.

[174] S. Mendoza, E. Bustos, J. Manriquez, L. A. Godinez, Voltammetric Techniques. In Agricultural and Food Electroanalysis, A. Escarpa, M. C. Gonzalez, M. A. Lopez, Eds.; John Wiley & Sons: Chichester, UK; Ltd.7yy7:West Sussex, UK, pp. 23–48. ISBN 9781119961864, 2015.

[175] N. Elgrishi, K. J. Rountree, B. D. McCarthy, E. S. Rountree, T. T. Eisenhart, J. L. Dempsey, A Practical Beginner's Guide to Cyclic Voltammetry, Journal of Chemical Education, Vol.95, 2018, pp. 197–206.

[176] A. J. Bard, L. R. Faulkner, Electrochemical Methods: Fundamentals and Applications, 2nd ed.; Willey: Hoboken, NJ, USA, ISBN 9780123813749, 2001.

[177] Z. Altintas, A. Takiden, T. Utesch, M. A. Mroginski, B. Schmid, F. W. Scheller, R. D. Süssmuth, Integrated Approaches Toward High-Affinity Artificial Protein Binders Obtained via Computationally Simulated Epitopes for Protein Recognition, Advanced Functional Materials, Vol.29, 2019, pp. 1–11.

[178] R. Tchinda, A. Tutsch, B. Schmid, R. D. Süssmuth, Z. Altintas, Recognition of Protein Biomarkers using Epitope-Mediated Molecularly Imprinted Films: Histidine or Cysteine Modified Epitopes? Biosensors & Bioelectronics, Vol.123, 2019, pp. 260–268.

[179] M. Arvand, S. Abbasnejad, N. Ghodsi, Graphene Quantum Dots Decorated with Fe3O4 Nanoparticles/Functionalized Multiwalled Carbon Nanotubes as a New Sensing Platform for Electrochemical Determination of l-DOPA in Agricultural Products, Analytical Methods, Vol.8, 2016, pp. 5861–5868.

[180] M. Hasanzadeh, N. Hashemzadeh, N. Shadjou, J. Eivazi-Ziaei, M. Khoubnasabjafari, A. Jouyban, Sensing of Doxorubicin Hydrochloride Using Graphene Quantum Dot Modified Glassy Carbon Electrode, Journal of Molecular Liquids, Vol.221, 2016, pp. 354–357.

[181] M. Hasanzadeh, S. Tagi, E. Solhi, A. Mokhtarzadeh, N. Shadjou, A. Eftekhari, S. Mahboob, An Innovative Immunosensor for Ultrasensitive Detection of Breast Cancer Specific Carbohydrate (CA 15-3) in Unprocessed Human Plasma and MCF-7 Breast Cancer Cell Lysates Using Gold Nanospear Electrochemically Assembled onto Thiolated Graphene Quantum Dots, International Journal of Biological Macromolecules, Vol.114, 2018, pp. 1008–1017.

[182] K. K. Mistry, K. Layek, T. N. Chell, C. R. Chaudhuri, H. Saha, Design and Development of an Amperometric Immunosensor Based on Screen-Printed Electrodes, Analytical Methods, Vol.8, 2016, pp. 3096–3101.

[183] N. J. Ronkainen, S. L. Okon, Nanomaterial-Based Electrochemical Immunosensors for Clinically Significant Biomarkers, Materials, Vol.7, 2014, pp. 4669–4709.

[184] T. Hu, L. Zhang, W. Wen, X. Zhang, S. Wang, Enzyme Catalytic Amplification of miRNA-155 Detection with Graphene Quantum Dot-Based Electrochemical Biosensor, Biosensors & Bioelectronics, Vol.77, 2016, pp. 451–456.

[185] A. Mars, M. Hamami, L. Bechnak, D. Patra, N. Raouafi, Curcumin-Graphene Quantum Dots for Dual Mode Sensing Platform: Electrochemical and Fluorescence Detection of APOe4, Responsible of Alzheimer's Disease, Analytica Chimica Acta, Vol.1036, 2018, pp. 141–146.

[186] Y. Zhu, S. Lu, A. Gowri Manohari, X. Dong, F. Chen, W. Xu, Z. Shi, C. Xu, Polydopamine Interconnected Graphene Quantum Dots and Gold Nanoparticles for Enzymeless H2O2 Detection, Journal of Electroanalytical Chemistry, Vol.796, 2017, pp. 75–81.

[187] J. Ju, W. Chen, In Situ Growth of Surfactant-Free Gold Nanoparticles on Nitrogen-Doped Graphene Quantum Dots for Electrochemical Detection of Hydrogen Peroxide in Biological Environments, Analytical Chemistry, Vol.87, 2015, pp. 1903–1910.

[188] H. Malekzad, M. Hasanzadeh, N. Shadjou, A. Jouyban, Highly Sensitive Immunosensing of Prostate Specific Antigen Using Poly Cysteine Caped by Graphene Quantum Dots and Gold Nanoparticle: A Novel Signal Amplification Strategy, International Journal of Biological Macromolecules, Vol.105, 2017, pp. 522–532.

[189] E. Katz, I. Willner, Probing Biomolecular Interactions at Conductive and Semiconductive Surfaces by Impedance Spectroscopy: Routes to Impedimetric Immunosensors, DNA-sensors, and Enzyme Biosensors, Electroanalysis, 15, 2003, pp. 913–947.

[190] F. Mollarasouli, S. Kurbanoglu, S. A. Ozkan, The Role of Electrochemical Immunosensors in Clinical Analysis, Biosensors (Basel), Vol.9, No.3, 2019, 86.

[191] E. B. Bahadir, M. K. Sezgintürk, A. Review on Impedimetric Biosensors, Artificial Cells, Nanomedicine, and Biotechnology, Vol.44, 2016, pp. 248–262.

[192] J. S. Daniels, N. Pourmand, Label-Free Impedance Biosensors: Opportunities and Challenges, Electroanalysis, Vol.19, 2007, pp. 1239–1257.

[193] M. Prodromidis, Impedimetric Biosensors and Immunosensors. Proceeding Book of 2nd International Conference on Applied Engineering and Natural Sciences, Vol.8, 2007, pp. 69–71.

[194] A. Ravalli, G. Marrazza, Electrochemical-Based Biosensor Technologies in Disease Detection and Diagnostics, In Biosensors and Nanotechnology; Z. Altintas, Ed.; Wiley: Hoboken, NJ, USA, pp. 95–124, 2018.

[195] M. Masikini, S. N. Mailu, A. Tsegaye, N. Njomo, K. M. Molapo, C. O. Ikpo, C. E. Sunday, C. Rassie, L. Wilson, P. G. L., Baker, E. I. Iwuoha, A Fumonisins Immunosensor Based on Polyanilino-Carbon Nanotubes Doped with Palladium Telluride Quantum Dots, Sensors, Vol.15, No.1, 2015, pp. 529–546.

[196] H. Bhardwaj, C. Singh, R. K. Kotnala, G. Sumana, Graphene Quantum Dots-Based Nano-Biointerface Platform for Food Toxin Detection, Analytical and Bioanalytical Chemistry, Vol.410, 2018, pp. 7313–7323.

[197] M. Zhao, Direct Synthesis of Graphene Quantum Dots with Different Fluorescence Properties by Oxidation of Graphene Oxide Using Nitric Acid, Applied Sciences, Vol.8, No.8, 2018, 1303.

[198] A. B. Ganganboina, R. Doong, Graphene Quantum Dots Decorated Gold-Polyaniline Nanowire for Impedimetric Detection of Carcinoembryonic Antigen, Nature, Vol.9, 2019, 7214.

[199] A. D. Chowdhury, K. Takemura, T.-C. Li, T. Suzuki, E. Y. Park, Electrical Pulse-Induced Electrochemical Biosensor for Hepatitis E Virus Detection, Nature Communications, Vol.10, 2019, pp. 4–7.

[200] S.M. Taghdisi, N.M. Danesh, M. Ramezani, N. Ghows, S.A.M. Shaegh, K. Abnous, A novel fluorescent aptasensor for ultrasensitive detection of microcystin-LR based on single-walled carbon nanotubes and dapoxyl, Talanta 166 (2017) 187–192.

[201] L. Lebogang, J. Jantra, M. Hedstr¨om, B. Mattiasson, Electrochemical flow-ELISA for rapid and sensitive determination of microcystin-LR using automated sequential injection system, Sensors 17 (2017) 1639.

[202] S. G. Ramaraj, A. Alrebh, D. Elamaran, H. Zhou, K. Huang, M. Almansoori, H. Yamahara, H. Tabata, Surface Acoustic Wave Gas Sensors: Recent Developments and Their Role in Sensing Technology, Materials Science and Engineering B-Advanced Functional Solid-State Materials, Vol.317, 2025, 118157.

[203] Y. A. Kumar, T. Ramachandran, A. Ghosh, A. G. Al-Sehemi, N. P. Reddy, M. A. Moniruzzaman, Review on In-Plane ordered MXenes-Based Materials in Addressing Challenges Faced by Biosensor Applications, Journal of Energy Storage, Vol.121, 2025, 116507.

[204] R. Jayabal, Addressing Challenges in Marine Ecosystems: Advanced Strategies for Wastewater Effluent Management and Contaminated Sediment Remediation, Results in Engineering, 2025, 104638.

[205] A. Chaouiki, M. Chafiq, N. Elboughdiri, I. Mahariq, J. H. Kang, Y.G. Ko, M. Abboud, Understanding Nanoscale Transport in Confined Spaces: Protecting Encapsulated Guests with Metal-Organic Frameworks, Applied Materials Today, Vol.44, 2025, 102676.

[206] I. Y. Massey, P. Wu, J. Wei, J. Luo, P. Ding, H. Wei, F. Yang, A Mini-Review on Detection Methods of Microcystins, Toxins (Basel), Vol.12, Nol.10, 2020, 641.

[207] V. Naresh, N. Lee, A Review on Biosensors and Recent Development of Nanostructured Materials-Enabled Biosensors, Sensors Vol.21, 2021, 1109.

[208] E. O. Polat, M. M. Cetin, A. F. Tabak, E. Bilget Güven, B. O. Uysal, T. Arsan, A. Kabbani, H. Hamed, S. B. Gül, Transducer Technologies for Biosensors and Their Wearable Applications, Biosensors (Basel), Vol.12, 2022, 385.

[209] M. Lee, S. H. Kim, D. Kim, H. J. Kim, Rapid and Easy Detection of Microcystin-LR Using a Bioactivated Multi-Walled Carbon Nanotube-Based Field-Effect Transistor Sensor, Biosensors (Basel), Vol.14, 2024, 37.

[210] R. Peltomaa, R. Barderas, E. Benito-Pena, M. C. Moreno-Bondi, Recombinant Antibodies and Their Use for Food Immunoanalysis, Analytical and Bioanalytical Chemistry, Vol.414, 2022, pp. 193–217.

[211] P. Bertani, W. Lu, Cyanobacterial Toxin Biosensors for Environmental Monitoring and Protection, Medicine in Novel Technology and Devices, Vol.10, 2021, 100059.

[212] I. Y. Massey, M. Al Osman, F. Yang, An Overview on Cyanobacterial Blooms and Toxins Production: Their Occurrence and

Influencing Factors, Toxin Reviews, Vol.41, 2022, pp. 326–346.

[213] A. O. Ogungbile, I. Ashur, I. Icin, O. H. Shapiro, S. Vernick, Rapid Detection and Quantification of Microcystins in Surface Water by an Impedimetric Immunosensor, Sensors and Actuators B: Chemical, Vol.348, 2021, 130687.

[214] S. Adjei-Nimoh, L. N. Rances, M. A. Tony, H. A. Nabwey, W. H. Lee, Rapid Microcystin-LR Detection using Antibody-Based Electrochemical Biosensors with a Simplified Calibration Curve Approach, Scientific Reports, Vol.14, 2024, 31968.

[215] J. Ozhikandathil, S. Badilescu, M. Packirisamy, Plasmonic Gold Decorated MWCNT Nanocomposite for Localized Plasmon Resonance Sensing, Scientific Reports, Vol.5, No.13181, 2015, pp. 1-11.

[216] E. G. Lee, K. M. Park, J. Y. Jeong, S. H. Lee, J. E. Baek, H. W. Lee, J. K. Jung, B. H. Chung, Carbon Nanotube-Assisted Enhancement of Surface Plasmon Resonance Signal, Analytical Biochemistry, Vol.408, No.2, 2011, pp. 206–211.

[217] N. Kakenov, O. Balci, S. Balci, C. Kocabas, Probing Molecular Interactions on Carbon Nanotube Surfaces Using Surface Plasmon Resonance Sensors, Applied Physics Letters, Vol.101, 2012, 223114.

[218] A. V. Ellis, K. Vijayamohanan, R. Goswami, N. Chakrapani, L. S. Ramanathan, P. M. Ajayan, G. Ramanath, Hydrophobic Anchoring of Monolayer-Protected Gold Nanoclusters to Carbon Nanotubes, Nano Letters, Vol.3, No.3, 2003, pp. 279–282.

[219] L. Jiang, L. Gao, Modified Carbon Nanotubes: An Effective Way to Selective Attachment of Gold Nanoparticles, Carbon, 41, 2003, pp. 2923–2929.

[220] Y. Ou, M. H. Huang, High-Density Assembly of Gold Nanoparticles on Multiwalled Carbon Nanotubes Using 1-Pyrenemethylamine as Interlinker, The Journal of Physical Chemistry B, 110, 2006, pp. 2031–2036.

[221] R. Zanella, E. V. Basiuk, P. Santiago, V. A. Basiuk, E. Mireles, I. Puente-Lee, J. M. Saniger, Deposition of Gold Nanoparticles onto Thiol-Functionalized Multiwalled Carbon Nanotubes, The Journal of Physical Chemistry B, Vol.109, No.34, 2005, pp. 16290–16295.

[222] H. C. Choi, M. Shim, S. Bangsaruntip, H. Dai, Spontaneous Reduction of Metal Ions on the Sidewalls of Carbon Nanotubes, Journal of the American Chemical Society, Vol.124, 2002, pp. 9058–9059.

[223] Y. Lin, K. A. Watson, M. J. Fallbach, S. Ghose, J. G. Smith Jr., D. M. Delozier, W. Cao, R. E. Crooks, J. W. Connell, Rapid, Solventless, Bulk Preparation of Metal Nanoparticle-Decorated Carbon Nanotubes, ACS Nano, Vol.3, No.4, 2009, pp. 871–884.

[224] Y. Zhang, H. Dai, Formation of Metal Nanowires on Suspended Single-Walled Carbon Nanotubes, Applied Physics Letters, Vol.77, 2000, pp. 3015–3017.

[225] J.-M. Yeh, K.-Y. Huang, S.-Y. Lin, Y.-Y., Wu, C.-C., Huang, S.-J., Liou, Noncovalent Interaction between Gold Nanoparticles and Multiwalled Carbon Nanotubes via an Intermediatory, Journal of Nanotechnology, 2009, Article ID 217469.

[226] R. Zhang, M. Hummelgård, H. Olin, Simple and Efficient Gold Nanoparticles Deposition on Carbon Nanotubes with Controllable Particle Sizes. Materials Science and Engineering B, Vol.158, 2009, pp. 48–52.

[227] L. Dobrzanski, M. Pawlyta, A. Krzton, B. Liszka, C. W. Tai, W. Kwasny, Synthesis and Characterization of Carbon Nanotubes Decorated with Gold Nanoparticles, Acta Physica Polonica A, Vol.118, No.3, 2010, pp. 483–486.

[228] X. Hou, L. Wang, X. Wang, Z. Li, Coating Multiwalled Carbon Nanotubes with Gold Nanoparticles Derived from Gold Salt Precursors, Diamond and Related Materials, Vol.20, 2011, pp. 1329–1332.

[229] V. Georgakilas, D. Gournis, V. Tzitzios, L. Pasquato, D. M. Guldi, M. Prato, Decorating Carbon Nanotubes with Metal or Semiconductor Nanoparticles, Journal of Materials Chemistry, Vol.17, No.26, 2007, pp. 2679–2694.

[230] A. Dobrzańska-Danikiewicz, D. Łukowiec, D. Cichocki, W. Wolany, Carbon Nanotubes Decorating Methods, Archives of Materials Science, Vol.54, 2013, pp. 53–61.

[231] L. Qu, L. Dai, Substrate-Enhanced Electroless Deposition of Metal Nanoparticles on Carbon Nanotubes, Journal of the American Chemical Society, Vol.127, 2005, pp. 10806–10807.

[232] L. Qu, L. Dai, E. Osawa, Shape/Size-Controlled Syntheses of Metal Nanoparticles for Site-Selective Modification of Carbon Nanotubes, Journal of the American Chemical Society, Vol.128, 2006, pp. 5523–5532.

[233] D. S. Kim, T. Lee, K. E. Geckeler, Hole- Doped Single- Walled Carbon Nanotubes: Ornamenting with Gold Nanoparticles in Water, Angewandte Chemie International Edition, Vol.45, 2006, pp. 104–107.

[234] K. Ding, Y. Wang, L. Liu, L. Liu, X. Zhang, Z. Guo, Hydrothermal Process Synthesized Electrocatalytic Multi-Walled Carbon Nanotubes-Inserted Gold Composite Microparticles toward Ethanol Oxidation Reaction, Journal of Applied Electrochemistry, Vol.43, 2013, pp. 567–574.

[235] E. Lorençon, A. S. Ferlauto, S. de Oliveira, D. R. Miquita, R. R. Resende, R. G. Lacerda, L. O. Ladeira, Direct Production of Carbon Nanotubes/Metal Nanoparticles Hybrids from a Redox Reaction between Metal Ions and Reduced Carbon Nanotubes, ACS Applied Materials & Interfaces, Vol.1, No.10, 2009, pp. 2104–2106.

[236] G. Lawson, F. Gonzaga, J. Huang, G. de Silveira, M. A. Brook, A. Adronov, Au–Carbon Nanotube Composites from Self-Reduction of Au3+ upon Poly (Ethylene Imine) Functionalized SWNT Thin Films, Journal of Materials Chemistry, Vol.18, No.14, 2008, pp. 1694–1702.

[237] L. Bokobza, J. Zhang, Raman Spectroscopic Characterization of Multi Wall Carbon Nanotubes and Composites, Express Polymer Letters, Vol.6, No.7, 2012, pp. 601-608.

[238] C. Zheng, M. Yin, B. Su, A. Peng, Z. Guo, X. Chen, X. Chen, A Novel Near-Infrared Light-Responsive Photoelectrochemical Platform for Detecting Microcystin-LR in Fish Based on Ag2S Cubes and Plasmonic Au Nanoparticles, Talanta, Vol.221, 2021,121447.

[239] V. Vogiazi, A. A. de la Cruz, E. A. Varughese, W. R. Heineman, R. J. White, D. D. Dionysiou, Sensitive Electrochemical Detection of Microcystin-LR in Water Samples via Target-Induced Displacement of Aptamer Associated [Ru(NH3)6]3+, ACS ES&T Engineering, Vol.1, 2021, pp. 1597–1605.

[240] J. Zhang, Z. Yang, B. Chai, L. Gao, J. Zhao, X. Xu, An Ultrasensitive Electrochemical Aptasensor for Microcystin-LR Detection Using Core-Satellite Gold Nanoparticle/Silver Nanocluster Nanoassemblies as Labels for Signal Amplification, Sensors & Actuators, B: Chemical, Vol.371, 2022, pp. 132586-132594.

[241] L. Zhou, R. Li, Z. Li, Q. Xia, Y. Fang, J. Liu, An Immunosensor for Ultrasensitive Detection of Aflatoxin B 1 with an Enhanced Electrochemical Performance Based on Graphene/Conducting Polymer/Gold Nanoparticles/the Ionic Liquid Composite Film on Modified Gold Electrode with Electrodeposition, Sensors & Actuators, B: Chemical, Vol.174, 2012, pp. 359–365.

[242] L. Reverté, B. Prieto-Simón, M. Campàs, New Advances in Electrochemical Biosensors for the Detection of Toxins: Nanomaterials, Magnetic Beads and Microfluidics Systems, A review, Analytica Chimica Acta, Vol.908, 2016, pp. 8–21.

[243] L. Hou, Y. Ding, L. Zhang, Y. Guo, M. Li, Z. Chen, X. Wu, An Ultrasensitive Competitive Immunosensor for Impedimetric Detection of Microcystin-LR via Antibody-Conjugated Enzymatic Biocatalytic Precipitation, Sensors & Actuators, B: Chemical, Vol.233, 2016, pp. 63–70.

[244] C. Gan, L. Ling, Z. He, H. Lei, Y. Liu, In-Situ Assembly of Biocompatible Core–Shell Hierarchical Nanostructures Sensitized Immunosensor for Microcystin-LR Detection, Biosensors & Bioelectronics, Vol.78, 2016, pp. 381–389.

[245] Z. He, J. Wei, C. Gan, W. Liu, Y. Liu, A Rolling Circle Amplification Signal-Enhanced Immunosensor for Ultrasensitive Microcystin-LR Detection Based on a Magnetic Graphene Functionalized Electrode, RSC Advances, Vol.7, No.63, 2017, pp. 39906–39913.

[246] P. Pang, X. Teng, M. Chen, Y. Zhang, H. Wang, C. Yang, W. Yang, C. J. Barrow, Ultrasensitive Enzyme-Free Electrochemical Immunosensor for Microcystin-LR Using Molybdenum Disulfide/Gold Nanoclusters Nanocomposites as Platform and Au@Pt Core-Shell Nanoparticles as Signal Enhancer, Sensors & Actuators, B: Chemical, Vol.266, 2018, pp. 400–407.

[247] J. Tian, H. Zhao, F. Yuan, X. Quan, S. Chen, Ultrasensitive Immunoassay of Microcystins-LR Using G-Quadruplex DNAzyme as an Electrocatalyst, International Journal of Environmental Analytical Chemistry, Vol.94, No.10, 2014, pp. 988–1000.

[248] C. Gan, B. Wang, J. Huang, A. Qileng, Z. He, H. Lei, W. Liu, Y. Liu,

Multiple Amplified Enzyme Free Electrochemical Immunosensor Based on g-Quadruplex/Hemin Functionalized Mesoporous Silica with Redox-Active Intercalators for Microcystin-LR Detection, Biosensors & Bioelectronics, Vol.98, 2017, pp. 126–133.

[249] H. W. Yu, J. Lee, S. Kim, G. H. Nguyen, I. S. Kim, Electrochemical Immunoassay Using Quantum Dot/Antibody Probe for Identification of Cyanobacterial Hepatotoxin Microcystin-LR, Analytical and Bioanalytical Chemistry, 394(8), 2009, pp. 2173–2181.

[250] X. Fu, Y. Feng, S. Niu, C. Zhao, M. Yang, Y. Yang, Sensitive Detection of Microcystin-LR by Using a Label-Free Electrochemical Immunosensor Based on Au Nanoparticles/Silicon Template/Methylene Blue Nanocomposite, Journal of Nanoscience and Nanotechnology, Vol.13, No.12, 2013, pp. 8245–8252.

[251] X. Fu, C. Zhao, X. Liu, J. Zhao, X. Niu, L. Zheng, Y. Yang, A Layer-by-Layer Assembly Label-Free Electrochemical Immunosensor for the Detection of Microcystin-LR Based on CHIT/PAMAM Dendrimer/Silver Nanocubes, International Journal of Environmental Analytical Chemistry, Vol.96, No.3, 2016, pp. 284–297.

[252] X. Sun, H. Shi, H. Wang, L. Xiao, L. Li, A Simple, Highly Sensitive, and Label-Free Impedimetric Immunosensor for Detection of Microcystin-LR in Water, Analytical Letters, Vol.43, No.4, 2010, pp. 533–544.

[253] G. Sun, J. Lu, S. Ge, X. Song, J. Yu, M. Yan, J. Huang, Ultrasensitive Electrochemical Immunoassay for Carcinoembryonic Antigen Based on Three-Dimensional Macroporous Gold Nanoparticles/Graphene Composite Platform and Multienzyme Functionalized Nanoporous Silver Label, Analytica Chimica Acta, Vol.775, 2013a, pp. 85-92.

[254] H. Sun, L. Wu, W. Wei, X. Qu, Recent Advances in Graphene Quantum Dots for Sensing, Materials Today, Vol.16, 2013b, pp. 433–442.

[255] V. Vogiazi, A. de la Cruz, S. Mishra, V. Shanov, W. R. Heineman, D. Dionysios D. D. Dionysiou, A Comprehensive Review: Development of Electrochemical Biosensors for Detection of Cyanotoxins in Freshwater, ACS Sensors, Vol.4, No.5, 2019, pp. 1151–1173.

[256] S. Loyprasert, P. Thavarungkul, P. Asawatreratanakul, B. Wongkittisuksa, C. Limsakul, P. Kanatharana, Label-Free Capacitive Immunosensor for Microcystin-LR Using Self-Assembled Thiourea Monolayer Incorporated with Ag Nanoparticles on Gold Electrode, Biosensors & Bioelectronics, Vol.24, No.1, 2008, pp. 78–86.

[257] S. Dawan, P. Kanatharana, B. Wongkittisuksa, W. Limbut, A. Numnuam, C. Limsakul, P. Thavarungkul, Label-Free Capacitive Immunosensors for Ultra-Trace Detection Based on the Increase of Immobilized Antibodies on Silver Nanoparticles, Analytica Chimica Acta, Vol.699, 2011, pp. 232–241.

[258] S. Bratakou, G. P. Nikoleli, C. G. Siontorou, D. P. Nikolelis, S. Karapetis, N. Tzamtzis, Development of an Electrochemical Biosensor for the Rapid Detection of Saxitoxin Based on Air Stable Lipid Films with Incorporated Anti-STX Using Graphene Electrodes, Electroanalysis, Vol.29, No.4, 2017, pp. 990–997.

[259] Z. Lin, H. Huang, Y. Xu, X. Gao, B. Qiu, X. Chen, G. Chen, Determination of Microcystin-LR in Water by a Label-Free Aptamer Based Electrochemical Impedance Biosensor, Talanta, 103, 2013, pp. 371–374.

[260] F. Yan, A. Erdem, B. Meric, K. Kerman, M. Ozsoz, O. A. Sadik, Electrochemical DNA Biosensor for the Detection of Specific Gene Related to Microcystis Species, Electrochemistry Communications, Vol.3, No.5, 2001, pp. 224–228.

[261] A. Erdem, K. Kerman, B. Mer, D. Ozkan, P. Kara, O. Oz, DNA Biosensor for Microcystis spp. Sequence Detection by Using Methylene Blue and Ruthenium complex as electrochemical hybridization Labels, Turkish Journal of Chemistry, Vol.26, 2002, pp. 851–862.

[262] I. O. K'Owino, S. K. Mwilu, O. A. Sadik, Metal-Enhanced Biosensor for Genetic Mismatch Detection, Analytical Biochemistry, Vol.369, No.1, 2007, pp. 8–17.

[263] E. Valério, L. M. Abrantes, A. S. Viana, 4-Aminothiophenol Self-Assembled Monolayer for the Development of a DNA Biosensor Aiming the Detection of Cylindrospermopsin Producing

Cyanobacteria, Electroanalysis, Vol.20, No.22, 2008, pp. 2467–2474.

[264] M. Lan, C. Chen, Q. Zhou, Y. Teng, H. Zhao, X. Niu, Voltammetric Detection of Microcystis Genus Specific-Sequence with Disposable Screen-Printed Electrode Modified with Gold Nanoparticles, Advanced Materials Letters, Vol.1, No.3, 2010, pp. 217–224.

[265] T. G. Drummond, M. G. Hill, J. K. Barton, Electrochemical DNA Sensors, Nature Biotechnology, Vol.21, No.10, 2003, pp. 1192–1199.

[266] S. Shahrokhian, M. Shamloofard, R. Salimian, Investigation of the Electrochemical Behavior of Tizanidine on the Surface of Glassy Carbon Electrode Modified with Multi-Walled Carbon Nanotube/Titan Yellow-Doped Polypyrrole, Journal of Electroanalytical Chemistry, Vol.823, 2018, pp. 146–154.

[267] E. Laviron, Adsorption, Autoinhibition and Autocatalysis in Polarography and in Linear Potential Sweep Voltammetry, Journal of Electroanalytical Chemistry and Interfacial Electrochemistry, Vol.52, No.3, 1974, pp. 355–393.

[268] C. Ye, X. Chen, D. Zhang, J. Xu, H. Xi, T. Wu, D. Deng, C. Xiong, J. Zhang, G. Huang, Study on the Properties and Reaction Mechanism of Polypyrrole@Norfloxacin Molecularly Imprinted Electrochemical Sensor Based on Three-Dimensional CoFe-MOFs/AuNPs, Electrochimica Acta, Vol.379, 2021, 138174.

[269] W. H. Qiao, L., Wang, H. C. Li, G. P. Li, J. J. Li, B. X. Ye, Electrochemical Behavior of Tectoridin and Its Sensitive Determination Based on L-arginine Modified Electrode, Talanta, Vol.144, 2015, pp. 726–733.

[270] L. Wang, W. Chen, D. Xu, B. S. Shim, Y. Zhu, F. Sun, L. Liu, C. Peng, Z. Jin, C. Xu, Simple, Rapid, Sensitive, and Versatile SWNT-Paper Sensor for Environmental Toxin Detection Competitive with ELISA, Nano Letters, Vol.9, No.12, 2009, pp. 4147–4152.

[271] J. P. Mensing, C. Poochai, S. Kerdpocha, C. Sriprachuabwong, A. Wisitsoraat, A. Tuantranont, Advances in Research on 2D and 3D Graphene-Based Supercapacitors, Advances in Natural Sciences: Nanoscience and Nanotechnology, Vol.8, 2017, pp. 2–9.

[272] S. Mishra, H. Nguyen, P. K., Adusei, Y. Y. Hsieh, V. Shanov, Plasma Enhanced Synthesis of N Doped Vertically Aligned Carbon Nanofibers on 3D Graphene, Surface and Interface Analysis, Vol.51, No.2, 2019, pp. 290– 297.

[273] C. Zhu, Z. Zeng, H. Li, F. Li, C. Fan, H. Zhang, Single-Layer MoS2-Based Nanoprobes for Homogeneous Detection of Biomolecules, Journal of the American Chemical Society, Vol.135, No.16, 2013, pp. 5998–6001.

[274] J. Lv, S. Zhao, S. Wu, Z. Wang, Upconversion Nanoparticles Grafted Molybdenum Disulfide Nanosheets Platform for Microcystin-LR Sensing, Biosensors & Bioelectronics, Vol.90, 2017, pp. 203-209.

[275] X. Qin, Y. Wang, B. Song, X. Wang, H. Ma, J. Yuan, Homogeneous Time-Resolved Fluoroimmunoassay of Microcystin-LR Using Layered WS2 Nanosheets as a Transducer, Methods and Applications in Fluorescence, Vol.5, No.2, 2017, 024007.

[276] G. Ertürk, B. Mattiasson, Capacitive Biosensors and Molecularly Imprinted Electrodes, Sensors, Vol.17, No.2, 2017, 390.

[277] W. Chen, G. Lv, W. Hu, D. Li, S. Chen, Z. Dai, Synthesis and Applications of Graphene Quantum Dots: A Review, Nanotechnology Reviews, Vol.7, 2018, pp. 157–185.

[278] L. Reverté, D. Garibo, C. Flores, J. Diogène, J. Caixach, M. Campàs, Magnetic Particle-Based Enzyme Assays and Immunoassays for Microcystins: from Colorimetric to Electrochemical Detection, Environmental Science & Technology, Vol.47, No.1, 2013, pp. 471–478.

[279] S. Ge, W. Liu, L. Ge, M. Yan, J. Yan, J. Huang, J. Yu, In Situ Assembly of Porous Au-Paper Electrode and Functionalization of Magnetic Silica Nanoparticles with HRP via Click Chemistry for Microcystin-LR Immunoassay, Biosensors & Bioelectronics, Vol.49, 2013, pp. 111–117.

[280] N. Bouaïcha, C. O. Miles, D. G. Beach, Z. Labidi, A. Djabri, N. Y. Benayache, T. Nguyen-Quang, Structural Diversity, Characterization and Toxicology of Microcystins, Toxins (Basel), Vol.11, No.12, 2019, 714.

[281] Editorial, Nanomaterials Definition Matters, The Definition and Classification of Nanomaterials in Regulations Leave too

Much Room for Interpretation, Nature Nanotechnology, Vol.14, 2019, pp. 193.

[282] L. Fan, R. Wu, J. J. Huang, P. Ravi Selvaganapathy, One-Step Fabrication of the Novel Electrochemical Sensing Platform for the Ultrasensitive Determination of Microcystin-LR, Sensors & Actuators: B. Chemical, Vol.390, No.133961, 2023, pp. 1-10.

[283] L. Chen, R. Tan, Y. Zhou, L. Zhang, S. Zhang, X. Li, Y. Cong, H. Li, P. Sun, H. Ueda, J. Dong, Development of an Open Sandwich ELISA for the Detection of Microcystin-LR, Microchemical Journal, Vol.158, 2020, 105325.

[284] Y. Li, S. Si, F. Huang, J. Wei, S. Dong, F. Yang, H. Li, S. Liu, Ultrasensitive Label-Free Electrochemical Biosensor for Detecting Linear Microcystin-LR Using Degrading Enzyme MlrB as Recognition Element, Bioelectrochemistry, Vol.144, 2022, 108000.

[285] A. P. M. Antonyraj, P. Nainangu, A. Sundaram Ganeshraja, A. Guru, K. Subramanian, M. D. Tanwar, V. Parimelazhagan, A. S. K. Kumar, Recent Advancements in Microcystin Detection: A Comprehensive Review of Immunosensors and Nucleic Acid-Based Biosensors for Efficient Monitoring in Drinking Water and Human Samples, Talanta Open, Vol.12, 2025, 100495.

[286] C. Hu, N. Gan, Y. Chen, L. Bi, X. Zhang, L. Song, Detection of Microcystins in Environmental Samples Using Surface Plasmon Resonance Biosensor, Talanta, Vol.80, 2009, pp. 407–410.

[287] M. Liu, H. Zhao, S. Chen, H. Yu, X. Quan, Colloidal Graphene as a Transducer in Homogeneous Fluorescence-Based Immunosensor for Rapid and Sensitive Analysis of Microcystin-LR, Environmental Science & Technology, Vol.46, 2012, pp. 12567–12574.

[288] C. Murphy, E. Stack, S. Krivelo, D. A. McPartlin, B. Byrne, C. Greef, M. J. Lochhead, G. Husar, S. Devlin, C. T. Elliott, R. J. O'Kennedy, Detection of the Cyanobacterial Toxin, Microcystin-LR, Using a Novel Recombinant Antibody-Based Optical-Planar Waveguide Platform, Biosensors & Bioelectronics, Vol.67, 2015, pp. 708–714.

[289] Z. Qi, R. Lu, S. Wang, C. Xiang, C. Xie, M. Zheng, X. Tian, X. Xu, Selective Fluorometric Determination of Microcystin-LR Using a Segment Template Molecularly Imprinted by Polymer-Capped Carbon Quantum Dots, Microchemical Journal, Vol.161, 2021, 105798.

[290] H. He, L. Zhou, Y. Wang, C. Li, J. Yao, W. Zhang, Q. Zhang, M. Li, H. Li, W. Dong, Detection of Trace Microcystin-LR on a 20 MHz QCM Sensor Coated with in Situ Self-Assembled MIPs, Talanta, Vol.131, 2015, pp. 8–13.

[291] K. Chen, M. Liu, G. Zhao, H. Shi, L. Fan, S. Zhao, Fabrication of a Novel and Simple Microcystin-LR Photoelectrochemical Sensor with High Sensitivity and Selectivity, Environmental Science & Technology, Vol.46, 2012, pp. 11955–11961.

[292] R. B. Queirós, J. P. Noronha, P. V. S. Marques, J. S. Fernandesd, M. G. F. Sales, Determination of Microcystin-LR in Waters in the Subnanomolar Range by Sol–gel Imprinted Polymers on Solid Contact Electrodes, Analyst, Vol.137, 2012, pp. 2437–2444.

Contribution of Individual Authors to the Creation of a Scientific Article (Ghostwriting Policy)

Prof. Dr. Delia Teresa Sponza and Post-Dr. Rukiye Öztekin took an active role in every stage of the preparation of this article.
The authors equally contributed in the present research, at all stages from the formulation of the problem to the final findings and solution.

Sources of Funding for Research Presented in a Scientific Article or Scientific Article Itself

The experimental phases of this research study were conducted at the National Research Council (NRC) of Canada, Research Centers, Ontario, Canada. The authors would like to thank this body for providing financial support.

Conflict of Interest

The authors have no conflicts of interest to declare that are relevant to the content of this article.

APPENDIX

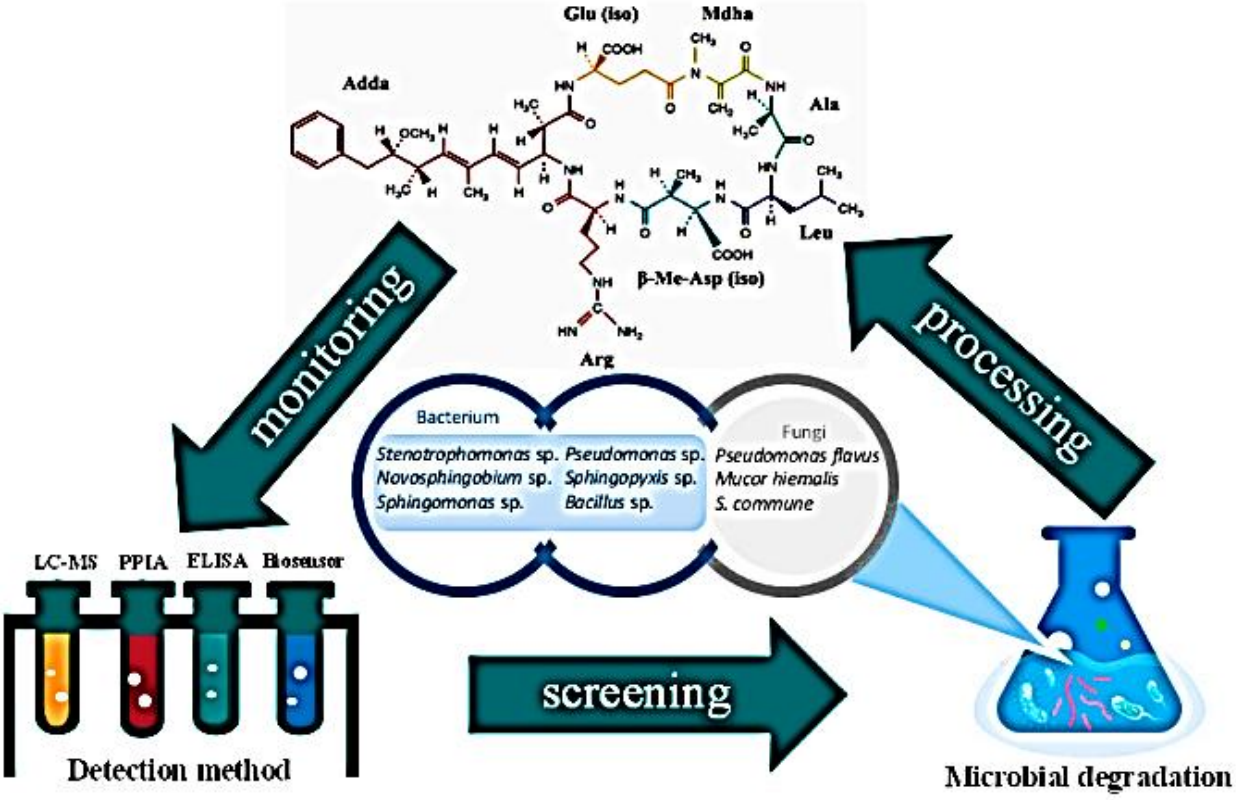

Fig. 1: The engineering system of MCs microbial degradation, [39]

Table 1. Comparative summary table

MC Detection Methods	**Nanomaterials Used**	**Sensor Configurations**	**Detection Limits**
Protein phosphatase inhibition assays (PPIA)	Gold NPs (Au NPs)	Electrochemical sensors	0.005 – 20 µg/l
Enzyme-linked immunosorbent assays (ELISA)	Multiwalled carbon nanotubes (MWCNTs)	Cyclic voltammetry (CV)	0.004 – 20 µg/l
High performance liquid chromatography (HPLC)	Graphene quantum dots (GQDs)	Linear scanning voltametry (LSV)	0.003 – 20 µg/l
Liquid chromatography-mass spectrometry (LC-MS)	AuNPs@MWCNTs/GQDs	Differential pulse voltammetry (DPV)	0.002 – 60 µg/l
Biosensors		Square wave voltammetry (SWV)	0.003 – 30 µg/l
		Voltammetric aptasensor	0.003 – 25 µg/l
		Biosensor	0.003 – 20 µg/l
		Biomedical GQDs sensors (a) Voltammetric GQD sensors (b) Amperometric GQD sensors (c) Impedimetric GQD sensors	 0.002 – 25 µg/l 0.002 – 20 µg/l 0.003 – 25 µg/l
		Electrochemical biosensors (a) Label-based immunosensors (b) Label-free immunosensors (c) DNA and Aptasensors (c1) aptasensors (c2) DNA Biosensors	 0.004 – 28 µg/l 0.004 – 27 µg/l 0.004 – 20 µg/l 0.004 – 20 µg/l 0.003 – 20 µg/l

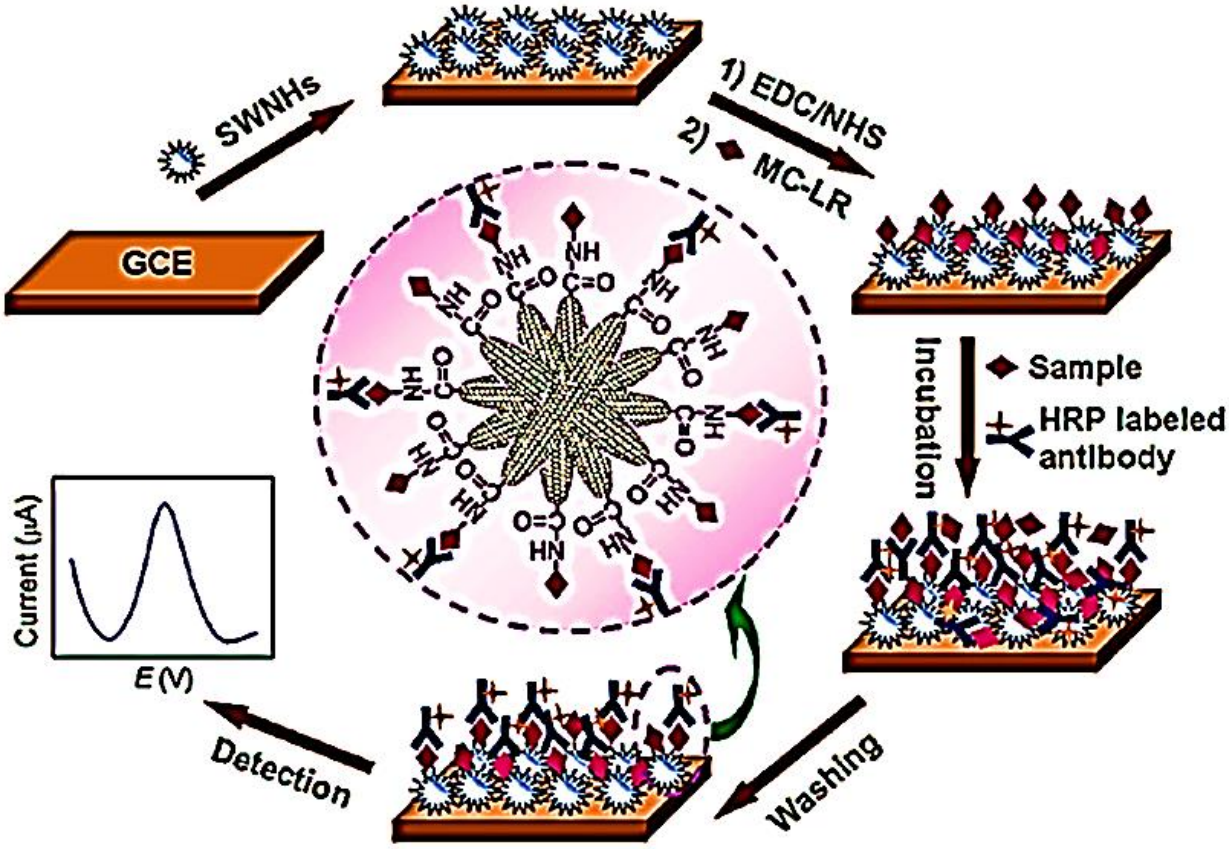

Fig. 2: The MC-LR immunosensor preparation and detection procedure [EDC: 1-ethyl-3-(3-dimethylaminopropyl) carbodiimide, GCE: Glassy-carbon electrode; HRP: horseradish peroxidase, NHS: N-hydroxysuccinimide, SWNH: single-walled carbon nanohorn], [42], [43]

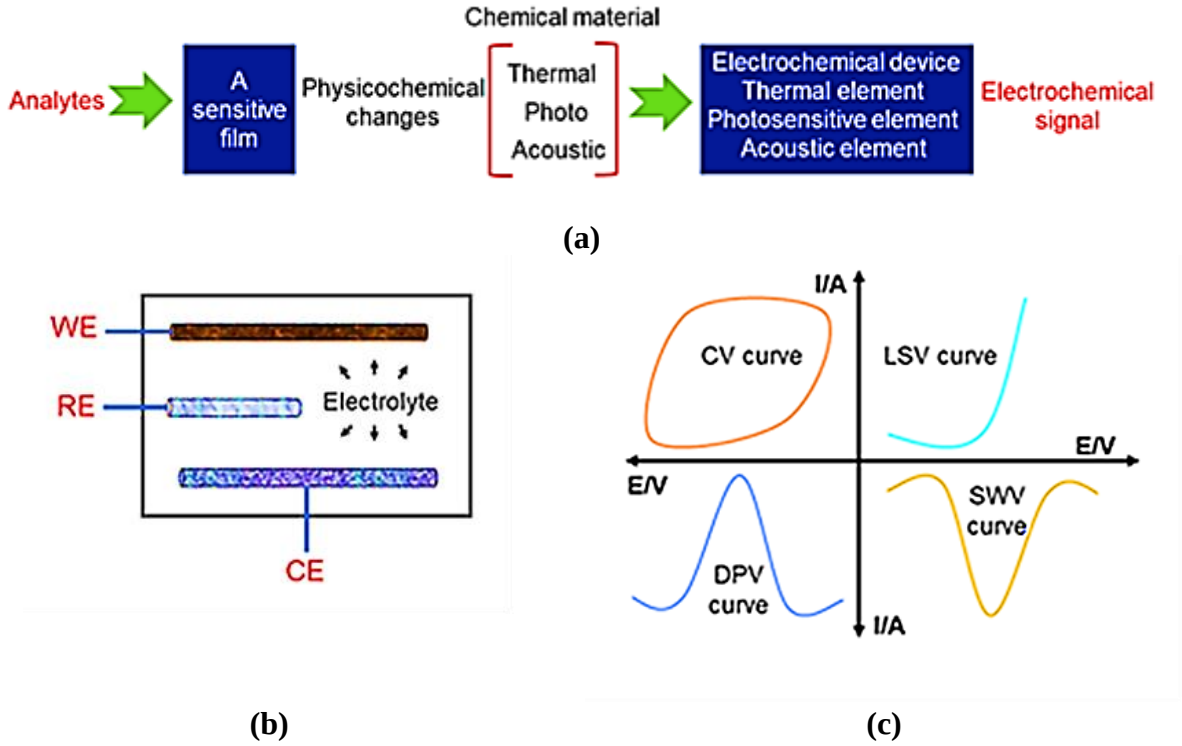

Fig. 3: The electrochemical sensors principle and test methods: (a) an electrochemical sensor detection principle, (b) an electrochemical sensor basic configuration and (c) the diagrams of cyclic voltammetry (CV), linear sweep voltammetry (LSV), differential pulse voltammetry (DPV), and square wave voltammetry (SWV) curves, respectively, [44]

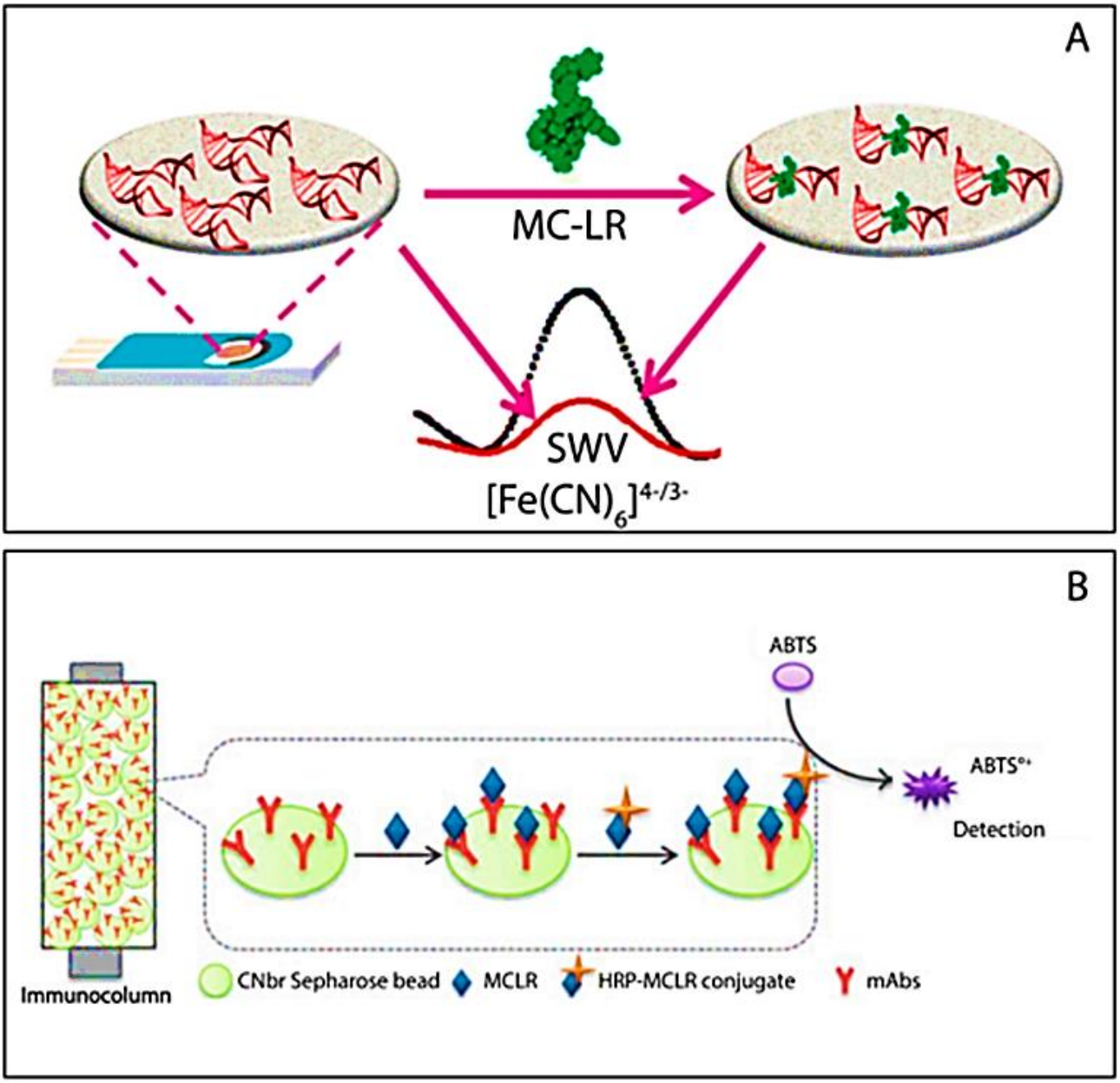

Fig. 4: Schematic configuration of (A) MC-LR detection based on SWV on aptamer-functionalized GSPE schematic diagram, [6], and (B) the extraction taking place in the immunocolumn, [80]

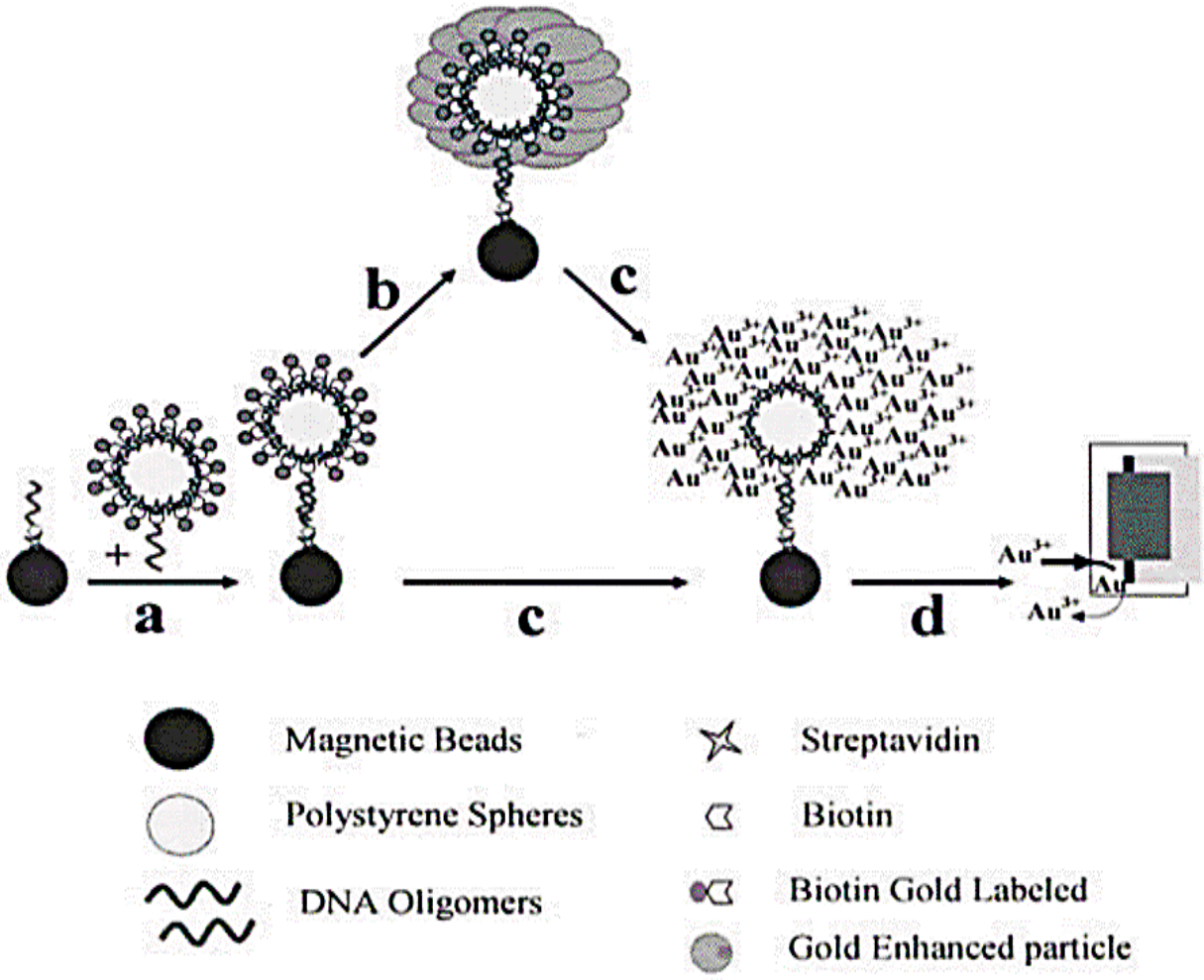

Fig. 5: Enhanced analytical protocol: (a) hybridization event, (b) catalytic enlargement, (c) Au dissolution and (d) stripping detection, respectively, [88]

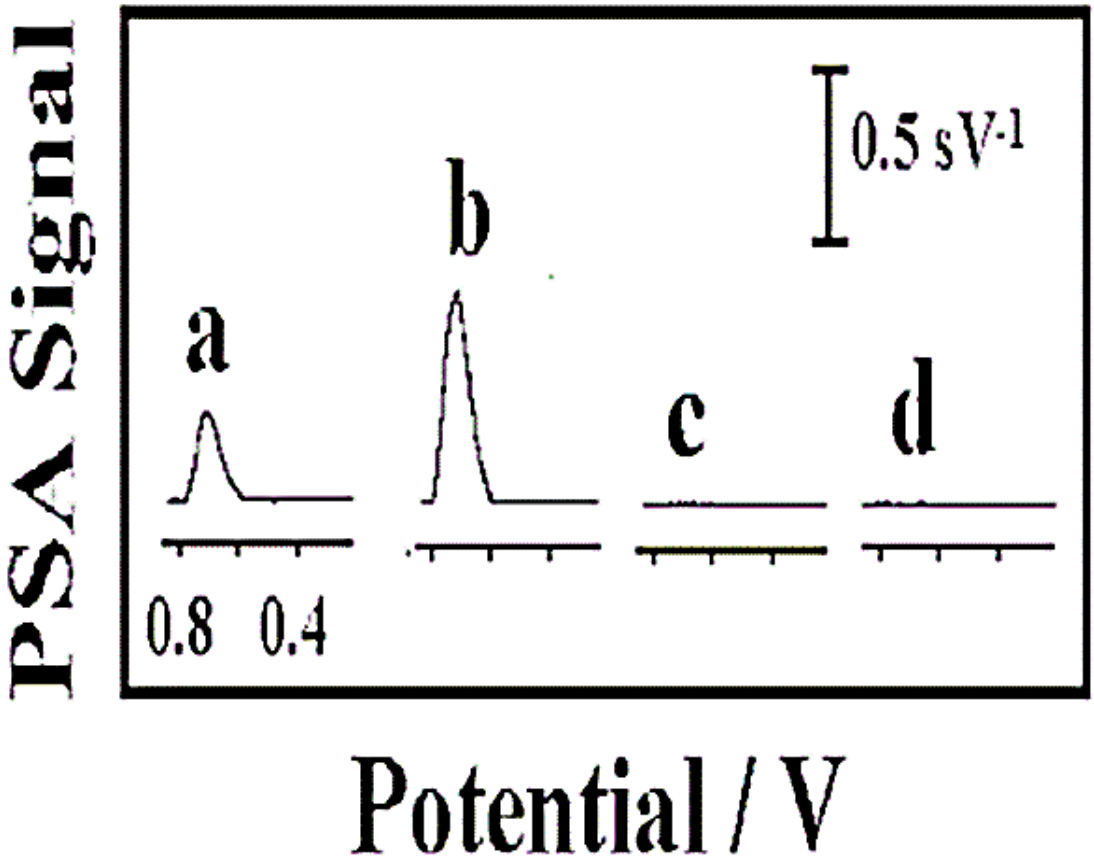

Fig. 6: Chronoamperometric stripping hybridization response of the single- (a) and multi- (b-d) particle protocols to (a) 500 ng/ml target, (b) 1 ng/ml target, (c) 1000 ng/ml non-complementary DNA and (d) control solution containing 20 µg Au-tagged beads, [88]

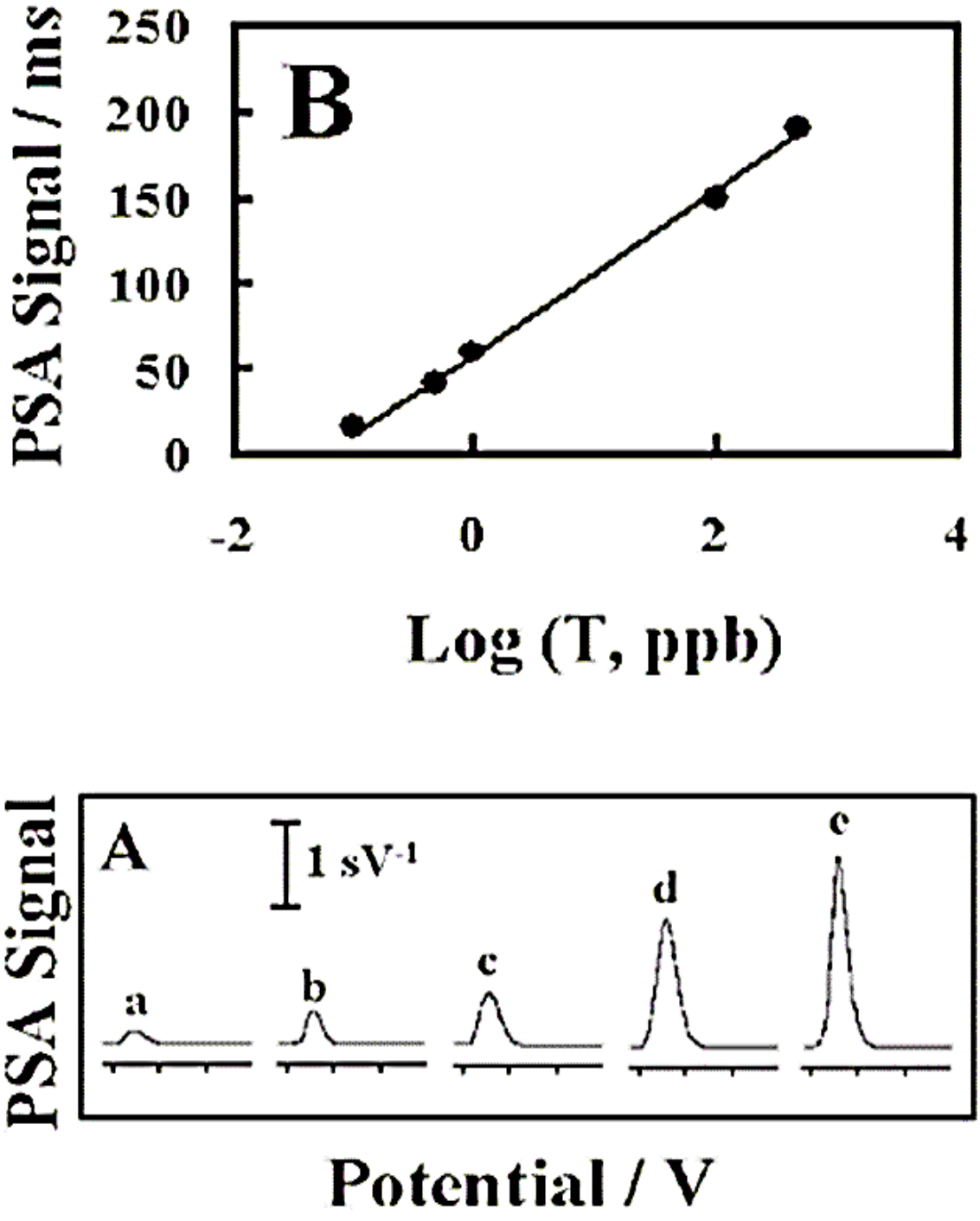

Fig. 7: Chronoamperometric signal for increased E908X-WT DNA level: (a) 0.1 ng/ml, (b) 0.5 ng/ml, (c) 1.0 ng/ml, (d) 100 ng/ml and (e) 500 ng/ml, respectively, [88]

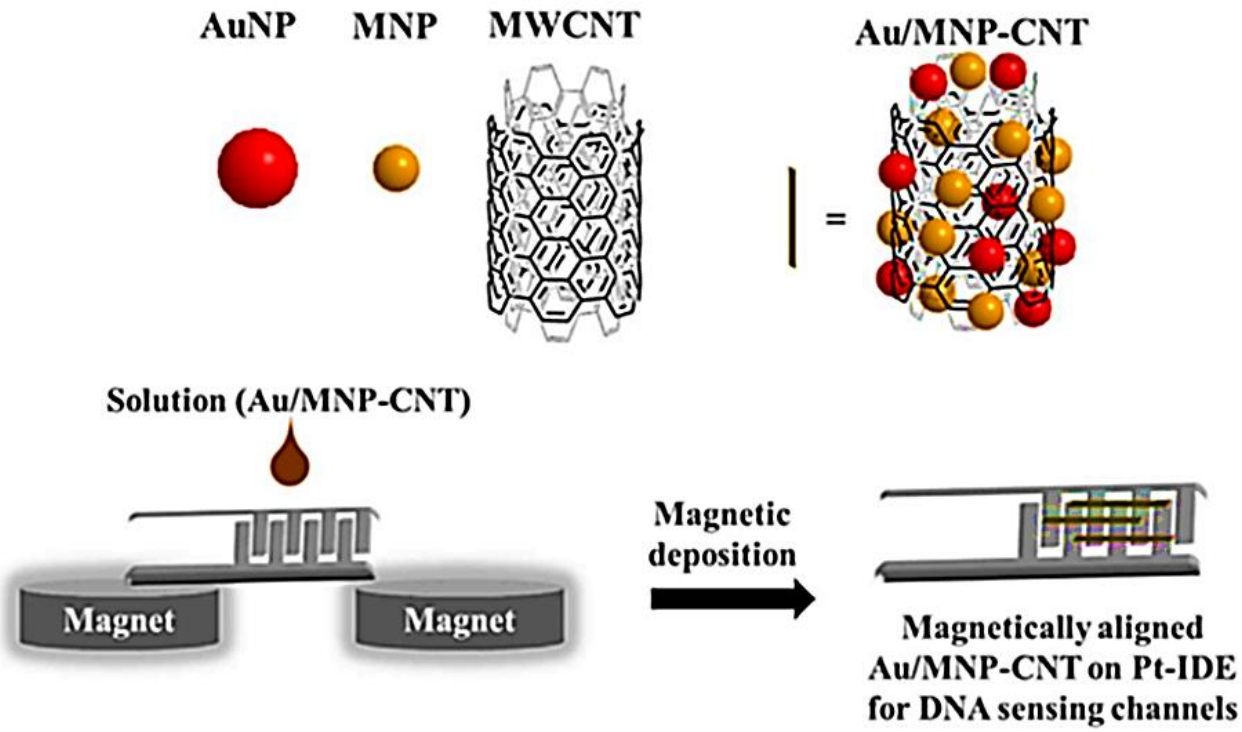

Fig. 8: Demonstration of production of magnetically aligned Au/magnetic NPs decorated with CNT on Pt-IDE for the virus DNA detection platform, [117]

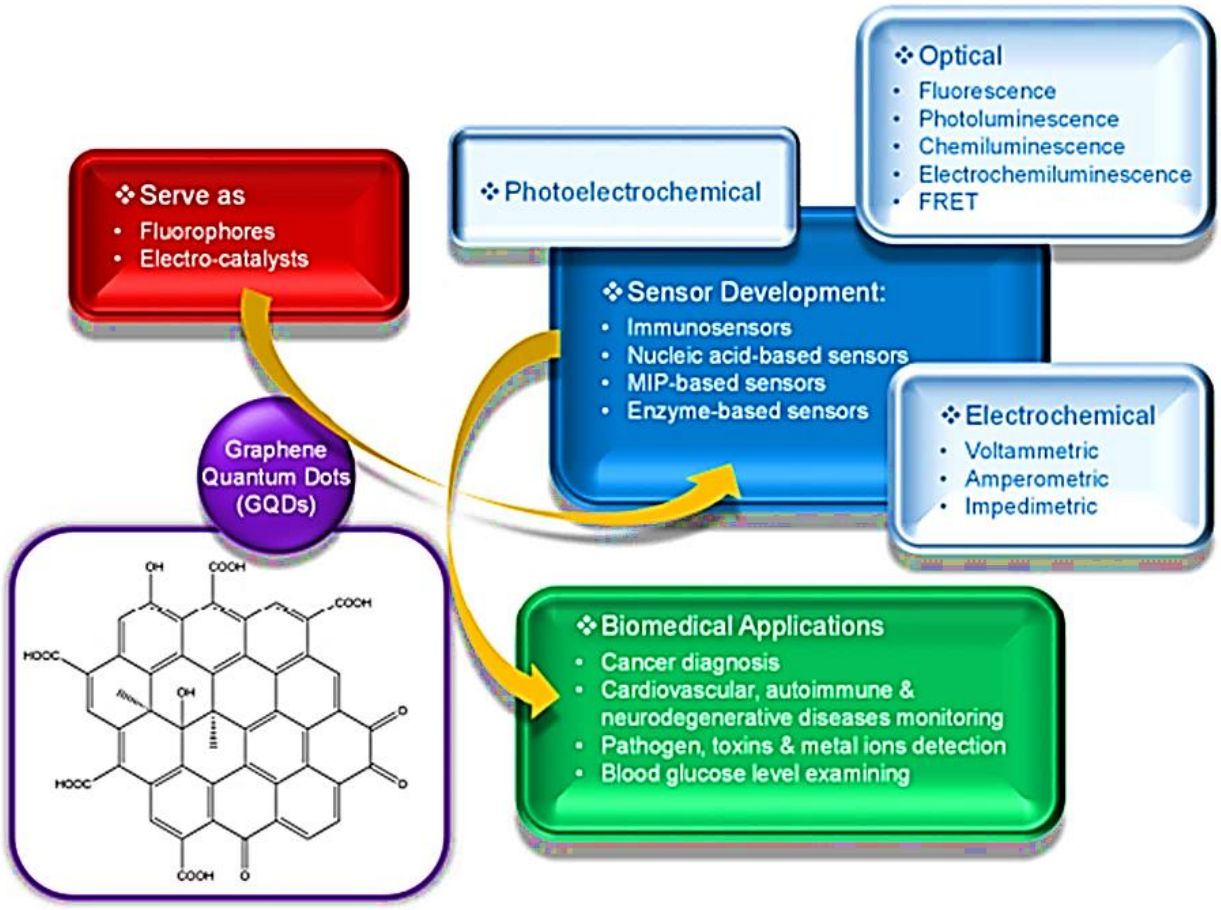

Fig. 9: Chemical structure and biomedical applications of GQDs in sensor development with GQDs, [154]

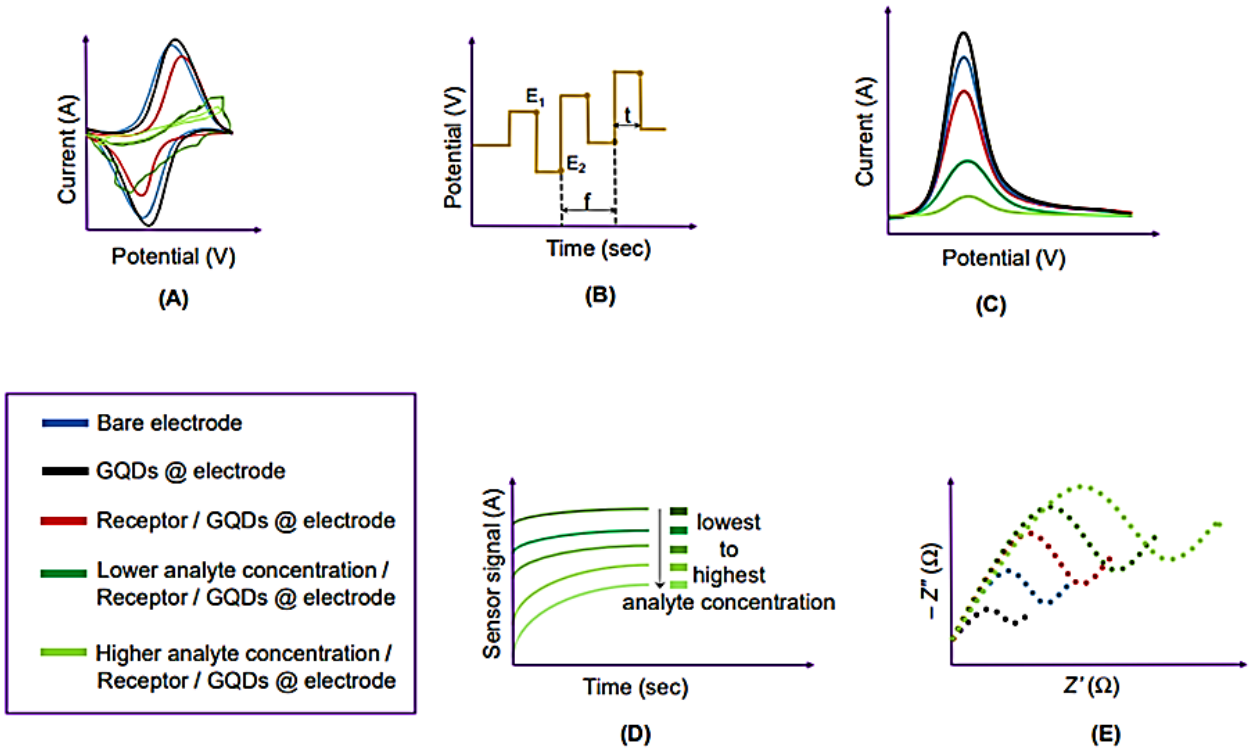

Fig. 10: (A) Cyclic voltammetry (CV), (B) Square wave voltammetry (SWV): where; t: time required for each pulse, f: frequency of each pulse, E1 and E2: initial and final pulse, respectively, (C) Target biomolecule detection by GQD-coated electrode based on SWV, (D) Ideal curves observed with amperometric measurements for varied concentrations of target biomolecules and (E) Electron impedance spectroscopy (EIS): a target analyte (i.e., Nyquist plot), [151]

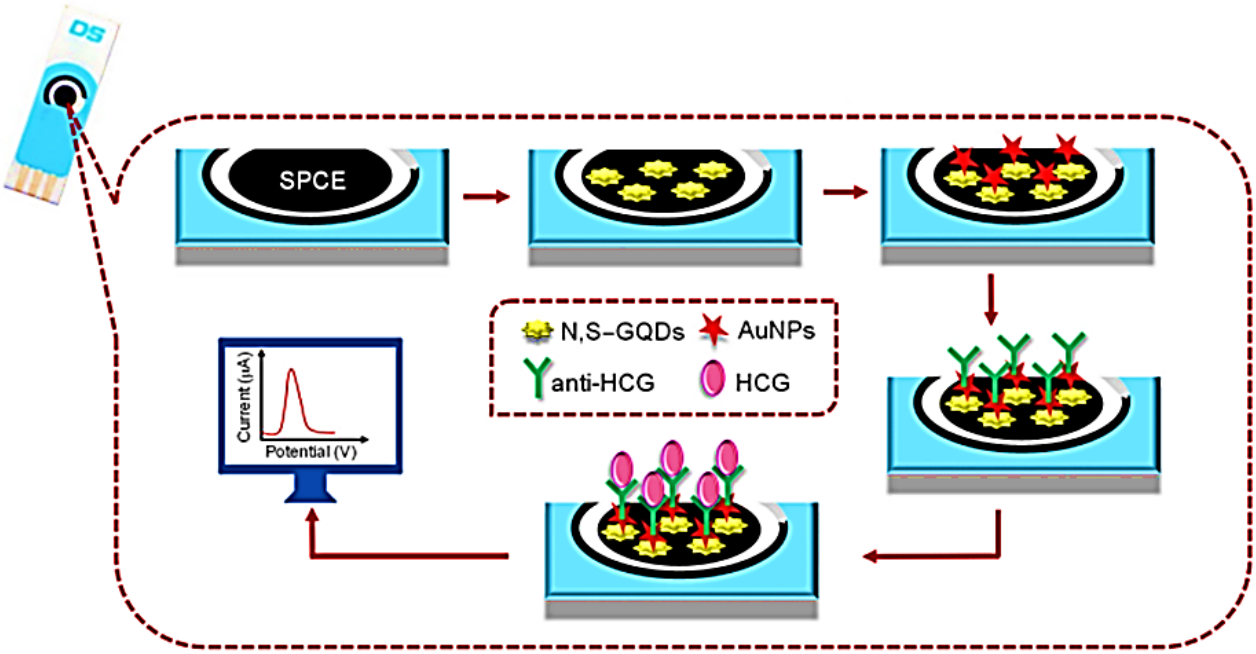

Fig. 11: Design of a GQD-based antibody sensor to monitor HCG levels, [151]

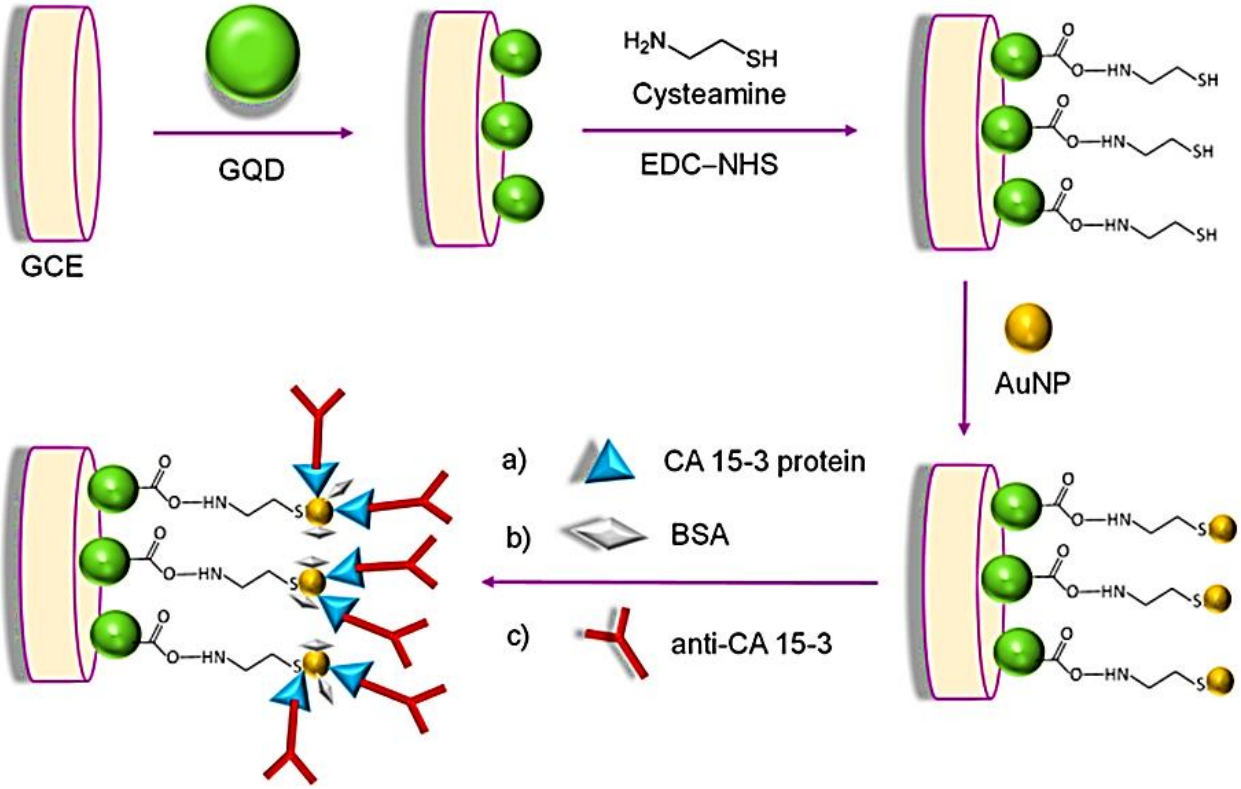

Fig. 12: Design to produce a GCE to detect breast cancer, [151]

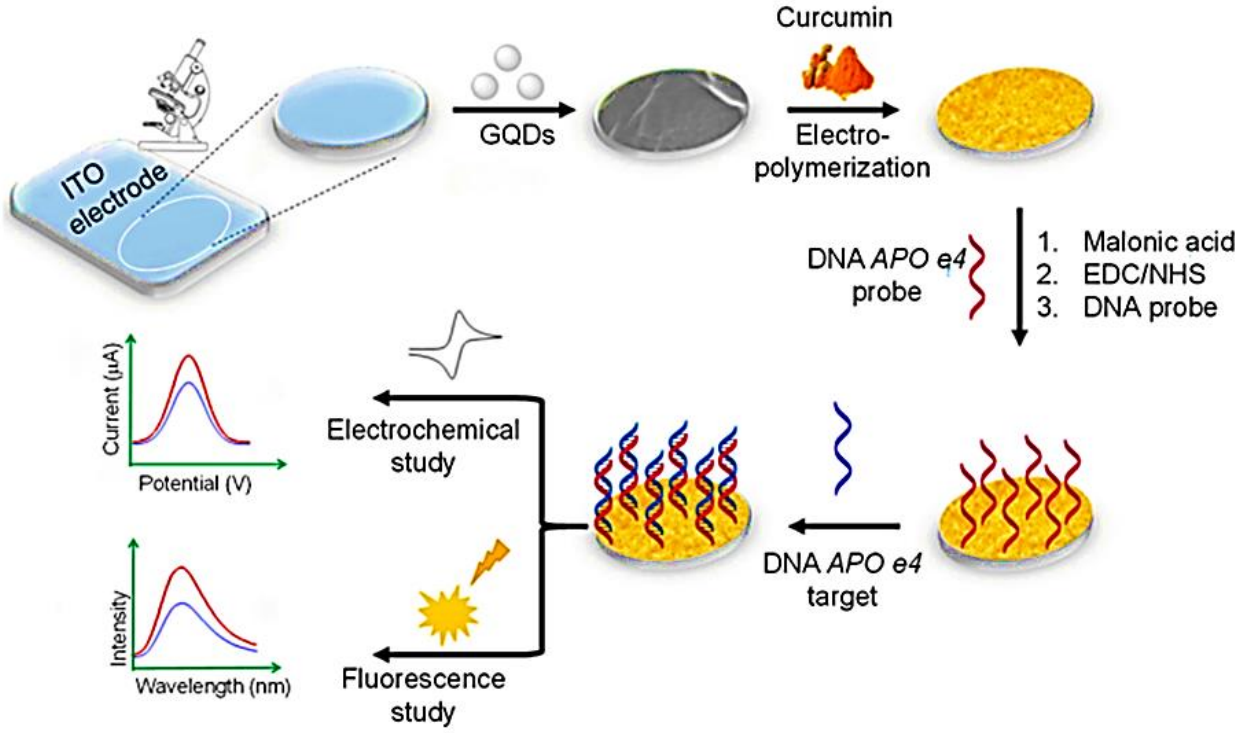

Fig. 13: Use of a n electrochemical and fluorescent-based DNA sensor in the experimental design of a PO e4 DNA, [185]

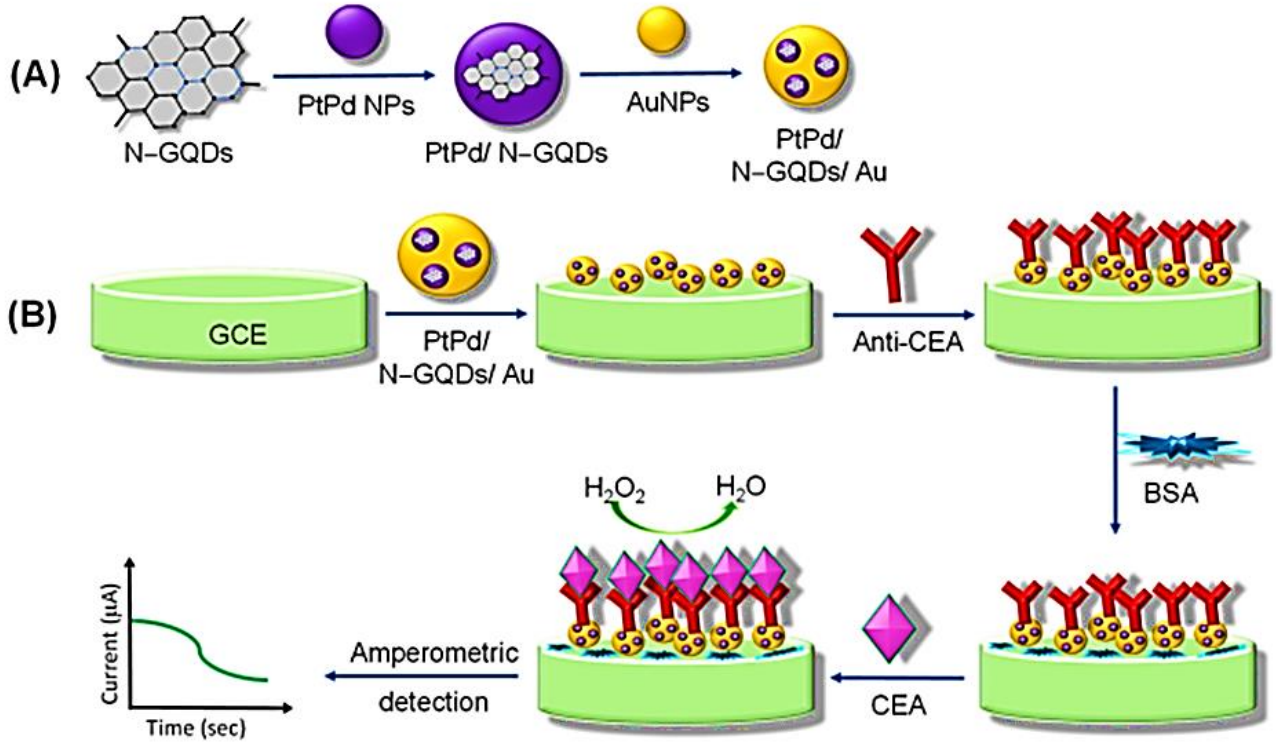

Fig. 14: (A) PtPd/N-GQDs/Au nanohybrid preparation steps and (B) design of a label-free amperometric antibody sensor for CEA detection, [151]

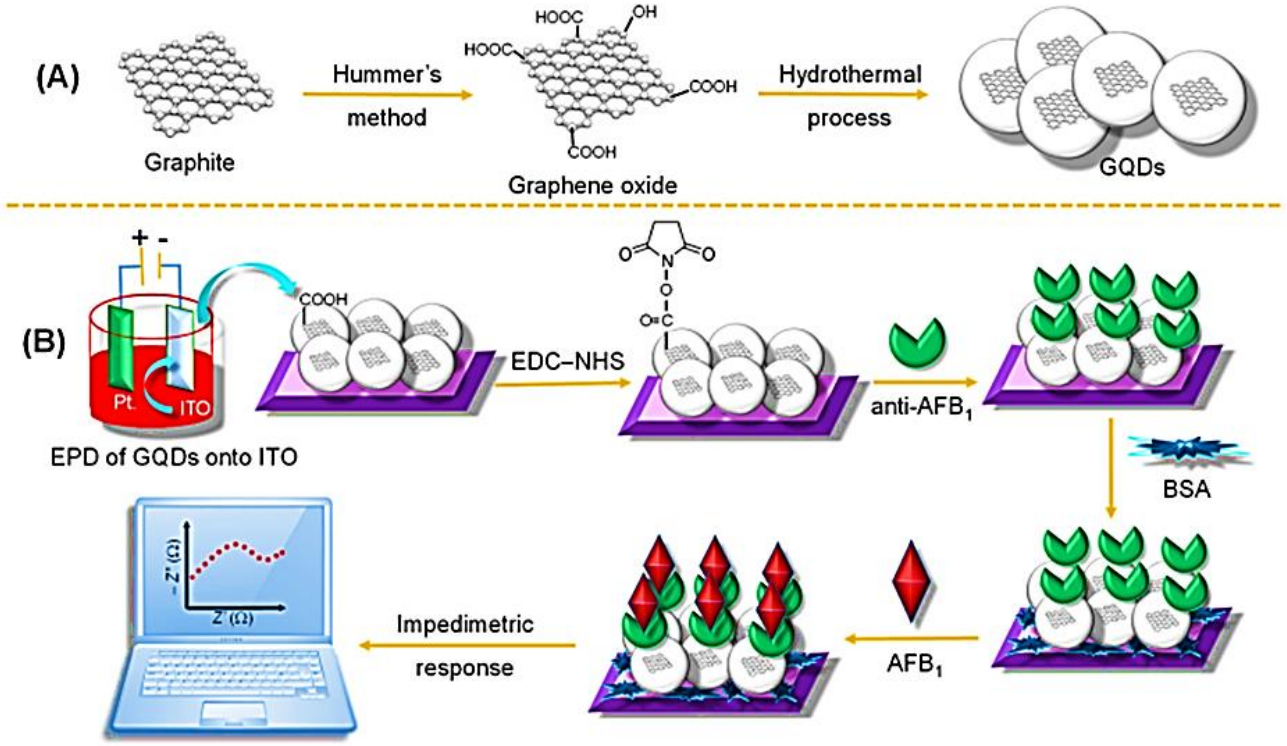

Fig. 15: (A) the preparation of GQDs and (B) the demonstration of the immunosensing platform for AFB1 with ITO-coated glass electrode with GQD function, [151]

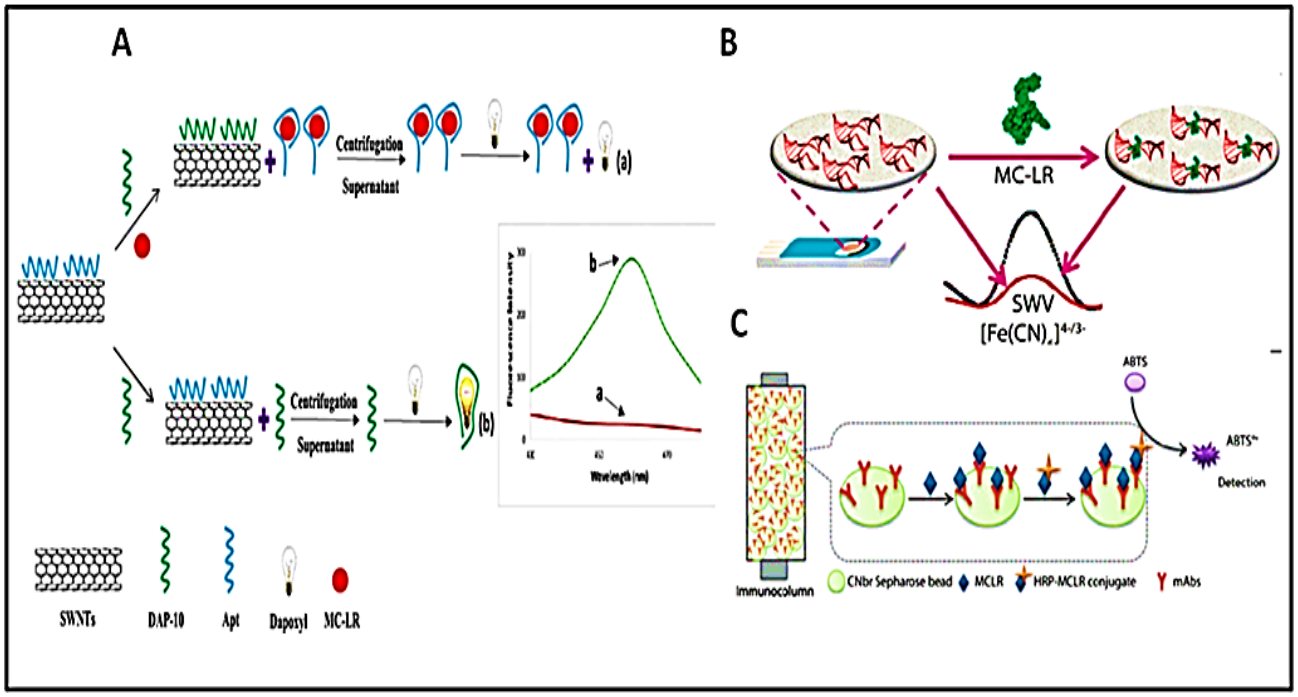

Fig. 16: (A) Illustration of a fluorescence method for MC-LR detection. When MC-LR is present, Apt attaches to it and then exits the SWNT interface. As a result, DAP10 could adhere to SWNT surfaces, leading to a modest level of fluorescence (a). An intense fluorescent signal exists in without the presence of MC-LR because the Apt persists on the SWNT interface and DAP-10 lacks the ability to attach to it (b), [200]. (B) MC-LR identification on an aptamer-functionalized GSPE by SWV, as shown schematically. (C) showing the removal procedure carried out in the immune column, [201]

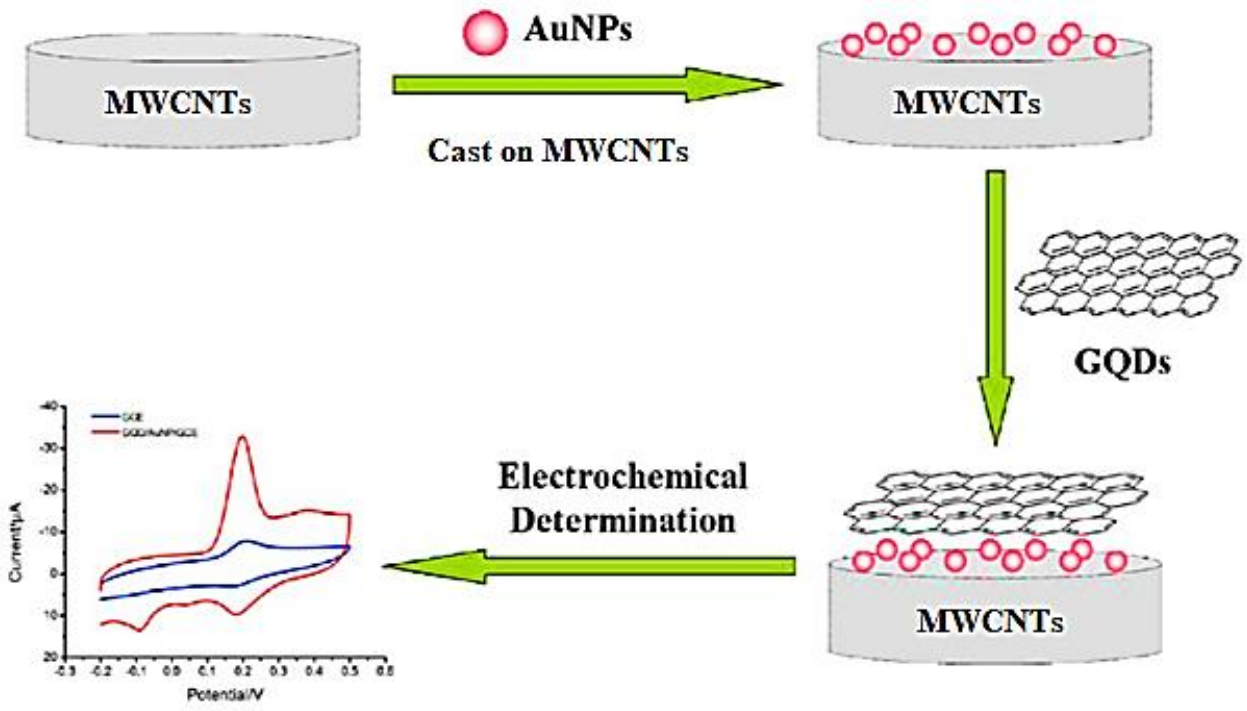

Fig. 17: The main mechanism of a u NPs@MWCNTs/GQDs with electrochemical sensor

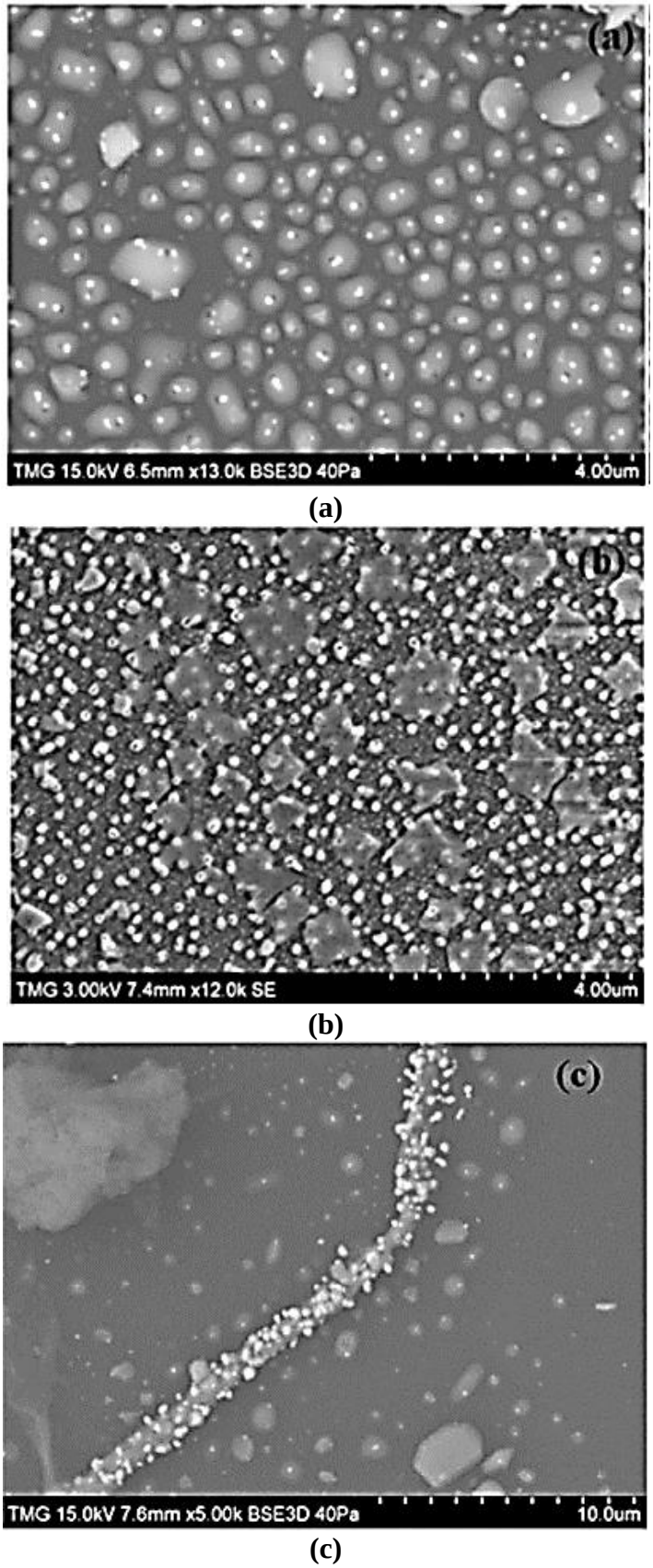

Fig. 18: (a) the nucleation of a u in the dried droplet of the precursor solution, (b) dispersed and growing Au crystals, (c) Au reduction in CNT bundles, [200]

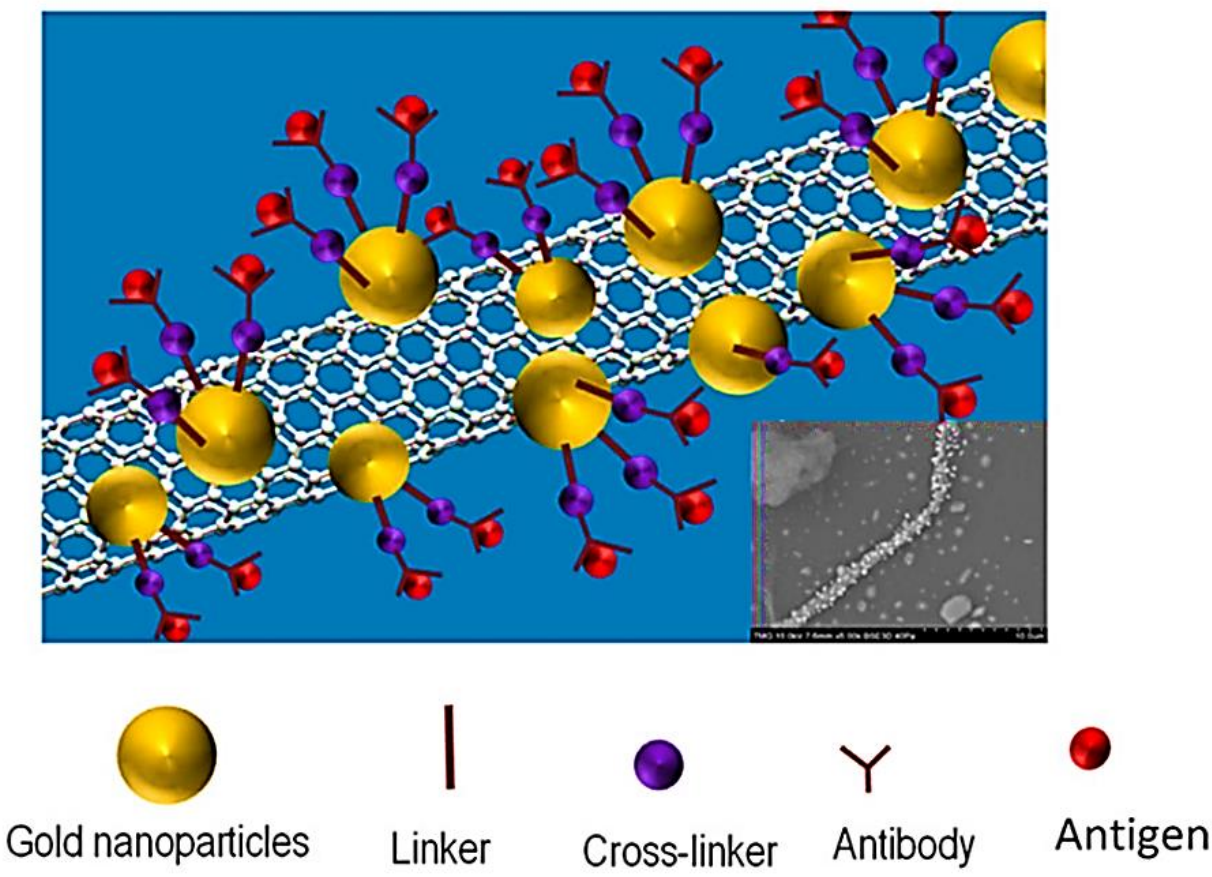

Fig. 19: CNTs locally decorated with Au NPs for plasmonic detection (the Au-CNT SEM images is shown in inset), [200]

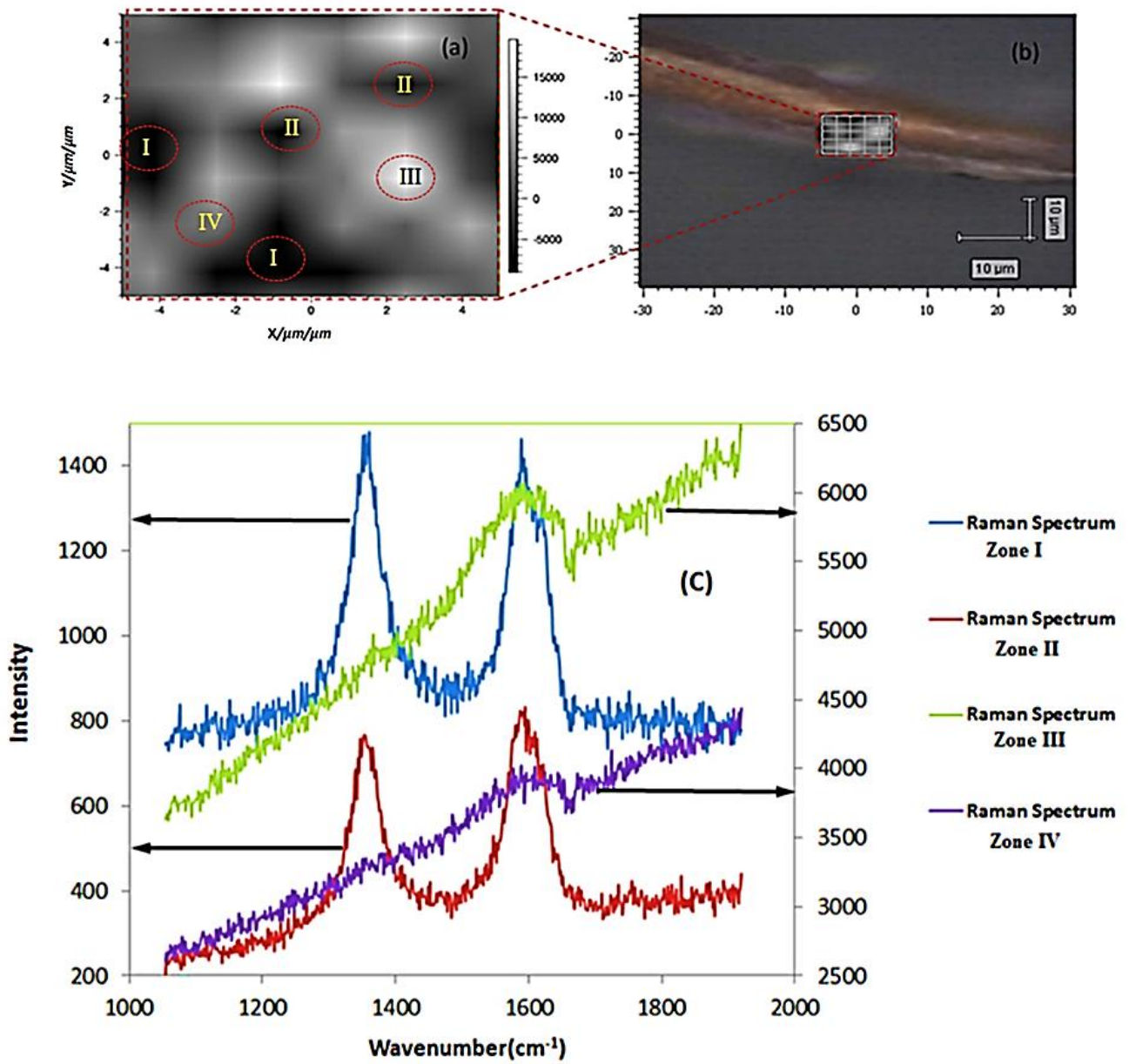

Fig. 20: Combined video and Raman image of a MWCNT covered by aggregates of a u NPs (a, b), and Raman spectra corresponding to measurements at different Zones on the sample (Zone I to Zone IV) of the area defined in (a) according to the mapping software (c). The Raman image (a) originates in the mapping of the ratio of the intensities of G (1590 cm−1) and D (1343 cm−1) lines, [237]

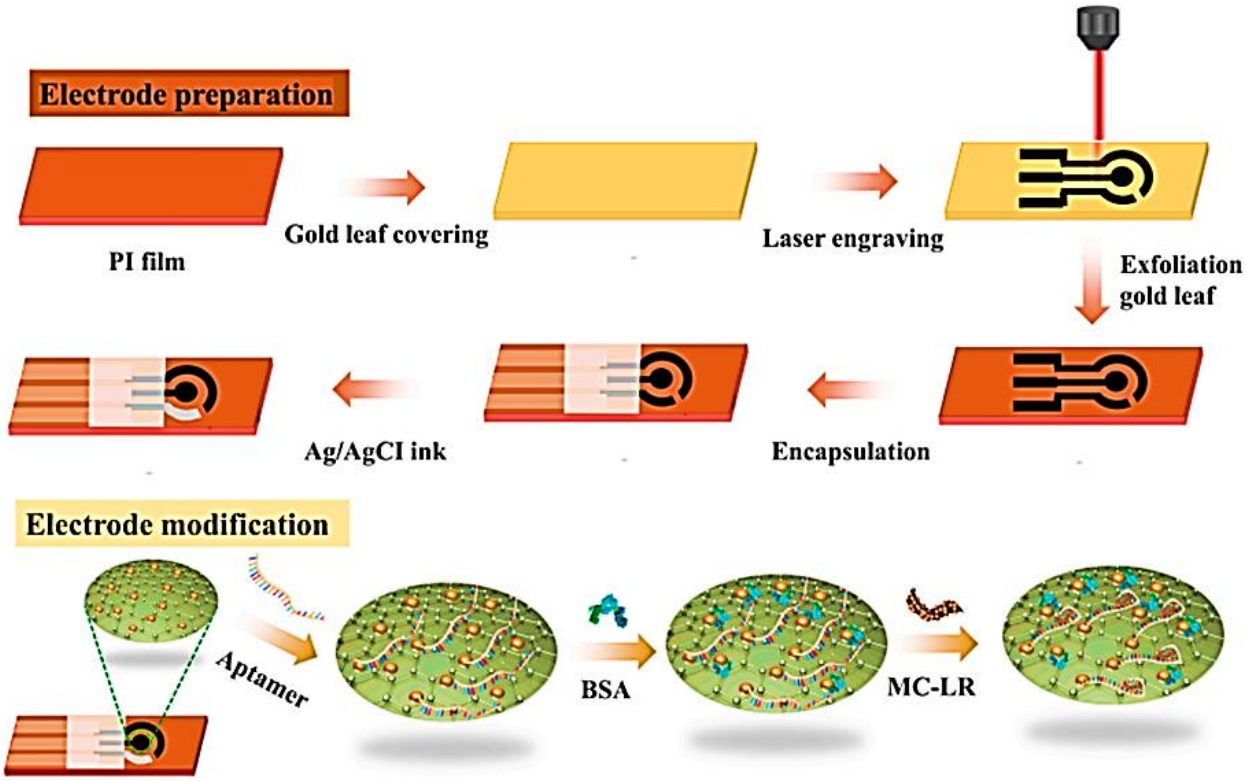

Fig. 21: the demonstration of preparation of LIG-Au electrodes and assembly of portable MC-LR aptasensors, [238]

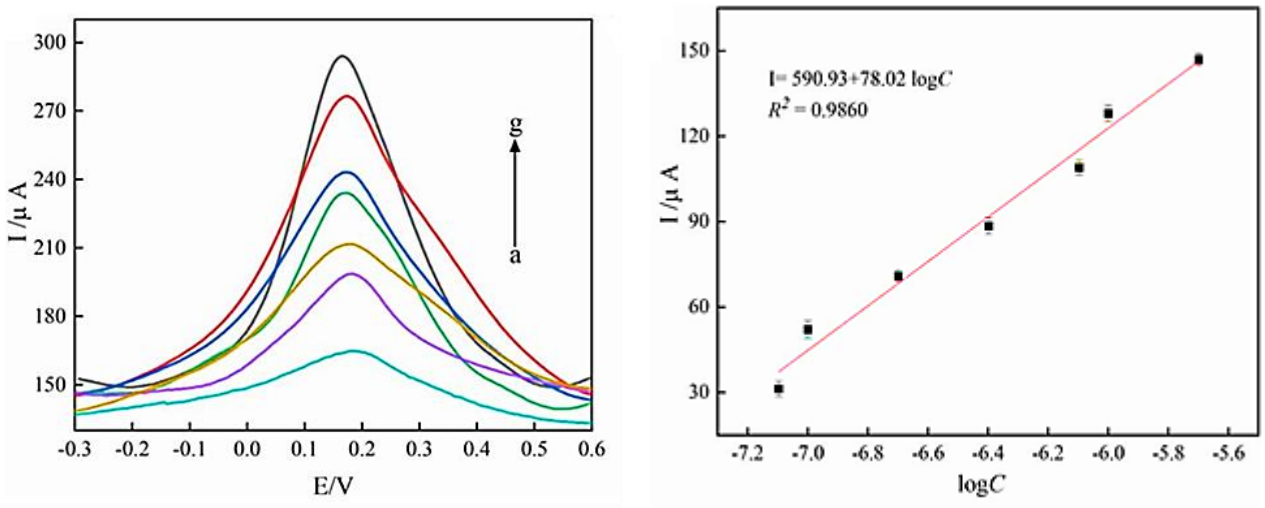

(a) **(b)**

Fig. 22: (A) DPV of the MIP/AuNPs@MWCNTs/GQDs/GCE toward different concentrations of MC-LR (a→g correspond to MC-LR concentrations of (a) 0.08, (b) 0.1, (c) 0.2, (d) 0.4, (e) 0.8, (f) 1.0, (g) 2.0 μg/l, respectively; (B) the linear relationship between the peak currents and the logarithm of concentrations

Table 2. The comparison of analytical methods or products for the analysis of MC-LR in water samples

Method	Linear range (µg/l)	LOD (µg/l)	References
Colorimetric sensor	1 - 100	-	[268]
Fluoroimmunoassay	0 - 500	0.93	[269]
Optical planar waveguide platform	0.21 – 5.9	0.19	[270]
MIP-coated CQDs fluorescent sensor	1 - 1000	0.0093	[271]
QCM sensor	0.0995 - 995	0.0398	[272]
MIP photoelectrochemical sensor	0.5 - 100	0.1	[273]
Sol-gel imprinted polymers on solid contact electrodes	0.77 – 2.0	0.75	[274]
Molecularly imprinted electrochemical sensor	0.08 – 2.0	0.0028	In this study

Table 3. Analytical methods used for MCs detection in water

Method	Sample	Recovery rate	LOD	Ref.
Competitive fluorescence immunoassay pseudo ELISA	Distilled water Lake water	90-110% 96-130%	0.03 µg/l for MC-LR $2.64x10^{-4}$ nM for MC-LR	[286]
Indirect competitive chemiluminescent enzyme immunoassay immunochromatography assay	Distilled water Distilled water	96.46% 91.3-111.0%	0.13 µg/l for MC-LR 0.1 µg/l for MC-LR	[287]
SPE-LC/MS	Tap water	94.1-103.2%	5.0 ng/l for six common MCs	[287]
MSPE-HPLC/UV	Distilled water	86-113%	0.08 µg/l for MC-LR	[288]
MIP coated QCDs fluorescent sensor	Distilled water	94.1-100.7%	0.0093 µg/l for MC-LR	[288]
Nanobiochar paper immunosensor	Distilled water	97.0-100.1%	0.017 µg/l for MC-LR	[286]
PPy/Cu2O molecularly imprinted composite film-based visible light-responsive photoelectrochemical sensor	Distilled water	98.19-102.83%	0.23 ng/l for MC-LR	[287]
Sol-gel imprinted polymers	Distilled water	101.2%	0.75 µg/l for MC-LR	[289]
Enzyme-free electrochemical immunosensor based on G-quadruplex/hemin functunalized mesophorous silica	Distilled water	93.6-109.1%	0.3 ng/l for MC-LR	[290]
Impedimetric immunosensor	Distilled water		3 ng/l for MC-LR	[291
Nonenzymatic immunosensor based on carbon nanofibers	Distilled water	98.0-99.2%	1.68 ng/l for MC-LR	[288]
C18-functionalized magnetic silica nanoparticles for solid phase extraction followed by HPLC-DAD	Distilled water	73.3-104%	0.056 µg/l for MC-LR	[291
Bioactivated sensor based on MWCNTs on filter paper	Freshwater		0.19 ng/ml for MC-LR	[292]
Fiber optical chemiluminescent biosensor	Distilled water	80-120%	0.03 µg/l for MC-LR	[286]

Real-time assembled aptasensor of plasmonic graphene oxide	Distilled water	98-103%	6.3 pM	[288]
Signal-on immunosensor	River water	94.8-120.0%	0.45 ng/ml for MC-LR	[290
Photoelectrochemical sensor	Tap water, pond water, and river water	96.4-113%	0.4 pM	[291]

Table 4. Comparison of various immunosensors for the detection of MC-LR in waters

Biosensors	**MCs variants**	**Recognition elements**	**LOD**	**Ref.**
Portable optical immunosensor	MC-LR	MC-LR OVA	0.28 µg/ml	[286]
Photoelectrochemical immunosensor	MC-LR	Monoclonal MC-LR antibody (Ab) to the MUA-Au NCs modified Au electrodes	0.011 pM	[287]
Fluorescent immunosensor	MC-LR	CdTe quantum dots	0.0440 ng/l	[288]
Label-free amperometric immunosensor	MC-LR	Antibody on an Au electrode coated with L-cysteine	20 ng/l	[289]
Electrochemical immunosensor	MC-LR	Antibody coated on Biochip	3 ng/l	[290]
Molybdenum disulfide/Au nanorods (NRs) composite-based electrochemical immunosensor	MC-LR	Antibody on the MoS_2/Au NRs nanocomposites	3 ng/l	[291]
Electrochemical	MC-LR	Antibody	0.6 ng/l	[292
Impedimetric immunosensor	MC-LR	Biotinylated nanobody (Nab A2) immobilized on a glassy carbon electrode	0.033 µg/l	[290]
QCM immunosensor	MC-LR	Au NP-mAb	0.1 µg/l	[291]